



Project Title: *Increasing scientific, technological and innovation capacity of Serbia as a Widening country in the domain of multiscale modelling and medical informatics in biomedical engineering (SGABU)*

Coordinating Institution:
University of Kragujevac (UKG)

Start date: 1st October 2020

Duration: 36 months

Related work package	WP6 - Bioengineering computational platform
Related task	Task 6.3. Development of materials needed for high quality learning, training and research
Lead beneficiary	UKG
Contributing beneficiaries	TUW, UOI, KUL, COVU
Deliverable type*	Report
Dissemination level**	PU
Document version	V1.0
Contractual Date of Delivery	31/03/2023
Actual Date of Delivery	31/03/2023

Authors	UKG (Tijana Geroski, Nenad Filipovic)
Contributors	UKG (Smiljana Tomasevic, Aleksandra Vulovic, Milos Ivanovic, Aleksandar Atanasijevic, Andreja Zivic, Jelena Zivkovic) UOI (Themis Exarchos, Mary Roumpi, Orestis Gaides) TUW (Christian Hellmich, Stefan Scheiner, Niketa Ukaj) KUL (Hans van Oosterwyck, Fernando Perez Boerema, Jorge Barrasa Fano) COVU (Djordje Jakovljevic)
Reviewers	COVU (Djordje Jakovljevic), KUL (Hans van Oosterwyck)



This project has received funding from the European Union's Horizon 2020 research and innovation programme under grant agreement No 952603

Version history

Version	Description	Date of completion
0.1	Table of Content	09/02/2023
0.2	Completion of Sections 1, 2.1, 2.3	21/02/2023
0.3	Completion of Help files (Appendix)	20/03/2023
0.4	Completion of Sections 2.2, 3-5	22/03/2023
0.5	Formatting and proofreading of the report	24/03/2023
0.6	Internal review (COVU, KU Leuven)	27/03/2023
0.7	Final correctios of the report	30/03/2023
1.0	Submission of the final report	31/03/2023

Executive summary

The activities in **Task 6.3. Development of materials needed for high quality learning, training and research** are focused on providing short tutorials including guidelines, case studies and best practice examples in order to facilitate students' learning and training. All partners have contributed by providing relevant materials and adapting them to meet the specific learning and training needs, as well as by creating new materials based on the results achieved in the project. The results of Task 5.2 were used in the implementation of Task 6.3. The integration of subsystems (i.e. services of different platforms provided by twinning partners) relies on previously defined communication and integration protocols (Task 5.4) and designed architecture (Task 5.3), following the user requirements. Existing computer models for bone modelling, cancer modelling, cardiovascular diseases modelling and tissue engineering with patient specific databases have been successfully integrated within the SGABU. All these data together with the relevant learning and training materials are integrated into one cloud-based Biomedical engineering computational platform that is being evaluated for practical use. The evaluation and refinement of SGABU computational platform is a continuous process that will last during the project lifetime. The application of the platform will provide sustainability of project results toward maximizing the project impact.

The Deliverable D6.3 represents the outcome of Task 6.3, and it is structured as follows.

Section 1 – Introduction summarizes the main concept and objectives of the SGABU project.

Section 2 – Teaching and learning materials provides a description of help files, video tutorials and analytics of test users.

Section 3 – Deviation from the work plan is related to the reporting of any deviations from the workplan.

Section 4 – Conclusions summarizes main conclusions in the deliverable.

Section 5 – References comprehends main references used in this report.

Section 6 – Appendix describes all help files for datasets and models integrated within the SGABU platform.

Table of Contents

1	Introduction	10
2	Teaching and learning materials	11
2.1	Help files.....	11
2.2	Video tutorials.....	12
2.3	Analytics of test users	13
3	Deviation from the work plan	17
4	Conclusions	18
5	References	19
6	Appendix – Help files	20
6.1	Dataset – Baghdadite; Responsible partner - TUW	20
6.2	Dataset – Femur geometries; Responsible partner - UOI.....	24
6.3	Dataset – Stenosis cases; Responsible partner - UOI	30
6.4	Dataset – Oral cancer; Responsible partner - UOI.....	37
6.5	Dataset – Mechanobiology; Responsible partner - KUL	41
6.6	Dataset – TFMLAB data; Responsible partner - KUL.....	43
6.7	Dataset – LVAD; Responsible partner - COVU	49
6.8	Dataset – CORS; Responsible partner - COVU	54
6.9	Dataset – Hip joint; Responsible partner - UKG.....	57
6.10	Dataset – Electrospinning; Responsible partner - UKG.....	59
6.11	Model – BonePoreDense; Responsible partner - TUW.....	63
6.12	Model – BoneMinOrg; Responsible partner - TUW	67
6.13	Model – TissueEngUlt + TissueEngElast; Responsible partner - TUW	71
6.14	Model – Plaque progress; Responsible partner - UOI.....	76
6.15	Model – ASLI; Responsible partner - KUL.....	84
6.16	Model – TMFLAB; Responsible partner - KUL.....	91
6.17	Model – Biomaterial Corrosion; Responsible partner - UKG	96
6.18	Model – FEA of Femoral Bone; Responsible partner - UKG.....	104
6.19	Model – Parametric Heart; Responsible partner - UKG.....	110
6.20	Model – Smearred tumor growth model; Responsible partner - UKG	116
6.21	Model – Semicircular canal model; Responsible partner - UKG	120

List of Figures

Figure 1. The main dashboard of the SGABU platform.	11
Figure 2. Example Help file.	12
Figure 3. Age distribution of the SGABU platform test users.	14
Figure 4. Gender distribution of the SGABU platform test users.	14
Figure 5. Response to SGABU target fields.	15
Figure 6. Response to SGABU platform impressions.	15
Figure 7. Response to SGABU individual modules impressions.....	16
Figure 8. Main platform dashboard; (icon for Baghdadite is extracted from Figure 7(a): H. Kariem, M.-I. Pastrama, S.I. Roohani-Esfahani, P. Pivonka, H. Zreiqat, C. Hellmich ¹)	20
Figure 9. User Interface for Baghdadite module.	21
Figure 10. Exception handling.....	22
Figure 11. Results section: (a) Overview of input parameters, (b) figures	23
Figure 12. Main platform dashboard.....	24
Figure 13. The web page of the Femur Geometries dataset.	24
Figure 14. Computer-aided design (CAD) geometries of proximal trabecular bone tissue (a); cortical bone tissue (b); stem (c); and femoral head (d).	25
Figure 15. The Datasets tab and its options.	26
Figure 16. The GUI inside ParaView for the representation of trabecular bone in surface (a), surface with edges (b), wireframe (c) and points (d) type representation.	28
Figure 17. The GUI inside ParaView while in two-split window (a) and four-split window mode (b).....	29
Figure 18. Main platform dashboard.	30
Figure 19. An Artery with 2% DS on the platform.	31
Figure 20. An Artery with 79% DS on the platform.	31
Figure 21. A Bifurcated Artery with 80% DS on the platform.....	32
Figure 22. The (translated) surfaces of inner, outer and vessel rings.....	32
Figure 23. ParaView settings for the datasets (a) and the tools (b).	33
Figure 24. ParaView global settings.	33
Figure 25. An artery representation as a surface without any change in the mesh.....	34
Figure 26. An artery representation as points without any change in the mesh.	34
Figure 27. An artery representation as points with changes in the mesh (points size and opacity).....	35
Figure 28. A splitted view of the geometry of the artery.	35
Figure 29. A splitted view of the geometry of the ring.....	36
Figure 30. The buttons for split view and for screenshots, save or upload a file and other information. .	36
Figure 31. Main platform dashboard.	37
Figure 32. The genes information for all the patients.	38
Figure 33. The patient's id selection in the platform for the clinical information.....	38
Figure 34. Selection of previous/next patient's id and download the clinical information.	39
Figure 35. The main clinical information for each patient in the platform.	40
Figure 36. Main platform dashboard.....	41
Figure 37. Data visualization in SGABU platform.....	42
Figure 38. Main platform dashboard.....	43
Figure 39. Raw images tab.....	44
Figure 40. Filtered images tab.	45

Figure 41. Corrected images tab.....	46
Figure 42. Results: ParaView tab.	47
Figure 43. Results shown in ParaView.	48
Figure 44. Main platform dashboard.....	49
Figure 45. Clinical Characteristics of Studied Population.	50
Figure 46. Resting and Peak Exercise Cardiac and Physical Function Variables in HTx, Implanted and Explanted LVAD Patients, and Healthy Controls.....	51
Figure 47. Individual Data of Cardiac Pumping Capability in HTx, LVAD Implanted and LVAD Explanted Patients, and Healthy Controls.	51
Figure 48. Individual Data of Functional Capacity in HTx, LVAD Implanted and LVAD Explanted Patients, and Healthy Controls in Relation to Age.....	52
Figure 49. Cardiac Recovery Following LVAD Therapy In Advanced Heart Failure.....	52
Figure 50. Cardiac and Functional Capacities in LVAD Implanted, LVAD Explanted, and HTx Patients Expressed as % of Healthy Controls.....	53
Figure 51. Main platform dashboard.....	54
Figure 52. The results.....	55
Figure 53. Diagram: user can select graph type.....	56
Figure 54. Main platform dashboard.....	57
Figure 55. User Interface for Hip joint with femoral Implant dataset.....	58
Figure 56. Different dataset sections.....	58
Figure 57. Main platform dashboard.....	59
Figure 58. Electrospinning setup with flat negative electrode.....	60
Figure 59. Representation of fiber cone formation.....	61
Figure 60. Parameters for electrospinning process.....	62
Figure 61. Main platform dashboard; icon for BonePoreDens.....	63
Figure 62. User Interface for BonePoreDens module.....	64
Figure 63. Exception handling.....	65
Figure 64. Results section: (a) Overview of input parameters, (b) figures.....	66
Figure 65. Main platform dashboard; icon for BoneMinOrg.....	67
Figure 66. User Interface for BoneMinOrg module.....	68
Figure 67. Exception handling.....	69
Figure 68. Results section: (a) Overview of input parameters, (b) figures.....	70
Figure 69. Main platform dashboard.....	71
Figure 70. User Interface for TissueEngUlt model.....	72
Figure 71. Exception handling.....	72
Figure 72. Displayed results for the TissueEngElast model.....	74
Figure 73. Displayed results for the TissueEngUlt model.....	75
Figure 74. Locating the plague growth workflow in the SGABU platform.....	76
Figure 75. The dashboard of the plague growth workflow.....	77
Figure 76. Provision of show features upon successful uploading of the geometries.....	77
Figure 77. Visualization of the lumen geometry inside Paraview Glance.....	78
Figure 78. The template of the input parameters.....	78
Figure 79. Prompting to view the 3D animated results of the shear stress in the lumen.....	80
Figure 80. Viewing the results of the lumen shear stress inside Paraview Glance.....	81
Figure 81. Prompting to view the results of the oxidized LDL in the wall.....	82
Figure 82. Viewing the results of the OxLDL in the wall inside ParaView Glance.....	83

Figure 83. Main platform dashboard.....	84
Figure 84. User Interface of the ASLI module.....	85
Figure 85. Geometries generated by the four sample data sets.....	87
Figure 86. Result section of the ASLI module: a) <i>Workflows</i> section of the ASLI module with a successfully completed run, b) <i>Inputs</i> tab of the results window, c) <i>Results</i> tab of the results window and d) output visualization.....	88
Figure 87. Folder structure of the output of TFMLAB.....	92
Figure 88. GUI.....	93
Figure 89. Illustration of procedures for calculating sprout growth direction and average displacements that are used to analyze directionality of displacements.....	95
Figure 90. Main platform dashboard; marked CorrosionPit model.....	96
Figure 91. User Interface for CorrosionPit module.....	97
Figure 92. Exception handling.....	98
Figure 93. Running the workflow.....	98
Figure 94. Moore neighborhood is used to describe the effect of surrounding cells on the cell of interest.....	99
Figure 95. Corrosion state $S(u, t)$ at time steps $t = 2,3,4,5$	100
Figure 96. Inputs section – table form.....	101
Figure 97. Results section – table form.....	101
Figure 98. Steps section – figures.....	102
Figure 99. Downloading of results.....	103
Figure 100. Main platform dashboard.....	104
Figure 101. Input parameters.....	105
Figure 102. Default values and value ranges.....	105
Figure 103. Workflow execution.....	106
Figure 104. Workflow finished.....	106
Figure 105. Results window – input parameters.....	107
Figure 106. Results window – PAK tab.....	107
Figure 107. ParaView Glance.....	108
Figure 108. ParaView Glance – choosing results to visualize.....	108
Figure 109. Displacement results.....	109
Figure 110. Stress results.....	109
Figure 111. Main platform dashboard.....	110
Figure 112. User Interface for ParametricHeart module.....	111
Figure 113. Prescribing inlet and outlet time function for ParametricHeart module.....	112
Figure 114. Running the workflow.....	112
Figure 115. Inputs tab of the results section.....	113
Figure 116. Data tab of the results section.....	113
Figure 117. Video tab of the results section.....	114
Figure 118. Paraveiw tab of the results section.....	114
Figure 119. Paraview velocities of PAKF0001.vtk.....	115
Figure 120. Input parameters.....	116
Figure 121. Workflow running.....	116
Figure 122. Workflow finished.....	117
Figure 123. Review of the inputs once the workflow is finished.....	117
Figure 124. Diagram data (Displacements vs time).....	118



Figure 125. List of vtk files.	118
Figure 126. Visualization of the vtk file.....	119
Figure 127. Locating the semicircular canal workflow in the SGABU platform.....	120
Figure 128. The dashboard of the semicircular canal workflow.....	121
Figure 129. Input Tab in the Workflow results section.....	122
Figure 130. Displacement Tab in the Workflow results section.	122
Figure 131. Movie Tab in the Workflow results section.	123

List of Tables

Table 1. YouTube links for video tutorials of datasets.....	12
Table 2. YouTube links for video tutorials of models.	13
Table 3. Inputs for the Baghdadite workflow.	22
Table 4. Inputs for the BonePoreDensApp.....	65
Table 5. Inputs for the BoneMinOrgApp.	69
Table 6. Inputs for the TissueEng workflows.....	73
Table 7. Configuration file template.	85
Table 8. Description of the input parameters found in the configuration file.	89
Table 9. Inputs for the corrosion pit model.	99

List of Abbreviations

Abbreviation	Explanation
3D	Three-dimensional
ASLI	A simple lattice infiller
CA	Cellular Automata
CAD	Computer-Aided Design
CI	Cardiac Index
COVU	Coventry University
CPO	Cardiac Power Output
CSV	Comma-Separated Values
CV	Coefficient of Variation
DBP	Diastolic Blood Pressure
DMF	Dimethylformamide
DNA	Deoxyribonucleic Acid
DS	Degree of Stenosis
FE	Finite Element
GUI	Graphical User Interface
HR	Heart Rate
HUVECs	Human Umbilical Vein Endothelial Cells
IVS	Interventricular Septum
KUL	KU Leuven
LVAD	Left Ventricular Assist Device
LVID	Left Ventricular Internal Diameter
LVPW	Left Ventricular Posterior Wall
MAP	Mean Arterial Pressure
MLD	Minimum Lumen Diameter
PCL	Polycaprolactone
PEG	Polyethylene Glycol
PV	Pressure-Volume
QT	Cardiac Output
RDI	Research and Development Institution
RVD	Reference Vessel Diameter
SBP	Systolic Blood Pressure
SV	Stroke Volume
SVI	Stroke Volume Index
TFM	Traction Force Microscopy
THA	Total Hip Arthroplasty
UI	User Interface
UKG	University of Kragujevac
UOI	University of Ioannina
WP	Work Package

1 Introduction

The main aim of the Twinning action SGABU (**S**erbia, **G**reece, **A**ustria, **B**elgium, **U**nited Kingdom) is to enhance research capacity and capabilities of UKG in the field of bioengineering, as well as raise the research profile of its staff, improve networking activities and exchange through the collaboration with four research-intensive institutions: the University of Ioannina (UOI), Greece, the Technical University of Vienna (TUW), Austria, the Catholic University of Leuven (KUL), Belgium, and Newcastle University (UNEW), United Kingdom. These four European universities are widely recognized as leaders in research in the field of multiscale modelling for bone, cancer and cardiovascular disease, tissue engineering, bioinformatics, sensor informatics, imaging informatics and public health informatics in biomedical engineering. Exchange of knowhow and scientific experience between UKG and the EU partners will be accomplished through meetings at UKG and the partner institutions; study visits of staff members to the partner institutions and their labs; summer schools and workshops. One of the main project results is a computational platform for multiscale modelling in biomedical engineering which has been integrated, tested and validated in the areas of tissue engineering, cardiovascular disease, bone and cancer disease.

There are five general objectives of SGABU project:

1. Improve the quality of our research;
2. Make RDI more relevant to the needs of society in Serbia and all relevant stakeholders;
3. UKG to become a national and regional leader in the area of multiscale modelling;
4. Raise the international profile of UKG researchers;
5. Become more competitive within ERA.

One of the SGABU project goals is to create a Bioengineering computational platform that will be used to facilitate, modernize and improve teaching and learning process at UKG, but it will as well be of benefit to the other project partners as a complement to their curricula and in RDI activities. The integrated platform also includes relevant geometries, exe files and tutorials in order to facilitate the learning and training process and enable students to perform modelling and simulations virtually in the university laboratories (WP6). Such a platform is planned to be used at PhD level courses but can also be adapted to be used on the Master level. Moreover, this platform can be used for further validation and parametrization of models (WP7), providing new opportunities for research in the field of bioengineering and be offered to interested stakeholders, such as clinics, medical organizations and similar.

2 Teaching and learning materials

The main dashboard of the SGABU platform (Figure 1) is divided into sections for each field of research, each one of which includes a subsection of datasets and multiscale models. SGABU platform can be found on the link: <https://sgabu-test.unic.kg.ac.rs/login>

Upon accessing any of the modules, a help page automatically opens to provide guidelines on how to use a specific model/dataset, along with the theoretical background and resources for additional reading.

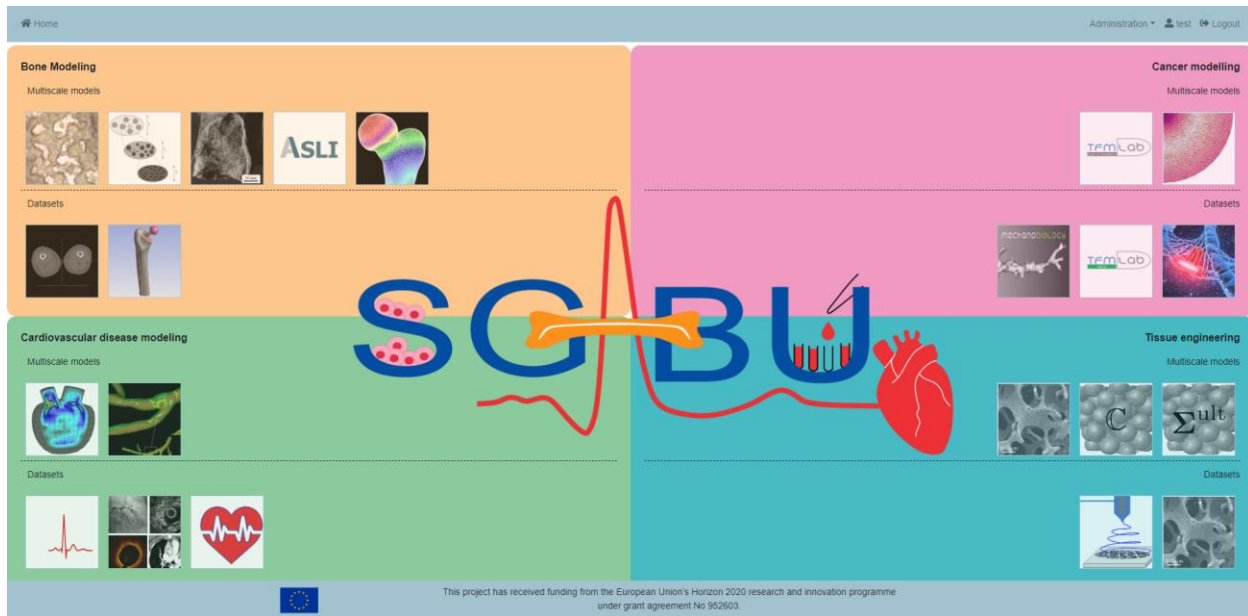


Figure 1. The main dashboard of the SGABU platform.

2.1 Help files

Each Help file contains a step by step tutorial of the theory behind the model, description of the model's use and user interface on the platform. At the end of the document, there are relevant references that can be accessed in order to investigate the methodology and results through published papers. One example of a Help file is depicted in Figure 2. After closing the Help file and working on the model integrated into the platform, the user can access the Help file at any time in the right upper corner mark with the question mark.

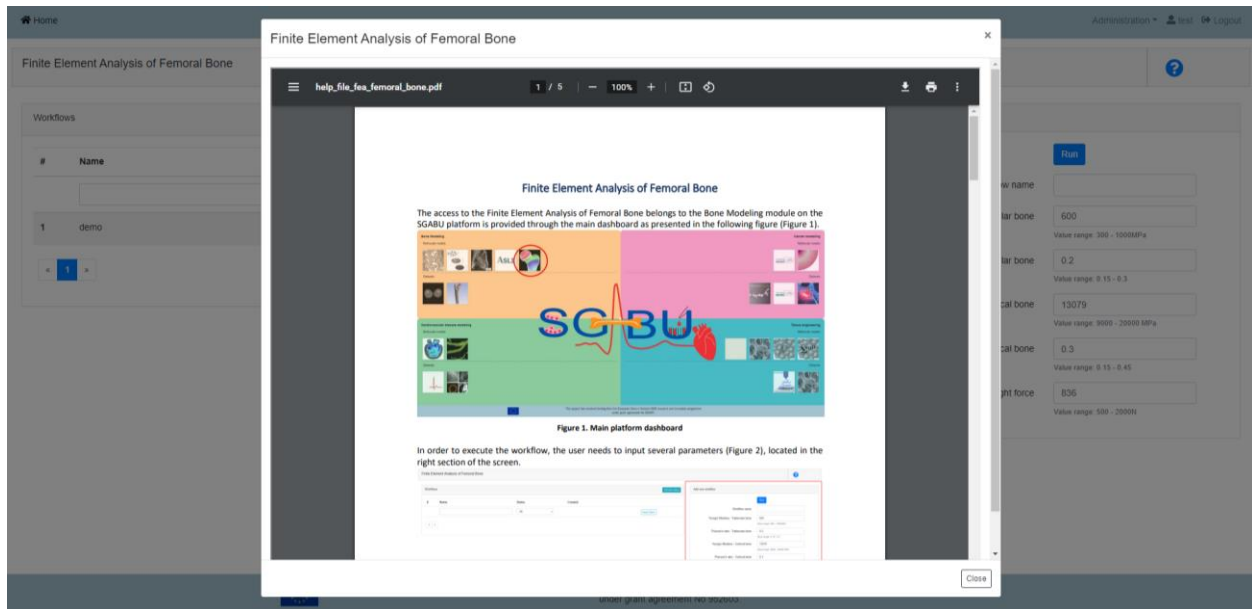


Figure 2. Example Help file.

2.2 Video tutorials

The importance of learning via video material has been recognised. As a result, a YouTube page of the SGABU project has been established and all the video files that represent a step by step tutorial of each dataset and model on the platform are created. In such a way, users can watch the video and repeat the steps given in this tutorial.

This page can be found on the link <https://www.youtube.com/@sgabuproject/videos>

The list of available links for each model is given in Table 1.

Table 1. YouTube links for video tutorials of datasets.

Dataset name	Dataset YouTube link	Responsible partner
Baghdadite	https://www.youtube.com/watch?v=8DzBYzpvGVU	TUW
Femur geometries	https://www.youtube.com/watch?v=9tO2CxQML_4	UOI
Stenosis cases	https://www.youtube.com/watch?v=02fU4c2qlgc	UOI
Oral cancer	https://www.youtube.com/watch?v=MIVzeViUnc4	UOI
Mechanobiology	https://www.youtube.com/watch?v=ilZVMR8IPSI	KUL
TFMLAB data	https://www.youtube.com/watch?v=aqEYBObTu6M	KUL
LVAD	https://www.youtube.com/watch?v=VI3DpD8k0uc&t=17s	COVU

CORS	https://www.youtube.com/watch?v=TY5EOqi04U0	COVU
Hip joint	https://www.youtube.com/watch?v=n97xkxOam6I&t=16s	UKG
Electrospinning	https://www.youtube.com/watch?v=Bbns21usa4&t=2s	UKG

The list of links for each model is given in Table 2.

Table 2. YouTube links for video tutorials of models.

Model name	Model description	Responsible partner
BonePoreDense	https://www.youtube.com/watch?v=EJ0n-Ef3BRs	TUW
BoneMinOrg	https://www.youtube.com/watch?v=zsqs0jsZ5Y	TUW
TissueEngUlt	https://www.youtube.com/watch?v=1rPxNliccol	TUW
TissueEngElast	https://www.youtube.com/watch?v=DsyBiols_x0	TUW
ASLI	https://www.youtube.com/watch?v=-3cb-JAdzO0	KUL
TMFLAB	https://www.youtube.com/watch?v=W8r8QHco7hc	KUL
Corrosion pit	https://www.youtube.com/watch?v=wVJNWMv5DdM	UKG
FEA of Femoral Bone	https://www.youtube.com/watch?v=DYqMhVBa62w	UKG
Parametric Heart	https://www.youtube.com/watch?v=SqxtkdeiRls	UKG
Smearred tumor growth model	https://www.youtube.com/watch?v=lpV0wBQ7R_w	UKG

Video tutorials of modules plaque progress and semi-circular canal are in the final stage of video editing and will be published on the YouTube page in April 2023.

2.3 Analytics of test users

The platform was tested among 21 users who were given access to the platform and afterwards were required to fill a questionnaire that would reflect their impressions of the SGABU platform. These potential users participated in the demonstration of the SGABU workshop named “SGABU platform” on 08/12/2022. At the beginning of the survey some personal information was requested for statistical reasons, although all the collected data were anonymized such that it would not be possible to identify afterwards each survey participant on the basis of his/her given responses. From the collected personal information, it was shown that the majority of the participants were at age up to 30 years old as they were

mostly Master’s and PhD degree students. The age distribution of the SGABU platform test users is shown in Figure 3. Out of the 20 participants, 11 were PhD students and 9 were MSc students. The nationalities of the participants were as following: 8 from Greece, 6 from Serbia, and one per countries India, Pakistan, Germany, Italy, Croatia, Bosnia and Herzegovina.

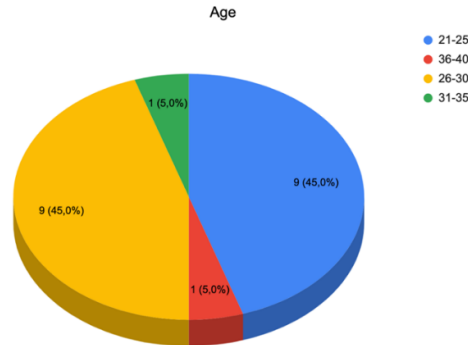


Figure 3. Age distribution of the SGABU platform test users.

The nationalities of the participants were as following: 8 from Greece, 6 from Serbia, and one per countries India, Pakistan, Germany, Italy, Croatia, Bosnia and Herzegovina. Out of the total number of participants, 13 were male and 7 were female (Figure 4).

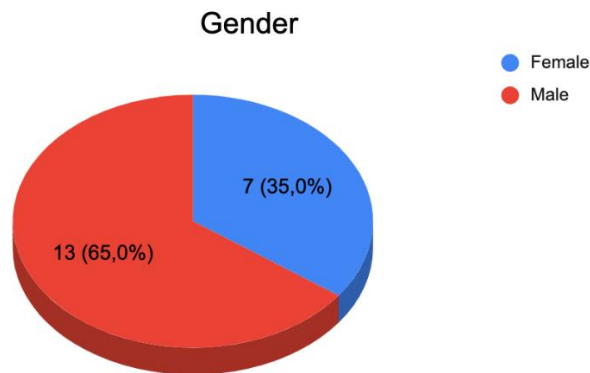


Figure 4. Gender distribution of the SGABU platform test users.

The users were then required to test the platform and its individual modules and respond to several questions. The main points in the survey were related to the efficiency, performance, complexity and usability of the presented platform and its tools. First request was related to check whether the existing modules were of interest to the users based on their education and research interests. This was reflected through the question “Which of demonstrated SGABU fields would you use in your daily practice?”. The responses are given in Figure 5. It can be seen that Cardiovascular module is of highest interest, yet all modules have captured the attention of the participants.

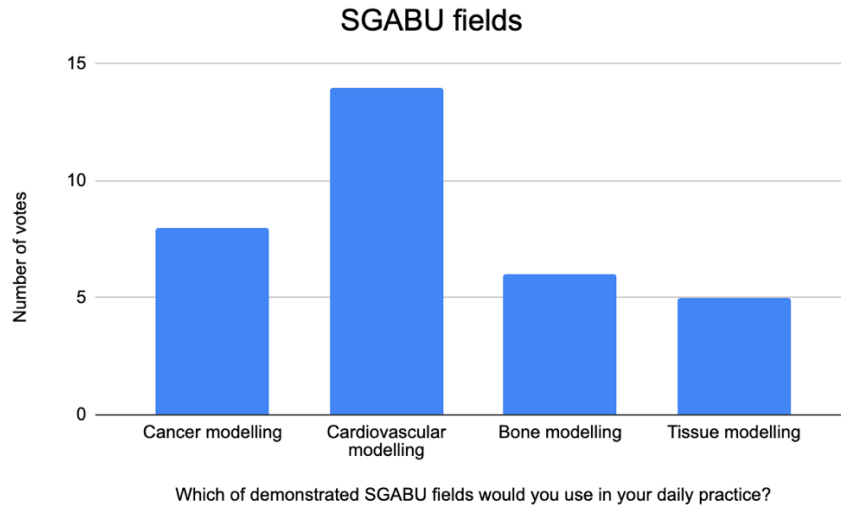


Figure 5. Response to SGABU target fields.

For requests related to their impressions of the overall platform, the users were required to respond in what degree they agree with several statements. This was reflected through the question “For each of the following statements, mark one box that best describes your impressions on the SGABU platform” (Figure 6). It can be seen that the majority of students liked the platform overall, although several participants were unsure whether they would use it in their everyday research. This may derive from the fact that some participants were not from any overlapping area of research with biomedical engineering and medical informatics and did not fully comprehend in a short time the platform and its modules.

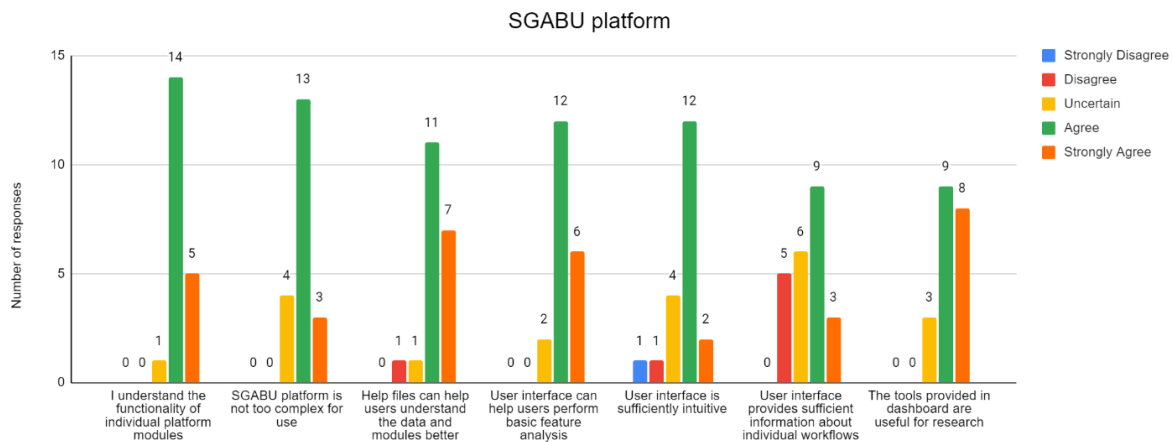


Figure 6. Response to SGABU platform impressions.

For requests related to their impressions of individual modules, the users were required to respond in what degree they agree with several statements. This was reflected through the question “For each of the following statements, mark one box that best describes your impressions on the SGABU modules” (Figure 7). Similarly, to the previous question, the vast majority of the students gave a positive review for the integrated models and datasets, however for a few participants some individual modules were hard to understand.

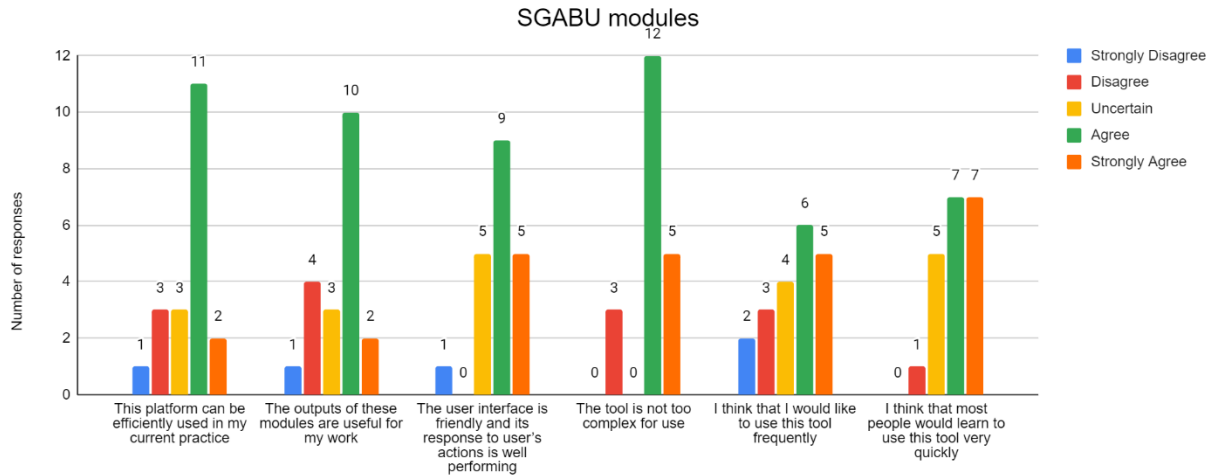


Figure 7. Response to SGABU individual modules impressions.

From the data obtained through the questionnaire, the generated information has guided the continuous development of the SGABU platform. Their responses provide great feedback for the improvement of the platform and its individual modules. However, it should be stated that from a technical point of view there are some limitations of the platform. Currently, the total upload capacity is 500MB and the machine is equipped with 24 cores to execute different workflows, which implies that the platform can accept up to 24 users who can concurrently run simulations using 1 core each. Although the platform is dedicated primarily to students of various levels of education, it has shown great potential to become a useful tool not just in education, but also in research and knowledge sharing.



3 Deviation from the work plan

There are no deviations from the workplan.

4 Conclusions

The deliverable D6.3 – *Materials for teaching and learning purposes* presents the outcome of *Task 6.3 Development of materials needed for high quality learning*. During the task implementation, training and research have been focused on providing short tutorials including guidelines, case studies and best practice examples in order to facilitate students’ learning and training. All partners have contributed by providing relevant materials and adapting them to meet the specific learning and training needs, as well as by creating new materials based on the results achieved in the project.

This deliverable provides a description of teaching and learning materials in the form of Help files and video tutorials in the cardiovascular, bone, tissue and cancer modelling fields. Apart from the platform, the deliverable presents the integrated datasets (10 in total) and models (11 in total) which are described in detail and can be used for teaching and learning purposes. It is important to note that the SGABU platform has been positively evaluated by test users. The further use and evaluation of the platform will enable sustainability of project results, as well as reaching targeted end-users and stakeholders.



5 References

References are incorporated as footnotes within the document.

6 Appendix – Help files

6.1 Dataset – Baghdadite; Responsible partner - TUW

Dataset - Baghdadite	Responsible partner - TUW
-----------------------------	----------------------------------

The access to the “Baghdadite” on the SGABU platform is provided through the second icon in the main dashboard for Tissue engineering as presented in Figure 8. Baghdadite ($\text{Ca}_3\text{ZrSi}_2\text{O}_9$) is a specific tissue engineering material. This workflow shows how respective data (from nanoindentation studies carried out on baghdadite by Kariem et al.¹) can be processed in order to give access to the material stiffness. Furthermore, the stiffness was determined alternatively via ultrasound measurements. The respective data can be downloaded through this workflow in form of a CSV-file.

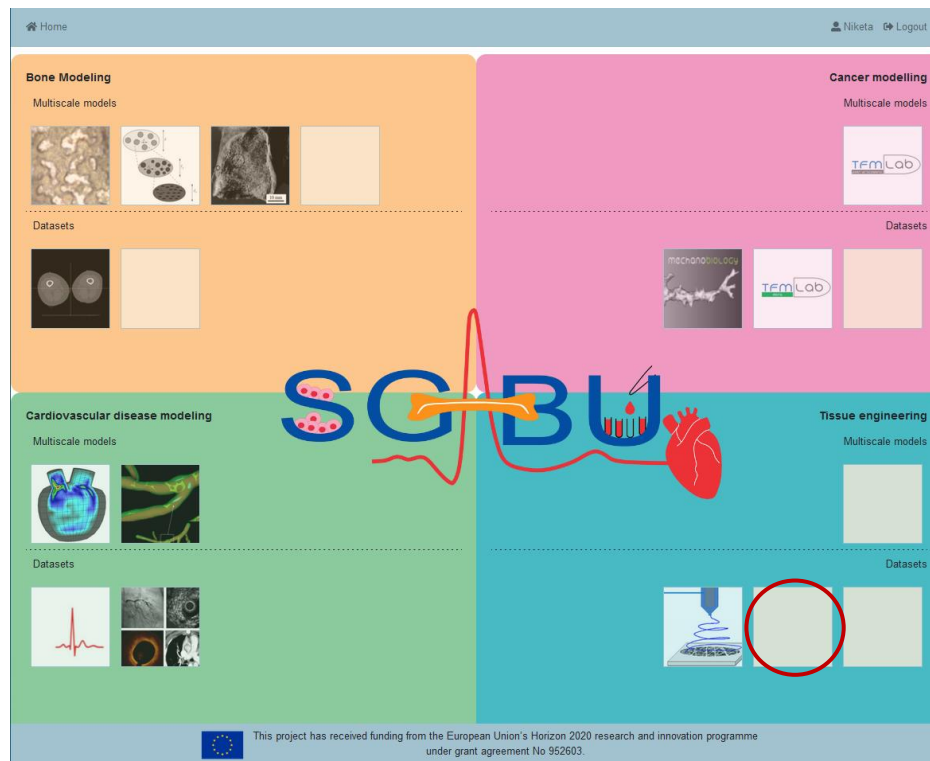


Figure 8. Main platform dashboard; (icon for Baghdadite is extracted from Figure 7(a): H. Kariem, M.-I. Pastrama, S.I. Roohani-Esfahani, P. Pivonka, H. Zreiqat, C. Hellmich¹)

¹ Kariem, H., Pastrama, M. I., Roohani-Esfahani, S. I., Pivonka, P., Zreiqat, H., & Hellmich, C. (2015). Micro-poro-elasticity of baghdadite-based bone tissue engineering scaffolds: a unifying approach based on ultrasonics, nanoindentation, and homogenization theory. *Materials Science and Engineering: C*, 46, pp. 553-564., doi:10.1016/j.msec.2014.10.072

After clicking the respective icon, a new window appears (see Figure 9). The basic execution unit in SGABU is a workflow. In the left section of the window, users are able to see names and status of the workflows. Possible statuses of the workflow are:

- Not yet executed
- Terminated
- Running
- Finished OK
- Finished Error

In the right section of the window, users can create new workflows for this submodule. Each of the forms needs to be filled out in order for the simulation to run.

Users are expected to fill out the following forms:

- Workflow name
- zz (standing for the fitting method)
- nz (standing for the number of peaks)
- vf2 (standing for the sigma-value for fitting)
- sz (standing for step size of stiffness distribution)
- tz (standing for step size of hardness distribution)
- emax (standing for max. Young's modulus)

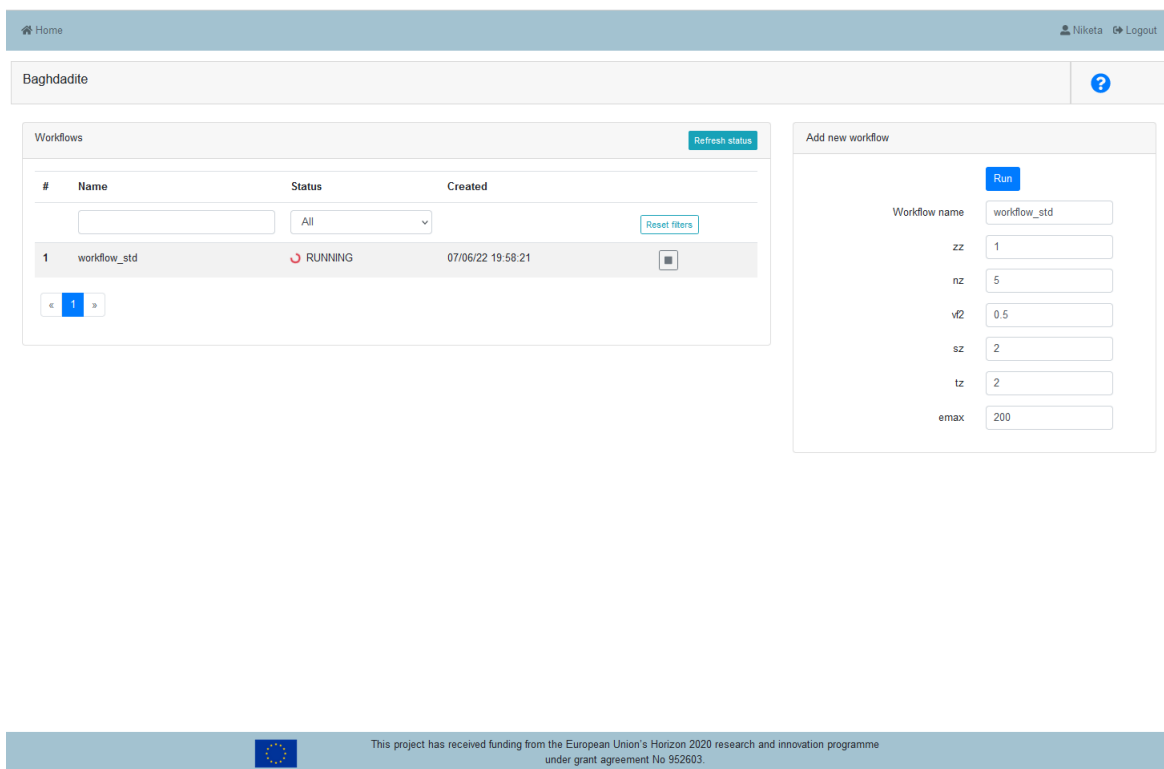


Figure 9. User Interface for Baghdadite module.

The workflow name can be freely chosen. For “zz” the value 1, for “nz” the value 5, for “vf2” a value between 0 and 1, for “sz” a value between 1 and 5, for tz a value between 1 and 5, and for emax a value between 150 and 250 should be entered. The exception handling is integrated into the user interface (UI) of the SGABU platform, see Figure 10.

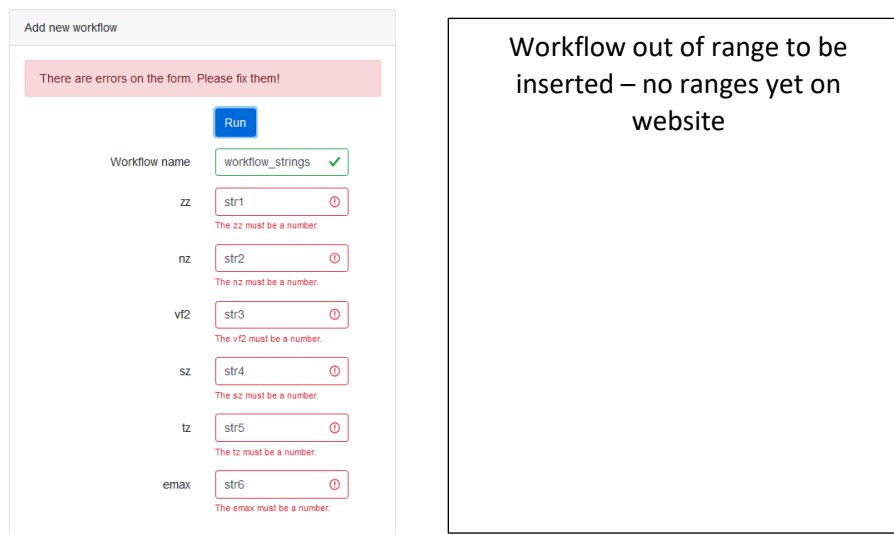


Figure 10. Exception handling.

Once everything is correctly filled, the workflow can be started. The user can monitor the current status of the workflow in the left section of the window. Table 3 shows the summarized information for the input parameters.

Table 3. Inputs for the Baghdadite workflow.

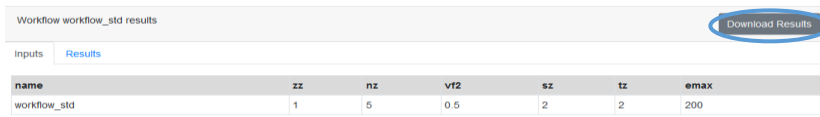
Name of the parameter	Label	Explanation	Unit	Range	Default value
Fitting method	zz	Fitting method 1... fitting based on pdf (probability density functions) 2... fitting based on cdf (cumulative distribution function)	/	1	1
Number of peaks	nz	Number of peaks	/	5	5
sigma-value for fitting	vf2	sigma-value (standard deviation) for fitting		0-1	0.5
Step size of stiffness distribution	sz	Step size of stiffness distribution	/	1-5	2
Step size of hardness distribution	tz	Step size of hardness distribution	/	1-5	2
Max. Young's modulus	emax	Max. Young's modulus	GPa	150-250	200

Results are displayed in the form of images. By clicking on the eye-icon a new window pops up, where the entered input parameters are shown in a table, see Figure 11(a). By switching to „Results“, two images appear, see Figure 11(b), showing (i) the results of the normal distribution of the elastic modulus E_R in [GPa], and (ii) the histogram of the modulus E_R , including the experimental data, sum of modeled distributions, and modeled Gaussian distributions.

The accompanying ultrasound data can be accessed through switching to the tab “Ultrasound data”. This data contains information on the studied sample, including diameter in [m], length in [m], length of microheterogeneities (pores) in [m], time of flight in [s], signal velocity in [m/s], wavelength in [m], density in [kg/m³], the normal stiffness component C_{1111} in [GPa], and porosity.

The results can also be downloaded, see blue circles in Figure 11, in form of figures and CSV files containing all the calculated values.

(a)



name	zz	nz	vt2	sz	tz	emax
workflow_std	1	5	0.5	2	2	200

(b)

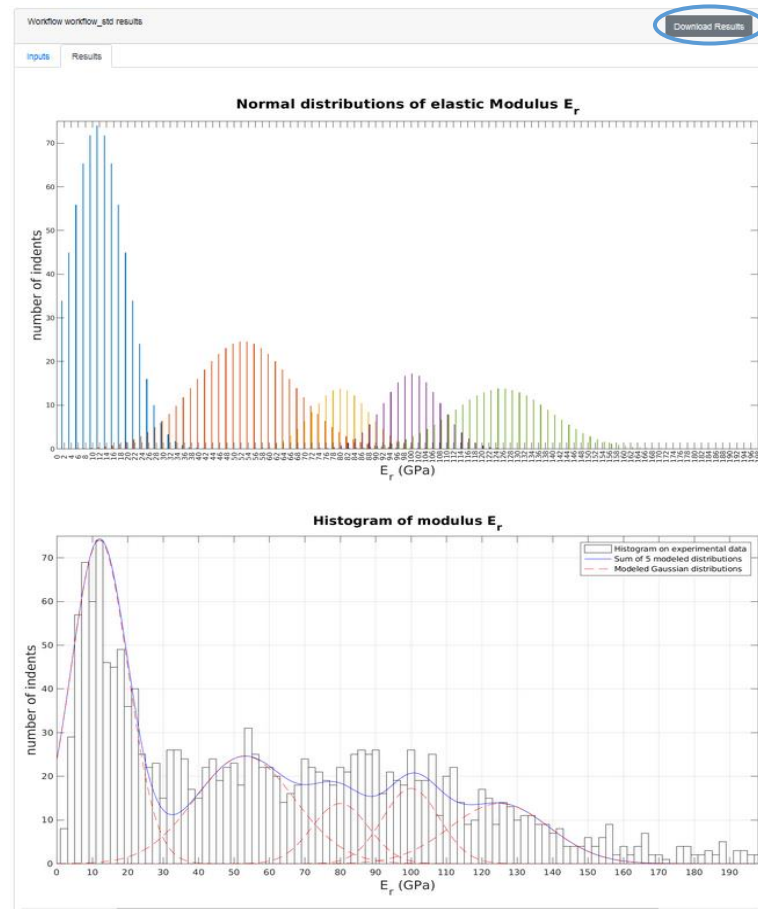


Figure 11. Results section: (a) Overview of input parameters, (b) figures.

6.2 Dataset – Femur geometries; Responsible partner - UOI

Dataset - Femur geometries	Responsible partner - UOI
-----------------------------------	----------------------------------

The Femur geometries dataset can be accessed via the Bone Modeling module in the main SGABU dashboard as presented in Figure 12.

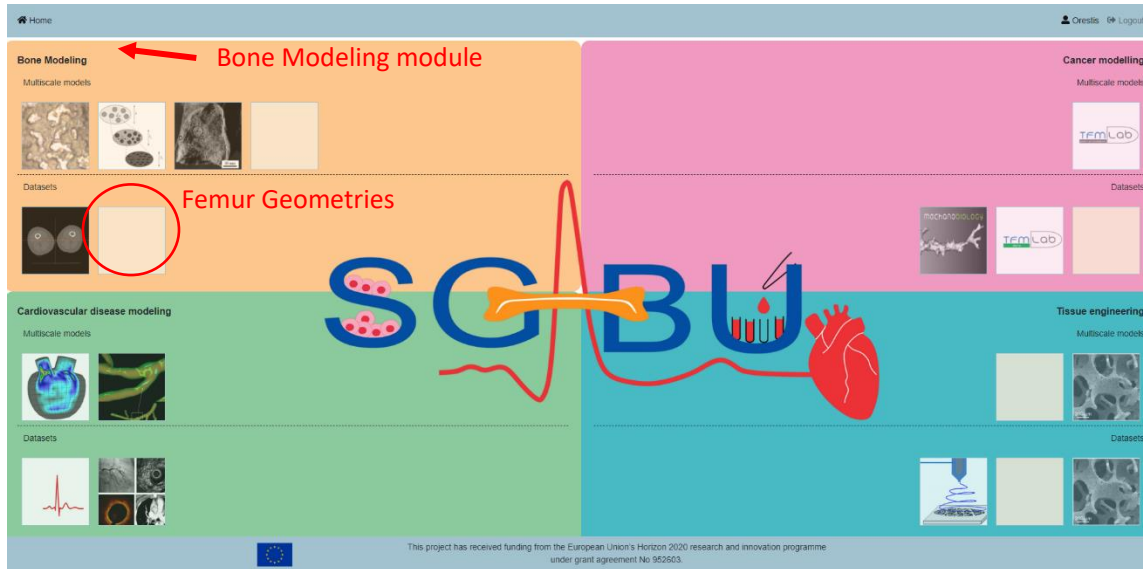


Figure 12. Main platform dashboard.

After selecting the Femur Geometries dataset, the platform will lead to the following page depicted in Figure 13, where the user may choose among the currently available computer-aided design (CAD) geometries for the prescribed bodies on the blue bounded boxes.

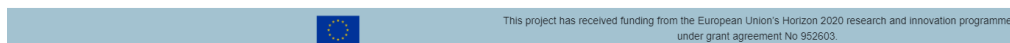
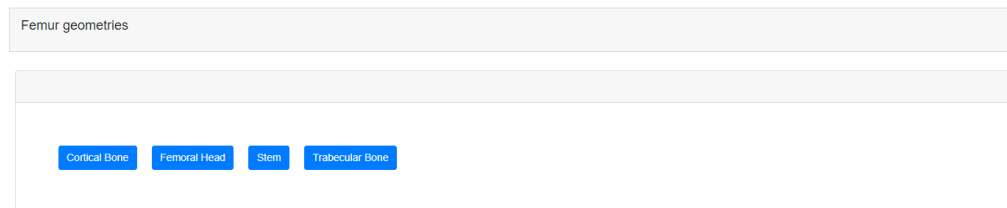


Figure 13. The web page of the Femur Geometries dataset.

This dataset contains the following geometries:

1. Proximal trabecular bone tissue, Fig. 14a
2. Cortical bone tissue, Fig. 14b
3. Stem (main body), Fig. 14c
4. Femoral head of stem, Fig. 14d

The geometries of the proximal trabecular and cortical bone tissue are osteotomized based on the surgical protocol of a conventional Total Hip Arthroplasty (THA) procedure. Furthermore, the cortical bone geometry comprises only the part of the proximal epiphysis and part of the midshaft higher than the isthmus.

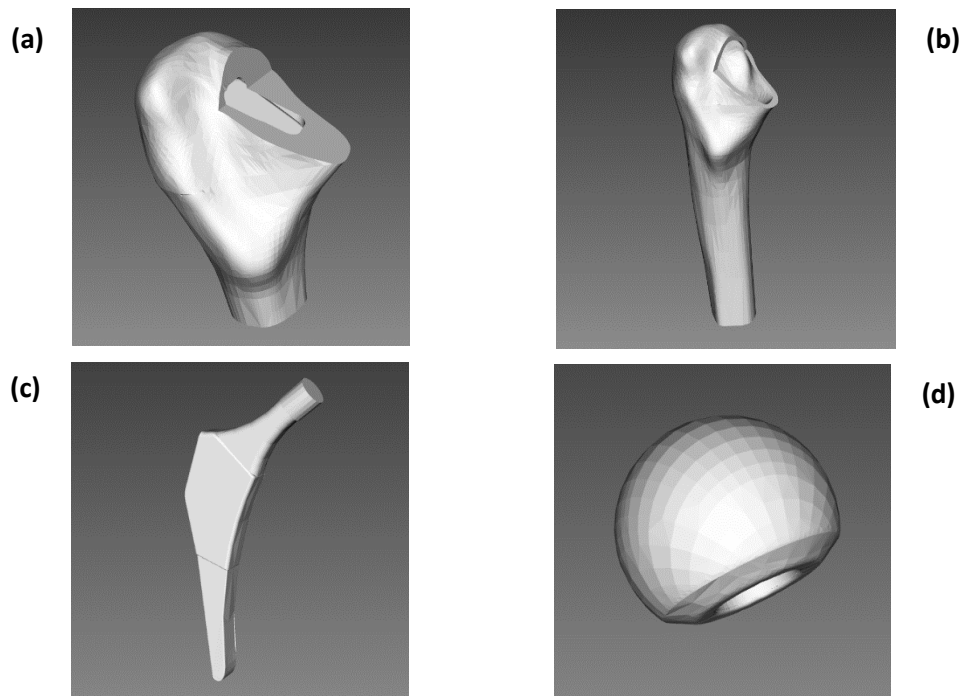


Figure 14. Computer-aided design (CAD) geometries of proximal trabecular bone tissue (a); cortical bone tissue (b); stem (c); and femoral head (d).

The CAD geometries are presented with the help of Paraview Glance, an open-source web application which facilitates the visualization of geometric objects. At the Datasets tab, as shown in Figure 15, the user may choose among several representation types (surface, surface with edges, wireframe and points), select a visualization color for the geometry, and inspect relevant data for the geometric object like the number of points (# of points) and number of cells (# of cells) that comprise the geometry of that object.

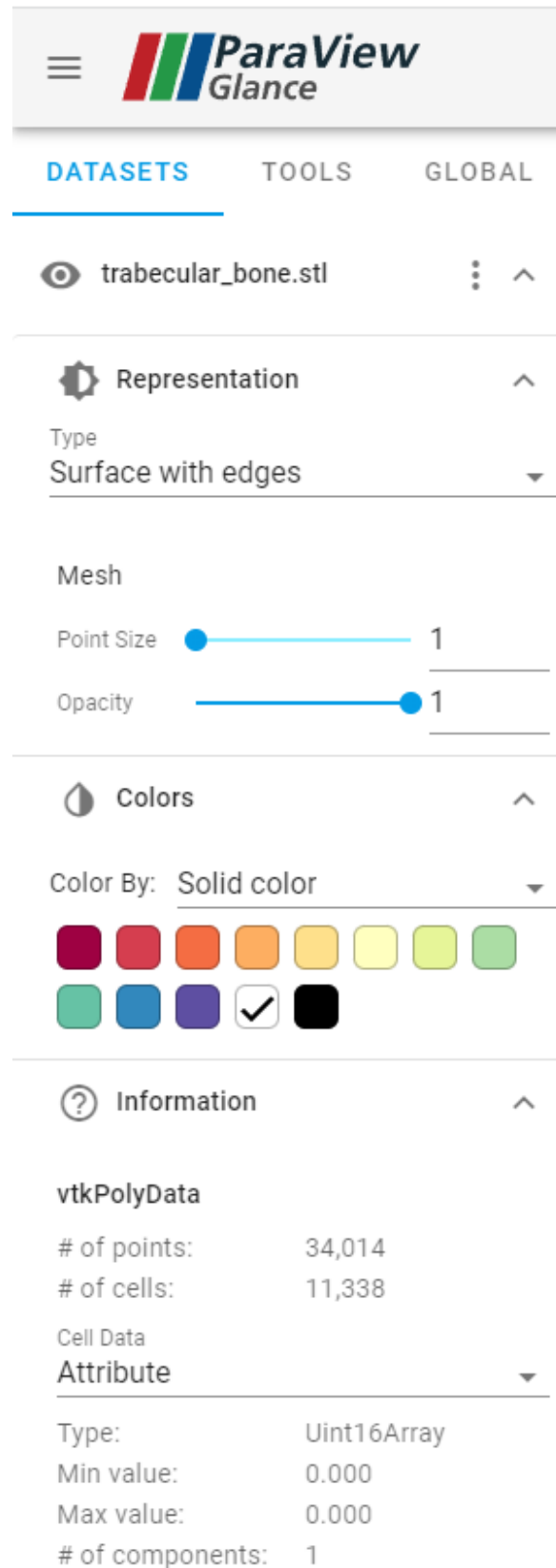
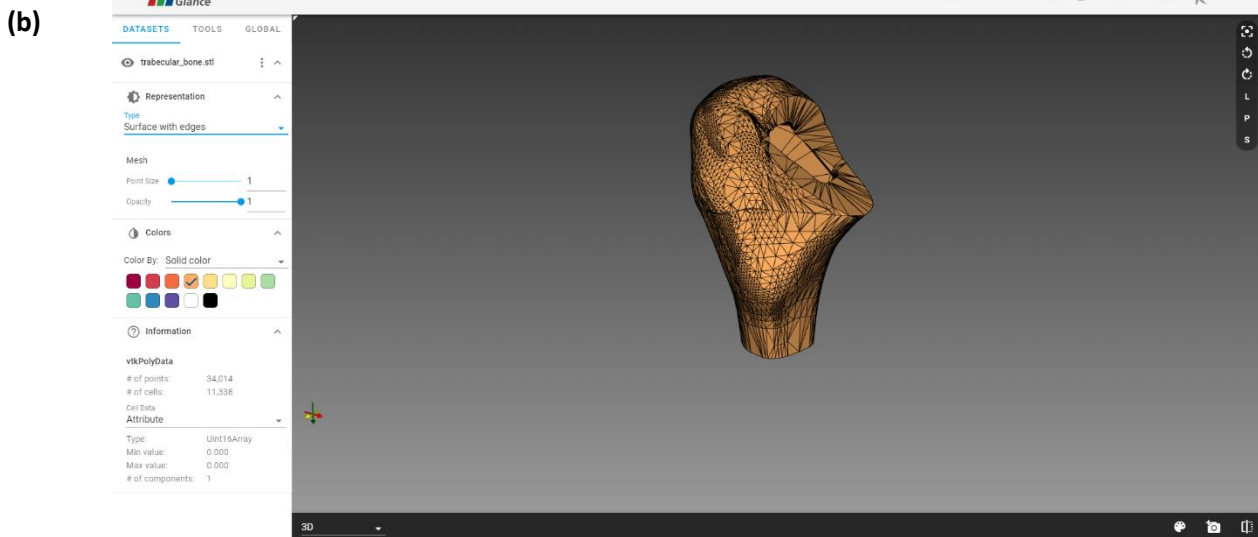
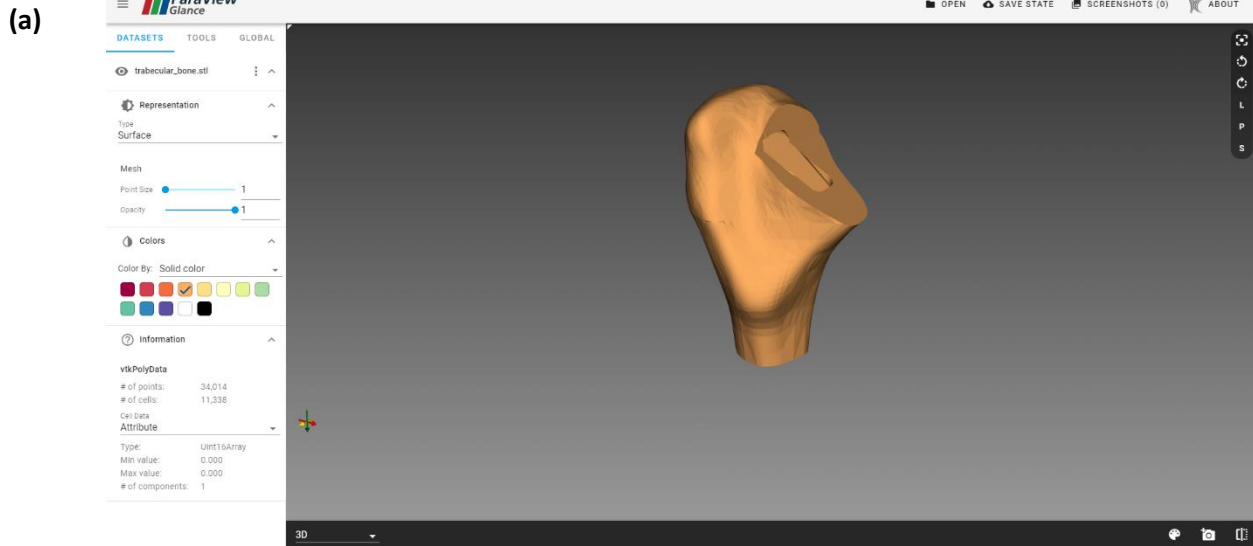
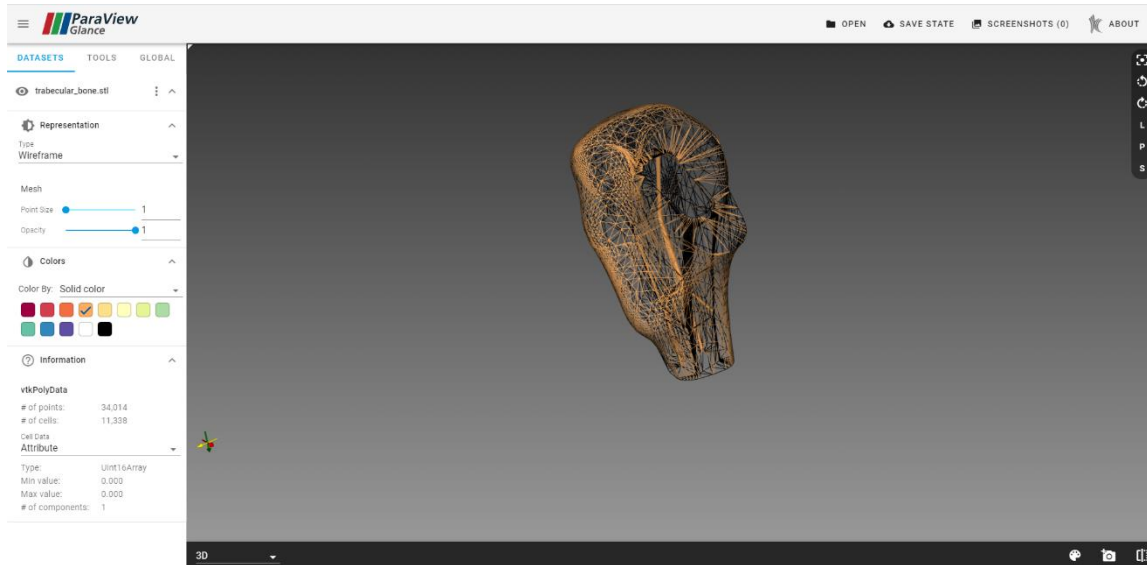


Figure 15. The Datasets tab and its options.

As an example, Figure 16 shows the graphical-user interface (GUI) of ParaView, where the trabecular bone tissue is shown in orange color for a surface type representation (Fig. 16a), for a surface with edges representation (Fig. 16b), for a wireframe representation (Fig. 16c) and for a points representation (Fig. 16d).



(c)



(d)

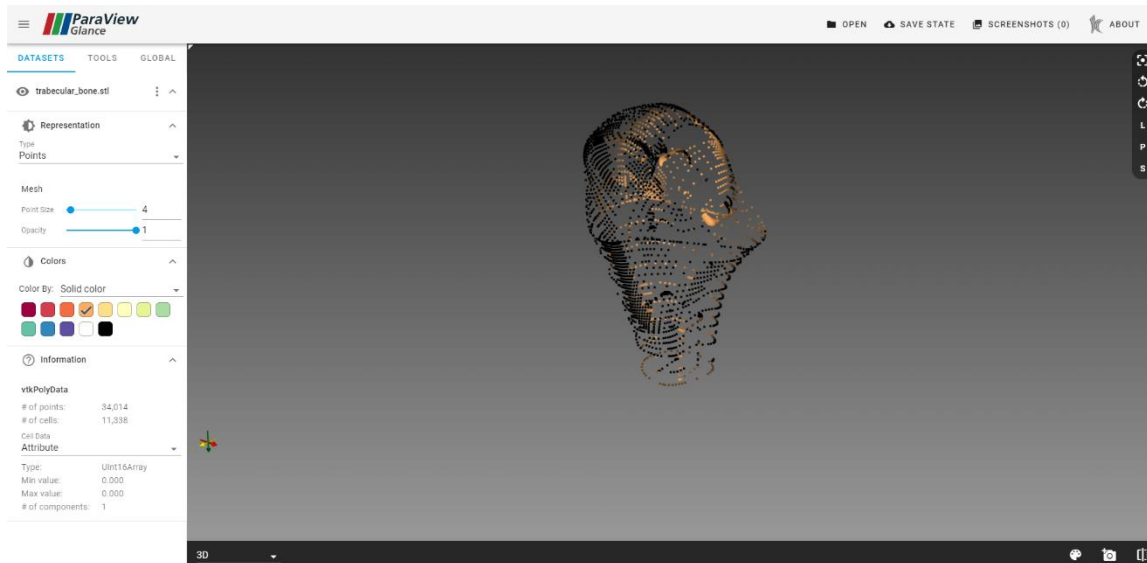


Figure 16. The GUI inside ParaView for the representation of trabecular bone in surface (a), surface with edges (b), wireframe (c) and points (d) type representation.

To rotate the object, press left mouse click and drag the mouse, while to zoom in and out press right mouse click and drag the mouse. Finally, several other useful options may be found in the lower right side of the geometry window (highlighted in Figure 17), where the user can change the color of the background, take a screenshot and split the geometry window into two or four windows as shown in Fig. 17a and Fig. 17b, respectively. The dataset is created using Solidworks², 3D slicer³ and Spaceclaim Ansys⁴, while more details in this area can be found in work of Gkaintes et al.⁵

² Solidworks (Dassault Systèmes): <https://www.solidworks.com/>

³ 3D Slicer image computing platform: <https://www.slicer.org/>

⁴ Spaceclaim Ansys, Pittsburgh, Pennsylvania, U.S.A: <https://www.ansys.com/>

⁵ Gkaintes, O. A., Potsika, V. T., Loukas, V. S., Gkiatas, I., Pakos, E., & Fotiadis, D. I. (2022). Computational modelling of Human Femur after Total Hip Arthroplasty. 44th Annual International Conference of the IEEE Engineering in Medicine & Biology Society (EMBC) (pp. 3947-3950). IEEE

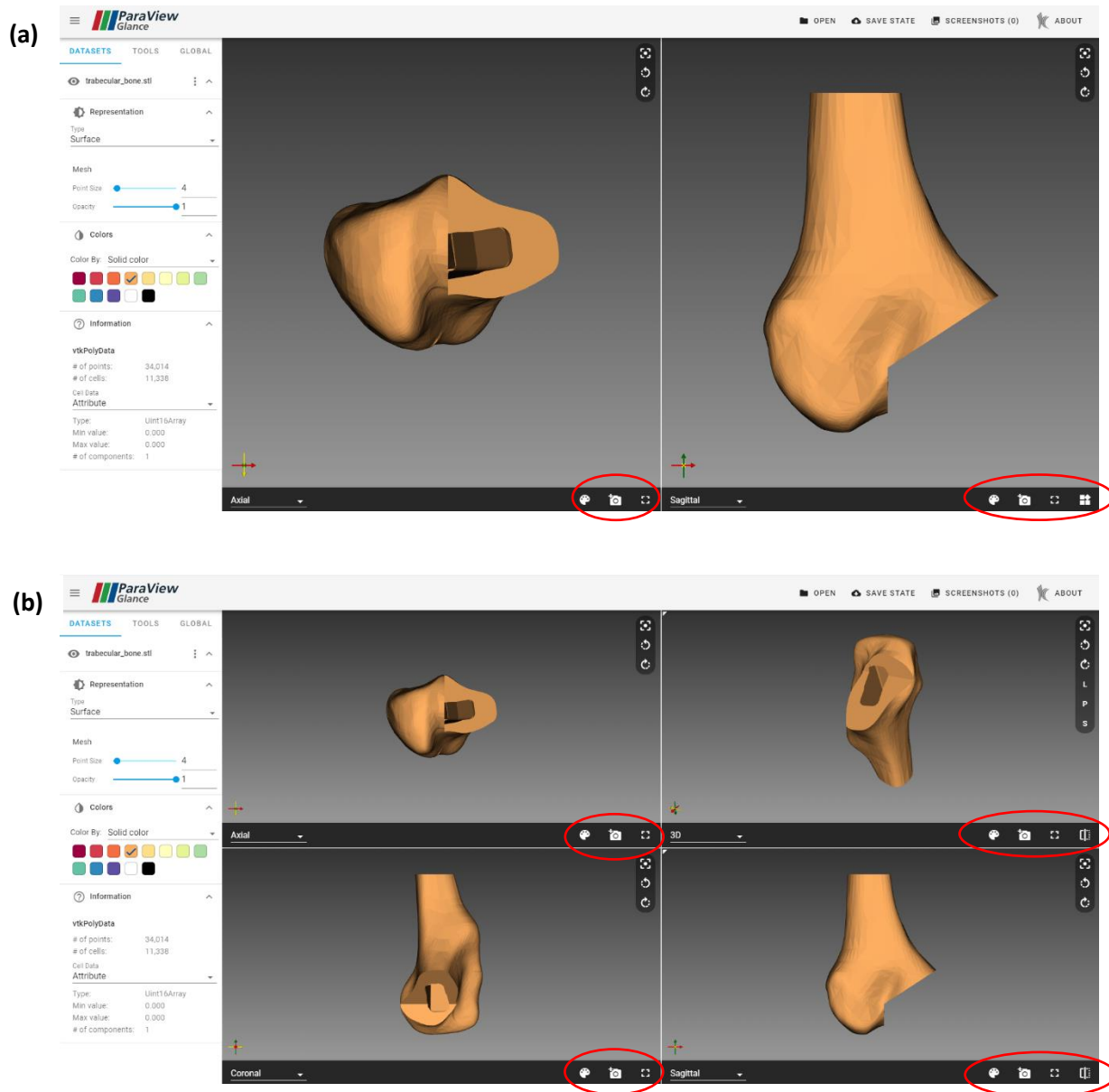


Figure 17. The GUI inside ParaView while in two-split window (a) and four-split window mode (b).

6.3 Dataset – Stenosis cases; Responsible partner - UOI

Dataset - Stenosis cases	Responsible partner - UOI
--------------------------	---------------------------

The Stenosis cases dataset can be accessed by the end user through the Cardiovascular disease modeling module, which lies on the main dashboard of the SGABU platform, as presented in the following Figure 18.

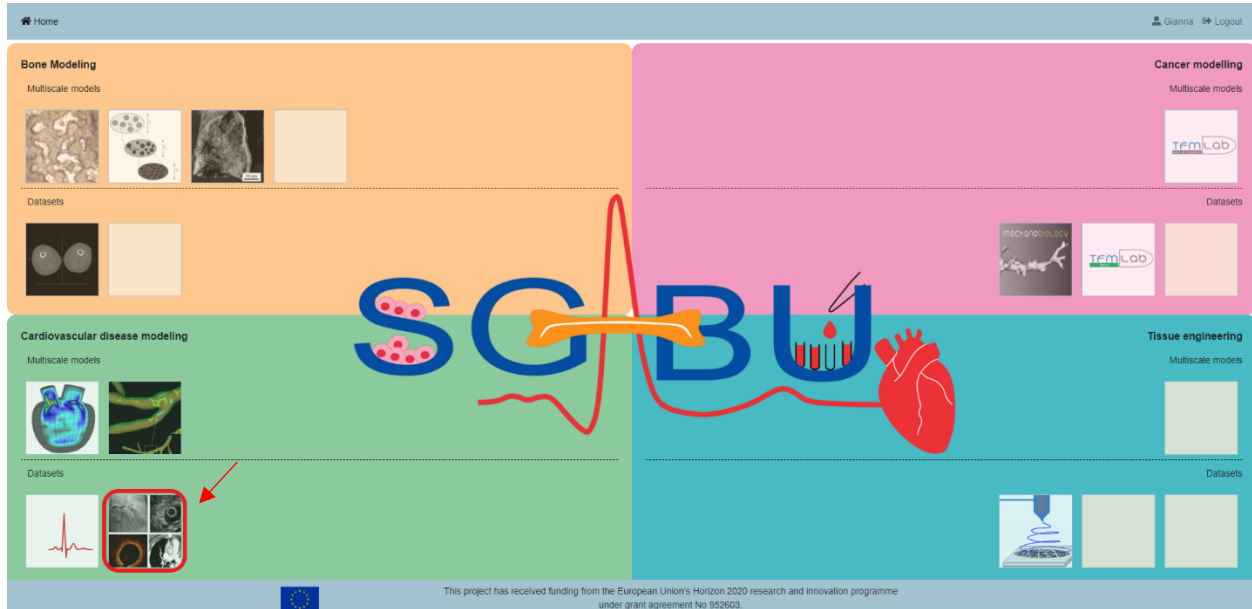


Figure 18. Main platform dashboard.

The dataset contains three (3) arterial cases with different degree of stenosis (DS), one with 2% DS (Figure 19), one with 79% DS (Figure 20) and one bifurcated segment with 80% DS (Figure 21). There are also other metrics which are represented on this field of the platform for each case. These metrics are the total vessel length (mm), the lesion vessel length (mm) which represents the stenosis area in the artery, the reference vessel diameter (RVD) (mm), the minimum lumen diameter (MLD) (mm) of the vessel and the percentage diameter stenosis.

D6.3 - Materials for teaching and learning purposes



Home Gianna Logout

Stenosis Cases ?

ARTERY WITH 2% STENOSIS ARTERY WITH 79% STENOSIS ARTERY WITH BIFURCATION

Vessel length (mm)	RVD (mm)	Lesion length (mm)	MLD (mm)	Percentage diameter stenosis
24	2.22	12	2.18	2

Translated Ring 1 Translated Ring 2 Translated Rotated Inset Translated Rotated Outer

This project has received funding from the European Union's Horizon 2020 research and innovation programme under grant agreement No 952603.

Figure 19. An Artery with 2% DS on the platform.

Home Gianna Logout

Stenosis Cases ?

ARTERY WITH 2% STENOSIS ARTERY WITH 79% STENOSIS ARTERY WITH BIFURCATION

Vessel length (mm)	RVD (mm)	Lesion length (mm)	MLD (mm)	Percentage diameter stenosis
84.08	3	45	0.63	79

Translated Ring 1 Translated Ring 2 Translated Rotated Inset Translated Rotated Outer

This project has received funding from the European Union's Horizon 2020 research and innovation programme under grant agreement No 952603.

Figure 20. An Artery with 79% DS on the platform.

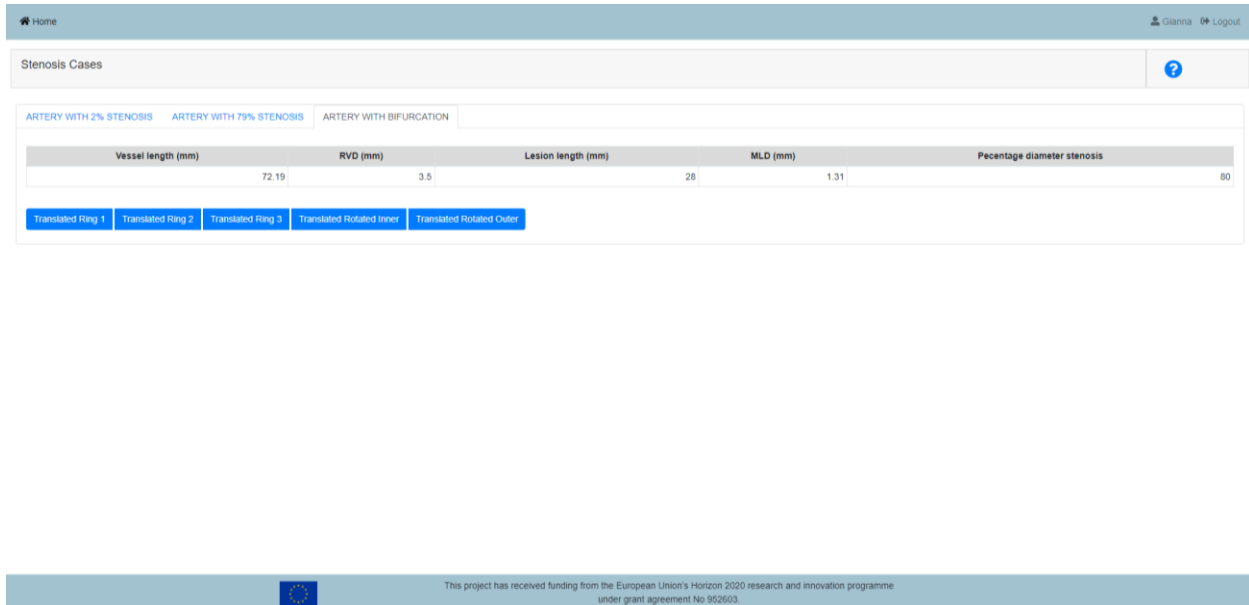


Figure 21. A Bifurcated Artery with 80% DS on the platform.

Apart from the metrics, the user can select the 3D arterial models for each case, i.e. the translated rings 1, 2 or 3 and the translated rotated inner and outer surfaces (Figure 22).

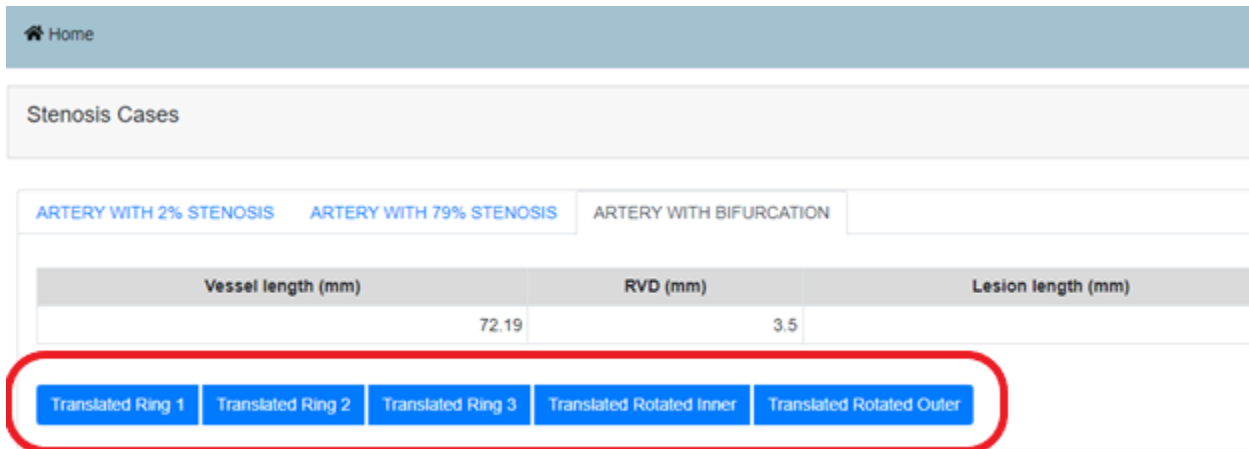


Figure 22. The (translated) surfaces of inner, outer and vessel rings.

**The Translation means that the artery geometry is positioned to have the “target” point at the origin of the general reference system (coordinates 0,0,0) and the Z axis target to the centerline indicating the flow direction.*

By clicking on each translated geometry, a new pop-up window will be launched, redirecting to the ParaView Glance, an open-source web visualizer, in which each segment is represented, and the user is able to select and process the datasets, the tools or the global settings (Figures 23, 24).

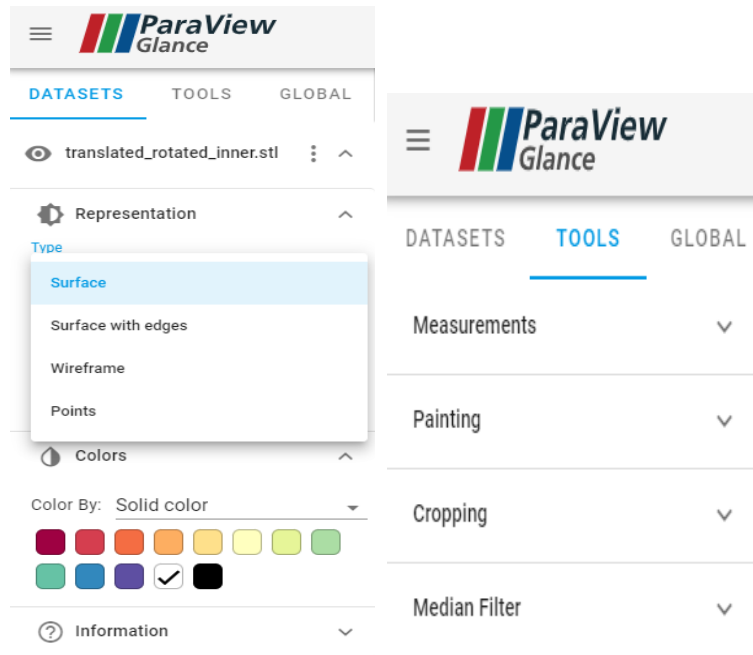


Figure 23. ParaView settings for the datasets (a) and the tools (b).

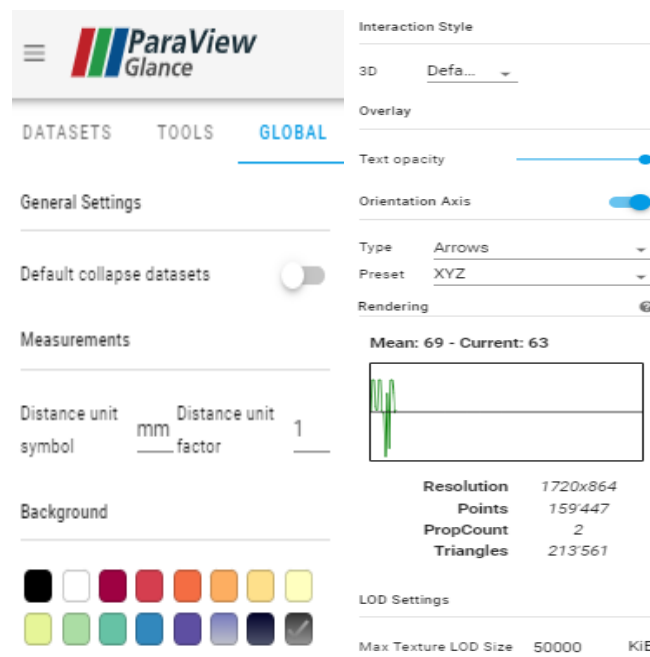


Figure 24. ParaView global settings.

The user is able to choose the type of the vessel’s representation such as surface, surface with edges, wireframes or points (Figure 23), change the mesh (points size, opacity), the color of the 3D model or the background and many other useful choices. In the next figures, the same artery is represented as (i) a surface without any change in the mesh (Figure 25), (ii) points without any change in the mesh (Figure 26) and (iii) points with specific point size and opacity on the mesh (Figure 27). Comparing these options, it is useful for the user to understand better the geometry and process many different parameters.

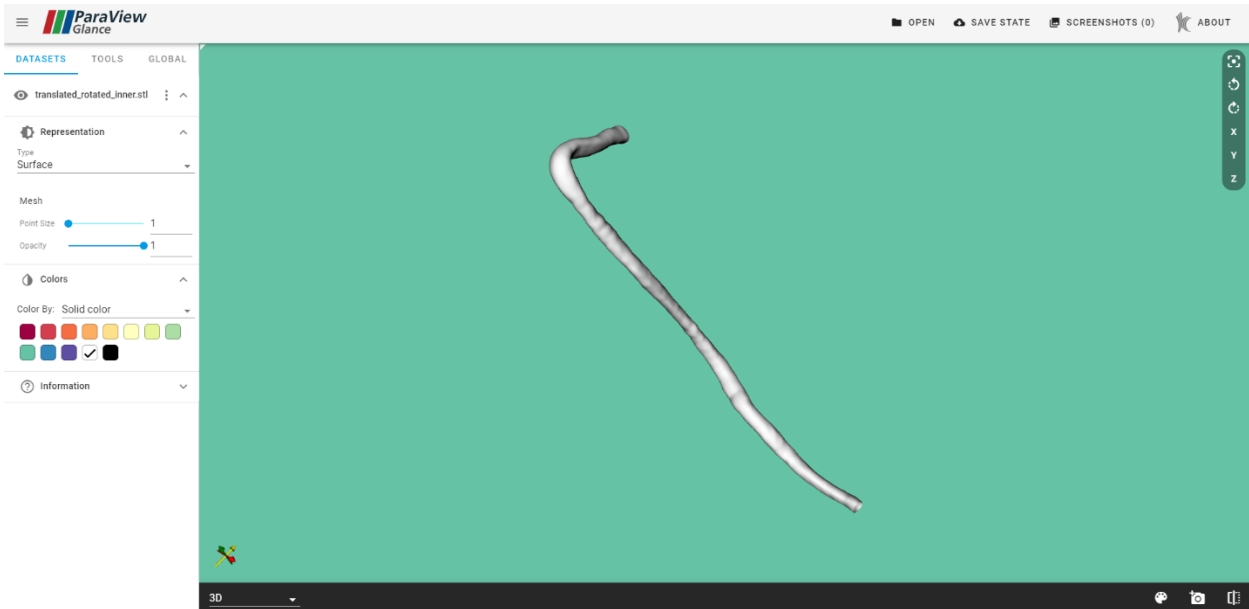


Figure 25. An artery representation as a surface without any change in the mesh.

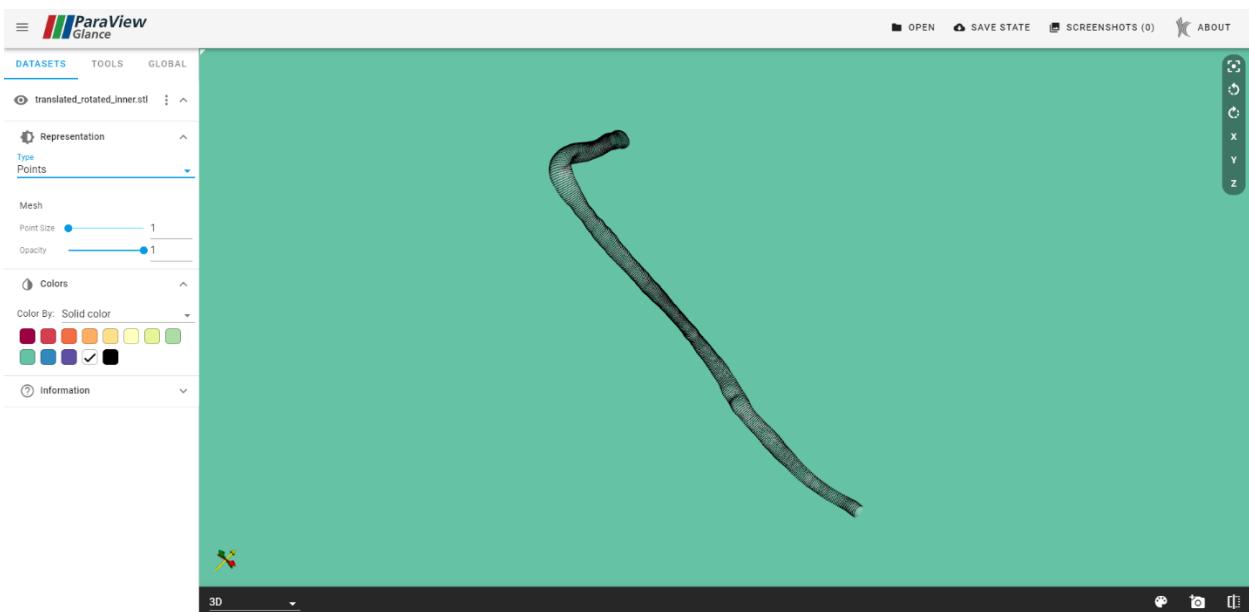


Figure 26. An artery representation as points without any change in the mesh.

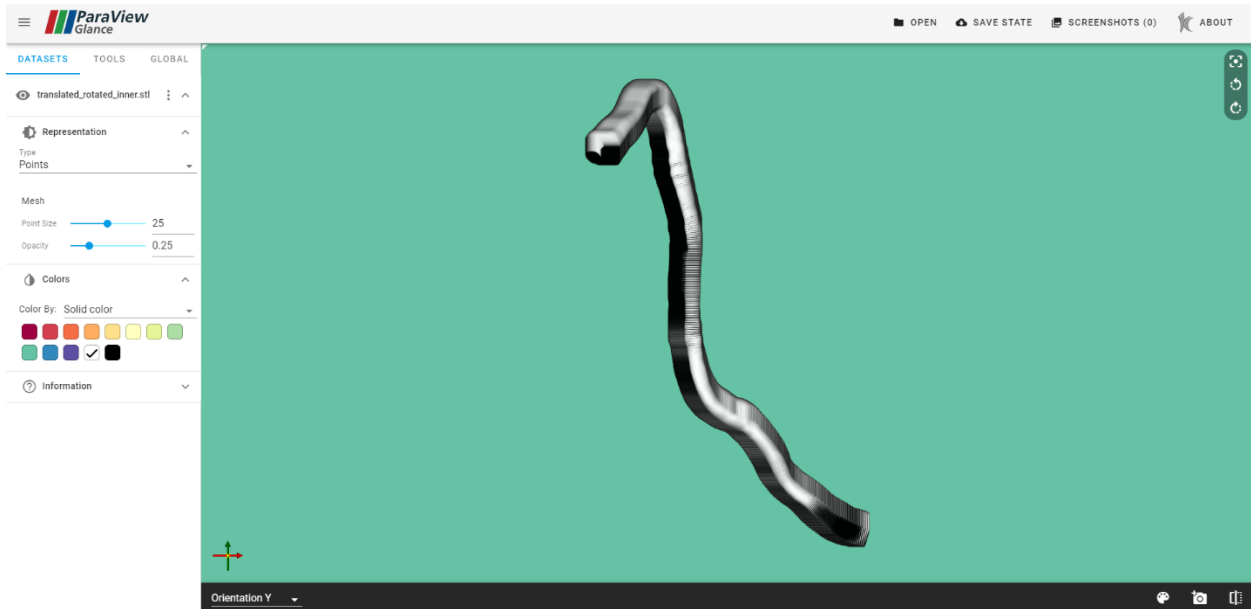


Figure 27. An artery representation as points with changes in the mesh (points size and opacity).

Another useful section for the user is that he/she can process and split the view of the geometry of artery (Figure 28) or for the ring (Figure 29), by choosing the 3D segment or different orientations X, Y, Z in order to study the artery in a great extent, by clicking on the last button on the right side of bottom page (Figure 30).

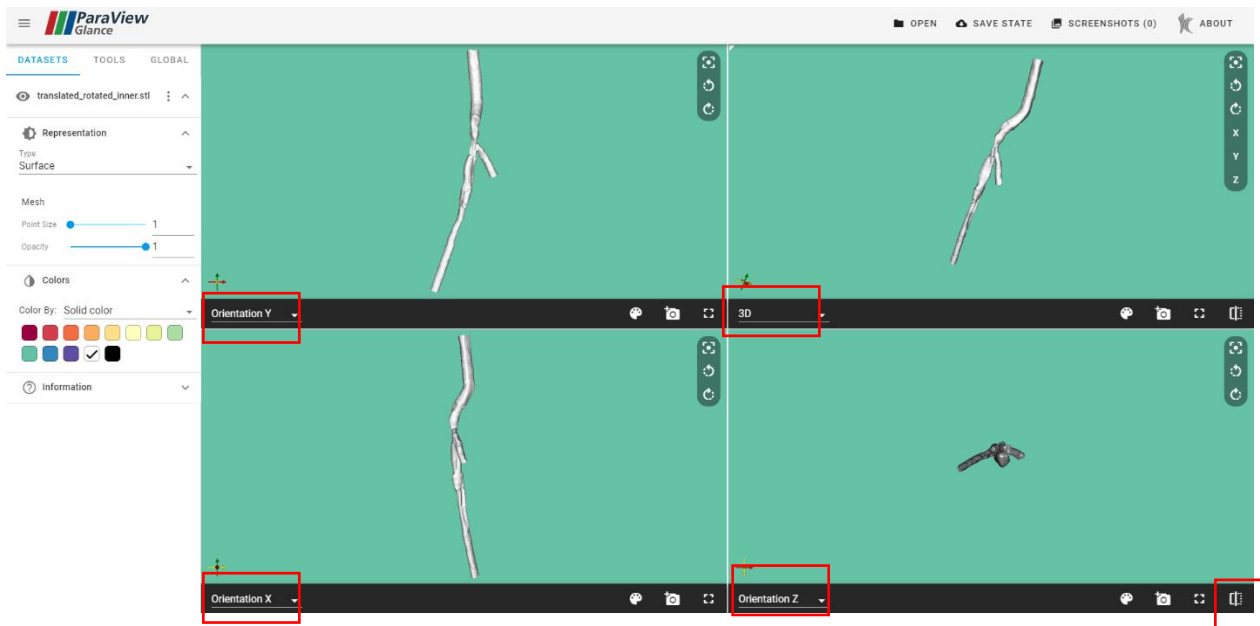


Figure 28. A splitted view of the geometry of the artery.

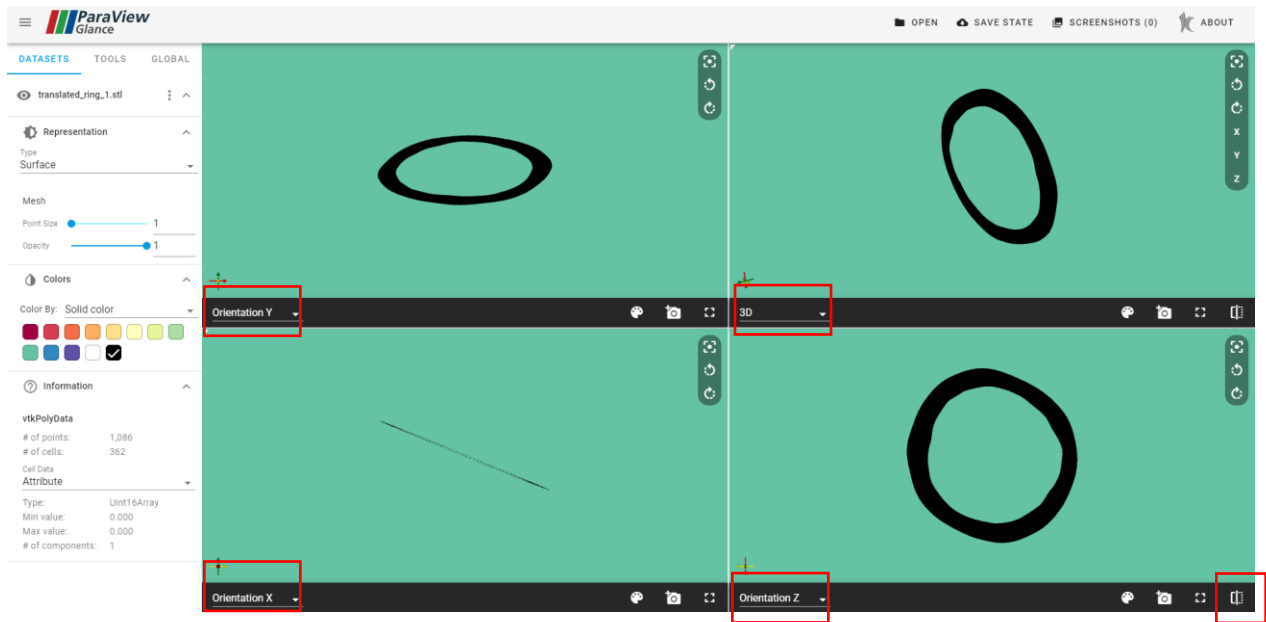


Figure 29. A splitted view of the geometry of the ring.

Furthermore, the user can save the whole process, or take some screenshots of the models, or open and upload any other file, by clicking in the upper buttons of the screen (Figure 30).

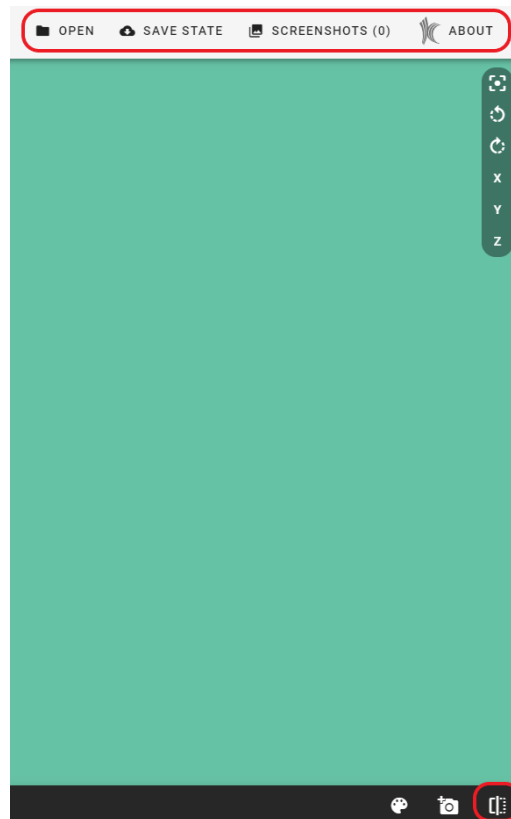


Figure 30. The buttons for split view and for screenshots, save or upload a file and other information.

6.4 Dataset – Oral cancer; Responsible partner - UOI

Dataset – Oral cancer	Responsible partner - UOI
------------------------------	----------------------------------

The oral cancer dataset can be accessed through the Cancer modeling module⁶, which resides in the main dashboard of the SGABU platform, as presented in the Figure 31.

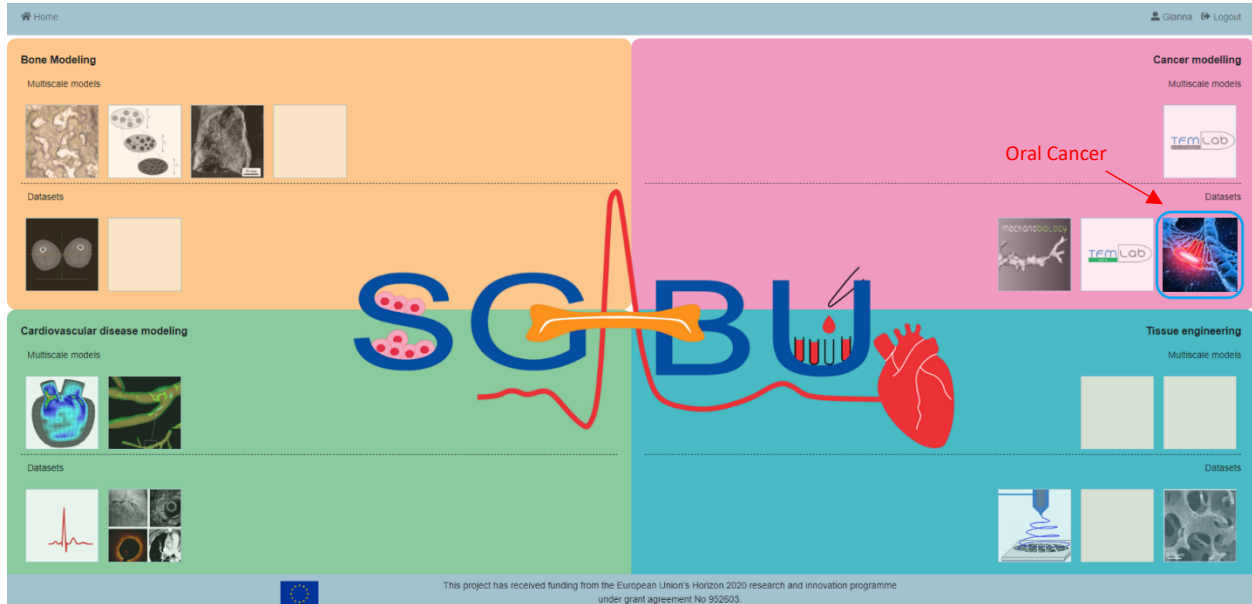


Figure 31. Main platform dashboard.

The dataset for Oral cancer contains four (4) .csv files that provide information about the blood and tissue genes of each patient (BloodGenomic_September2011 and TissueGenomic_September2011 files), the different timepoints for the genes of each patient (PRE_02_09_2011 file) and the information about the imaging that was used (Imaging_September2011 file). These all files can be downloaded easily, by clicking on the download button in the blue box on the right side of the screen (Figure 32).

⁶ Exarchos, K. P., Goletsis, Y., & Fotiadis, D. I. (2012). A multiscale and multiparametric approach for modeling the progression of oral cancer. *BMC medical informatics and decision making*, 12(1), 1-14.

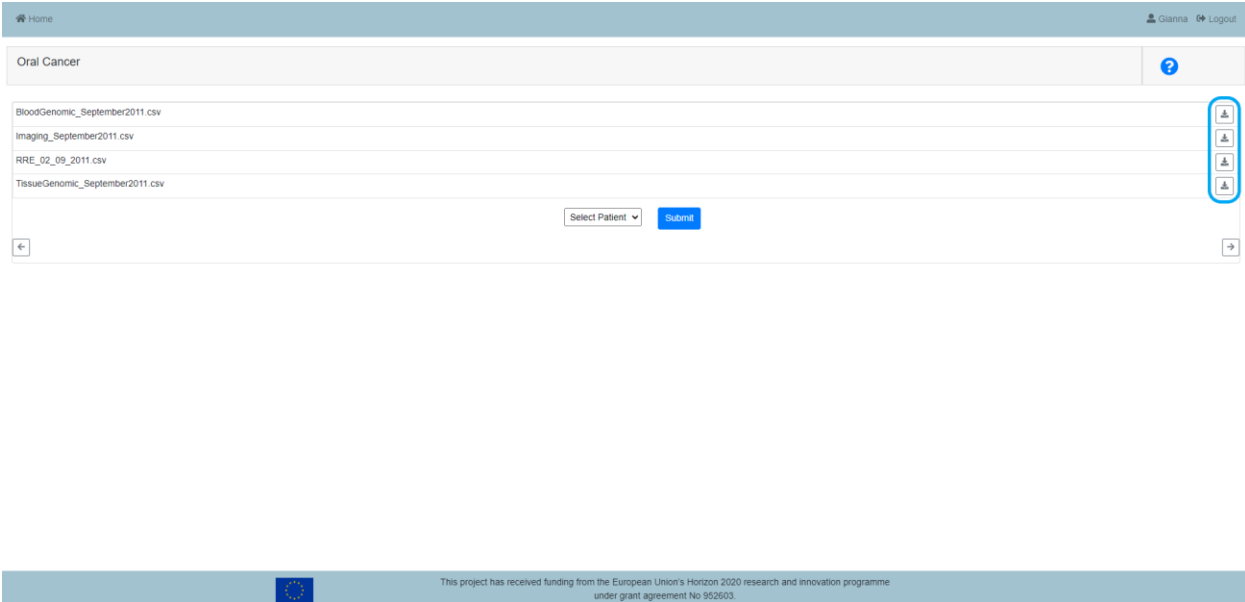


Figure 32. The genes information for all the patients.

The user can also select a specific patient id he/she prefers and click on the Submit button in order to acquire all the main clinical information for this patient (Figure 33).

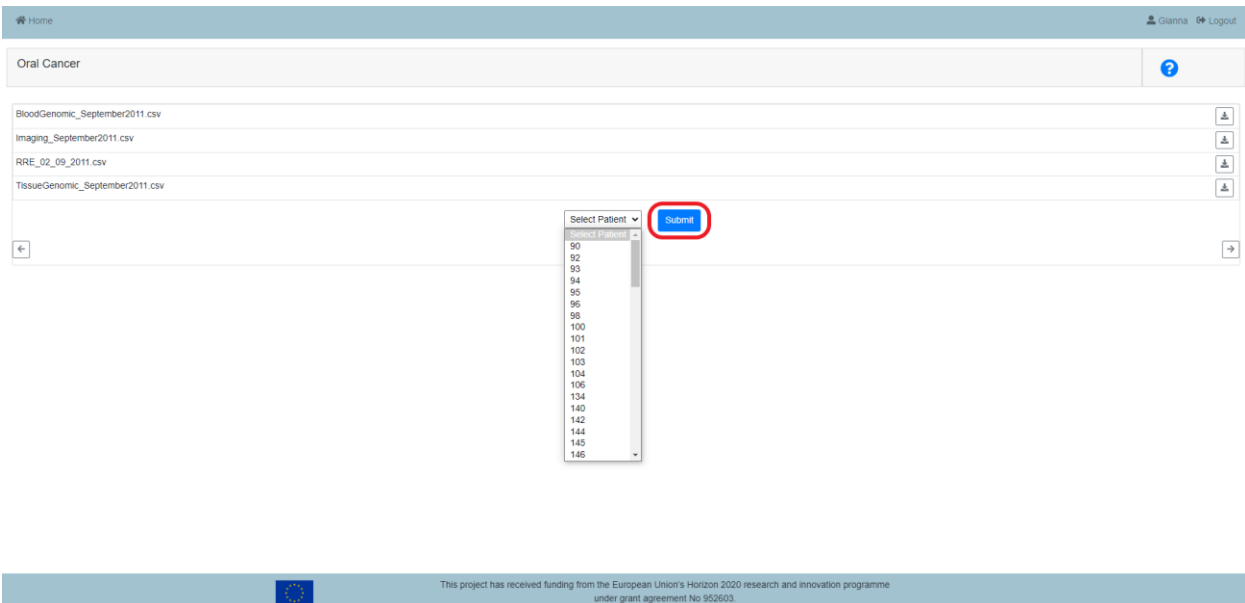
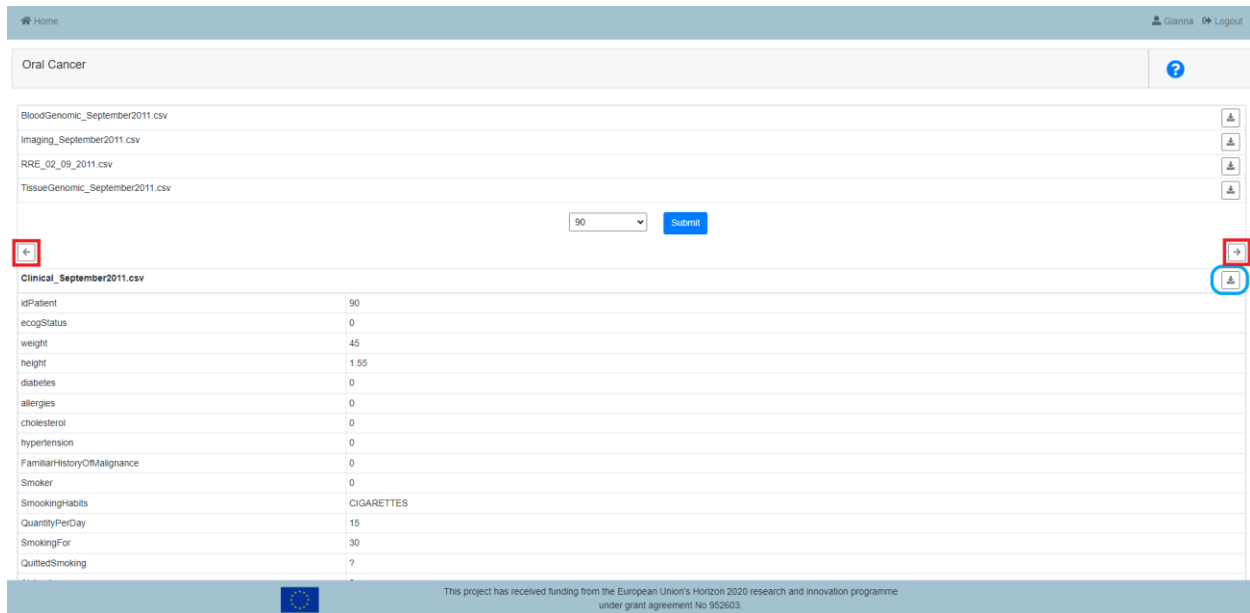


Figure 33. The patient’s id selection in the platform for the clinical information.

This information can be downloaded also in a .csv file format containing all the clinical information and the clinical characteristics for the specific patient by clicking the button in the blue box. There is also the capability to select the previous or the next patient by clicking the buttons in the red boxes (without choosing and submitting the patient’s id each time) (Figure 34).



Clinical_September2011.csv	
idPatient	90
ecogStatus	0
weight	45
height	1.55
diabetes	0
allergies	0
cholesterol	0
hypertension	0
FamiliarHistoryOfMalignance	0
Smoker	0
SmokingHabits	CIGARETTES
QuantityPerDay	15
SmokingFor	30
QuitiedSmoking	?

Figure 34. Selection of previous/next patient's id and download the clinical information.

The main clinical information for each patient can be visualized by the user, as it is depicted in the following figure (Figure 35) and more detailed information is provided in the “Clinical_September2011.csv” file for all the patients.

Clinical_September2011.csv	
idPatient	90
ecogStatus	0
weight	45
height	1.55
diabetes	0
allergies	0
cholesterol	0
hypertension	0
FamiliarHistoryOfMalignance	0
Smoker	0
SmokingHabit	CIGARETTES
QuantityPerDay	15
SmokingFor	30
QuittedSmoking	7
Alcohol	0
DrinkingHabit	7
MechanicalTrauma	0
DentalCusps	0
GalvanicCurrent	0
OralHygiene	ADEQUATE
Infection	0
TypeOfInfection	7
PhysicalAgents	0
TypeOfPhysicalAgent	7
DietDeficit	0
Fe_HaematicConcentration	7
PlummerVinson	0
Hb_HaematicConcentration	7
B12_VitaminHaematicConcentration	7
A_VitaminHaematicConcentration	7
E_VitaminHaematicConcentration	7
Foat	7
EatingHabit	NORMAL
BMI	18.7
SubstanceExposition	NO
PreneoplasticLesions	NO
ImmunosuppressionTreatments_Presence	0
ImmunDuration	7
ImmunType	7
TumorMaximumDiameter	35
max(pathologicdata_TumorThickness)	10
DepthOfInvasion	10
BasaloidFeatures	0
LymphoplasmacyticReaction	MILD
LymphovascularInvasion	1
PerineuralInvasion	1
DegreeOfCellularAtypia	HIGH
NuclearPleomorphism	MARKED
NumberOfMitosesPer10HPF	92
GradeOfDifferentiation	G3
SurgicalMargins	0
MarinecGimenoScore	7
AnerotheloidScore	7
DD_40Stain	7
P53_Stain	0
P16ink4Stain	0
EGFRStain	0
Cy5bO1Stain	7
K12Stain	60
HPV_DNA	1
TStaging	T2
NStaging	N1
MStaging	M0
	no_reoccurrence

Figure 35. The main clinical information for each patient in the platform.

6.5 Dataset – Mechanobiology; Responsible partner - KUL

Dataset - Mechanobiology	Responsible partner - KUL
---------------------------------	----------------------------------

The access to the *Mechanobiology* module^{7,8} on the SGABU platform is provided through the main dashboard as presented in the Figure 36.

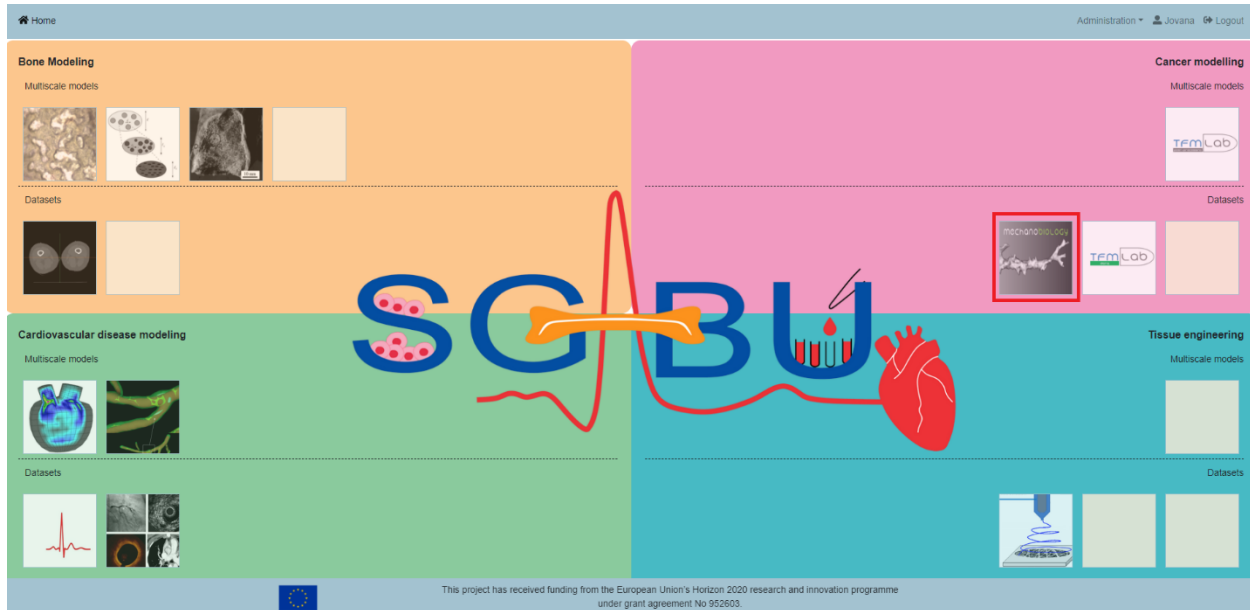


Figure 36. Main platform dashboard.

After clicking the respective icon, a new window appears (Figure 37). The user will see a panel with two tabs (labelled as 'Relaxed' and 'Stressed') and 4 images in each tab. These data correspond to a classical Traction Force Microscopy (TFM) experiment. In this experiment, cells cultured in vitro within a PEG hydrogel that contains fluorescent beads are imaged by means of confocal microscopy before and after the addition of mechanical inhibition. Since cells need to exert forces to migrate, they deform the surrounding hydrogel causing movements on the beads. TFM quantifies the movements of these beads and through constitutive equations recovers the cell forces. In SGABU, we provide a dataset that would allow for the computation of 3D cell forces around a growing angiogenic sprout. Both 'Relaxed' and 'Stressed' tabs show the same type of data:

- The first image on the **top left** shows a monolayer of Human Umbilical Vein Endothelial Cells (HUVECs) tagged with LifeAct-GFP. These cells are forming an angiogenic sprout that can be seen

⁷ J. Barrasa-Fano, A. Shapeti, Á. Jorge-Peñas, M. Barzegari, J. A. Sanz-Herrera and H. V. Oosterwyck, "TFMLAB: A MATLAB toolbox for 4D traction force microscopy," *SoftwareX*, vol. 15, 2021., doi: <https://doi.org/10.1016/j.softx.2021.100723>

⁸ "A MATLAB toolbox for 4D traction force microscopy," [Online]. Available: https://gitlab.kuleuven.be/MATrix/Jorge/tfmlab_public

in the center of the image. The user can scroll through the 90 z-slices of the confocal stack using the slider below the image.

- The second image on the **top right** shows the florescent beads present in the PEG hydrogel.
- The third image on the **bottom left** shows the bright field signal from the microscope. This is typically not used for TFM but it can be useful for the user to have a general view of the structures present in the image.
- The fourth image on the **bottom right** shows the nuclei of the cells. This signal corresponds to a Hoechst stain of the cells' DNA. This information is particularly useful to know how many cells are present in the image.

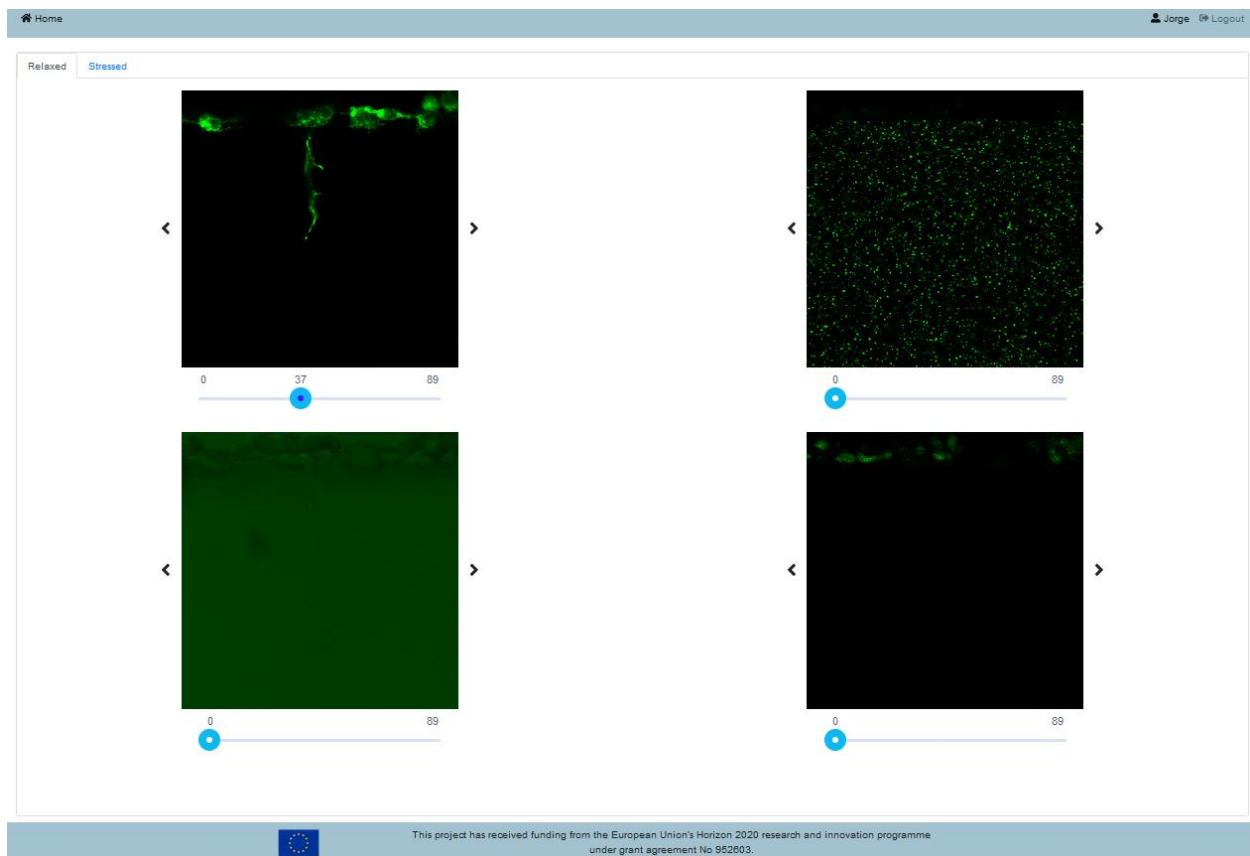


Figure 37. Data visualization in SGABU platform.

6.6 Dataset – TFMLAB data; Responsible partner - KUL

Dataset - TFMLAB data	Responsible partner - KUL
------------------------------	----------------------------------

The access to the TFMLAB data module on the SGABU platform is provided through the main dashboard as presented in the Figure 38.

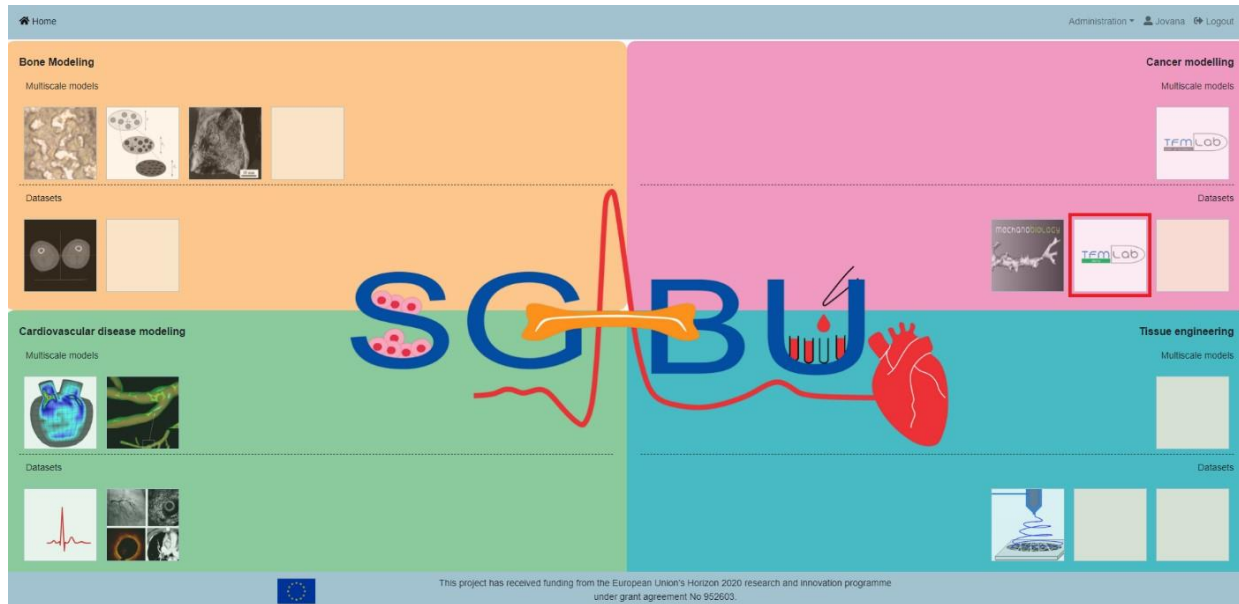


Figure 38. Main platform dashboard.

After clicking the respective icon, a new window showing different kinds of data appears. The data here shown correspond to raw and processed data from a 3D TFM experiment. In this experiment, cells cultured in vitro within a PEG hydrogel that contains fluorescent beads are imaged by means of confocal microscopy before and after the addition of mechanical inhibition. Since cells need to exert forces to migrate, they deform the surrounding hydrogel causing movements on the beads. TFM quantifies the movements of these beads and through constitutive equations recovers the cell forces. In SGABU, we provide a dataset showing all the intermediate steps that are needed to get to a measurement of the force-induced matrix displacements. The window has 4 different tabs that are reviewed below:

- **Raw images tab** (see Figure 39): this is the raw data that is needed for the TFM experiment. In this platform, we show only the data corresponding to the stressed state. Within these raw images (the user can scroll through the 90 z-slices of the confocal stack using the slider below the image) there are:
 1. Beads: shows the fluorescent beads present in the PEG hydrogel.
 2. Cell: shows a monolayer of HUVECs tagged with LifeAct-GFP. These cells are forming an angiogenic sprout that can be seen in the center of the image.
 3. Nuclei: shows the nuclei of the cells. This signal corresponds to a Hoechst stain of the cells' DNA. This information is particularly useful to know how many cells are present in the image.

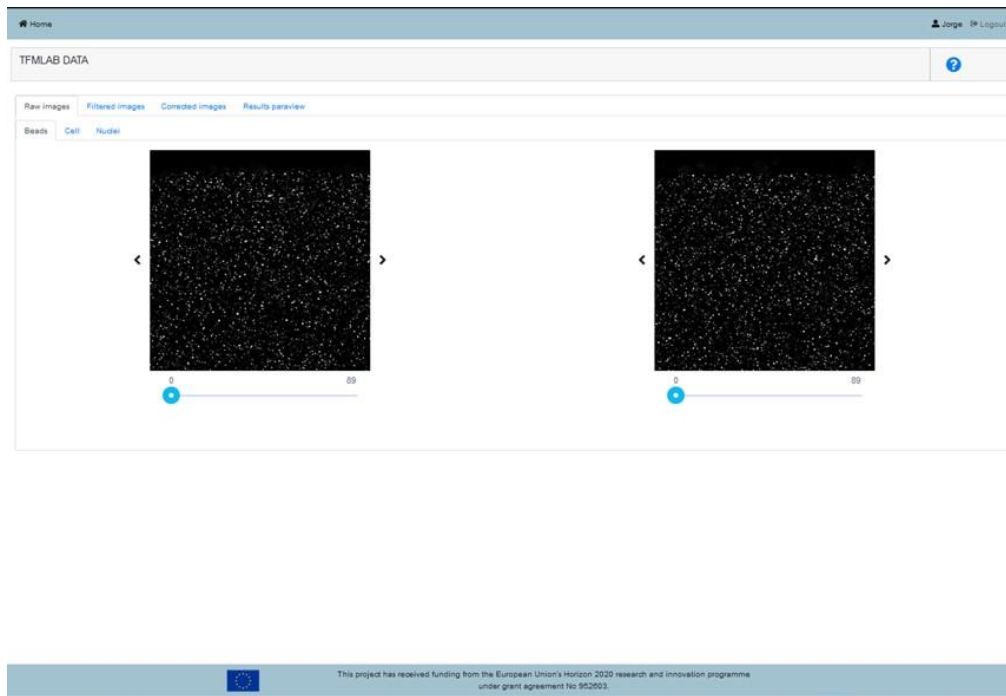


Figure 39. Raw images tab.

- **Filtered images tab** (see Figure 40): since raw microscopy files usually contain some noise, some filters are required. TFMLAB is a toolbox that offers all the necessary computational tools to process these images (link to the Gitlab repository and manual: https://gitlab.kuleuven.be/MAtrix/Jorge/tfmlab_public), more info on TFMLAB can be found in references^{7,8}. In SGABU we provide the intermediate results after applying these filters and operations. The user can see the raw image on the left and the processed image on the right. Typically, the noise is suppressed and the contrast is enhanced for all three channels (beads, cell, and nuclei).

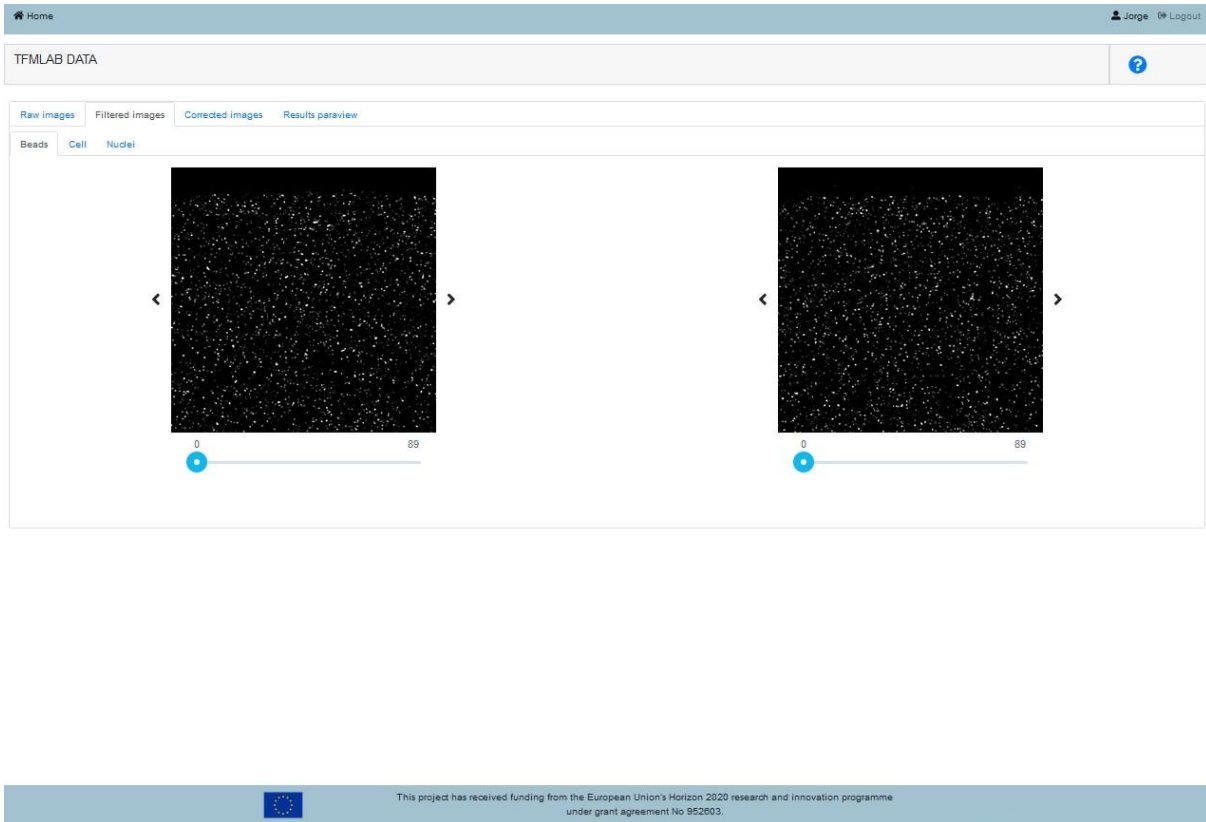


Figure 40. Filtered images tab.

- **Corrected images tab** (see Figure 41): shifts caused by the microscope stage have to be removed in order to only preserve the cell-induced matrix displacements. By applying for phasecorrelation-based rigid image registration, these effects are corrected. This tab shows the images (of all the channels) before (left) and after (right) correction. Moreover, a new channel is shown: Cell Seg. This is obtained by means of thresholding the cell channel. The cell segmentation is used for the following step of TFM.

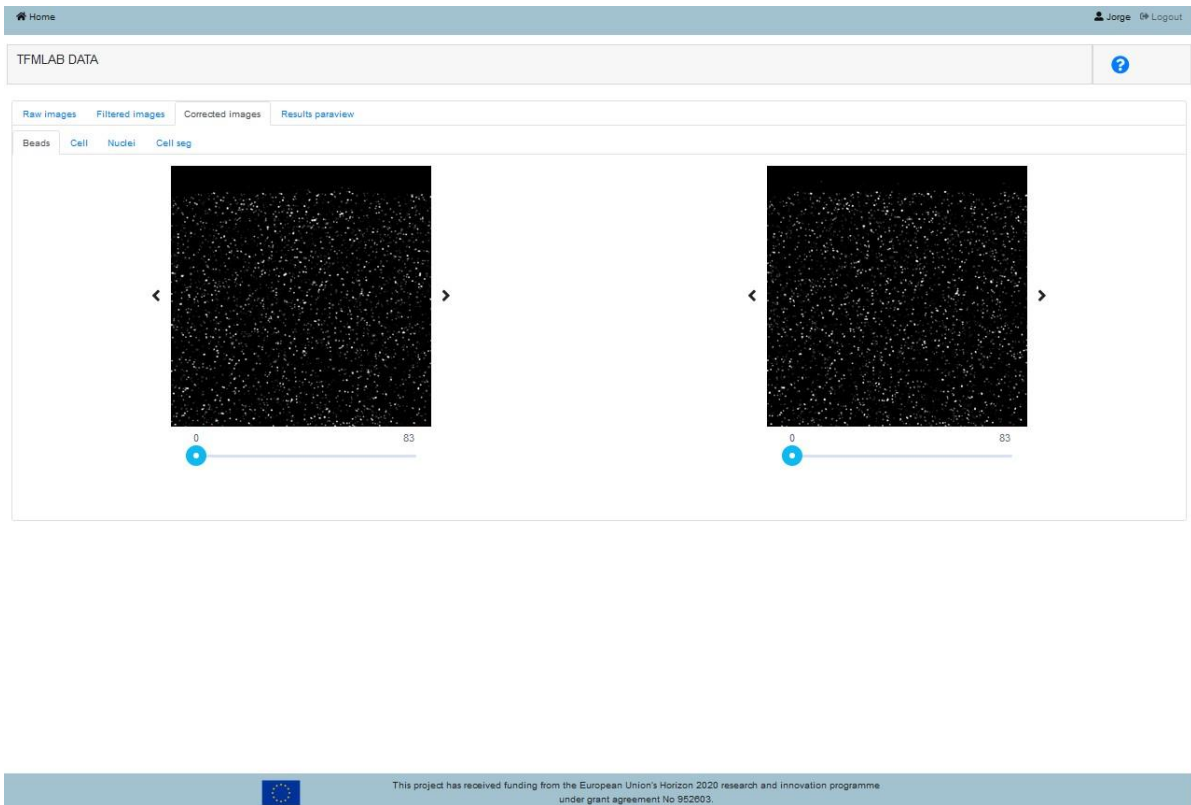


Figure 41. Corrected images tab.

- **Results ParaView tab** (see Figure 42 and Figure 43): the measured displacement field together with the cell segmentation can be seen in a 3D render provided by ParaView. First, click on the blue button “ParaView” (see Figure 42) and you will be directed to ParaView Glance – an online visualizer of ParaView (see Figure 43). The user can tune the way the results are plotted. There are two items in the render: the cell segmentation (in white) and the 3D displacement field (depicted by magnitude-colored arrows). The user can use the left-click of the mouse to rotate the sample and the mouse wheel to zoom in and out. The top tool bar can be used to save the current settings or take a screenshot of the render.



Figure 42. Results: ParaView tab.

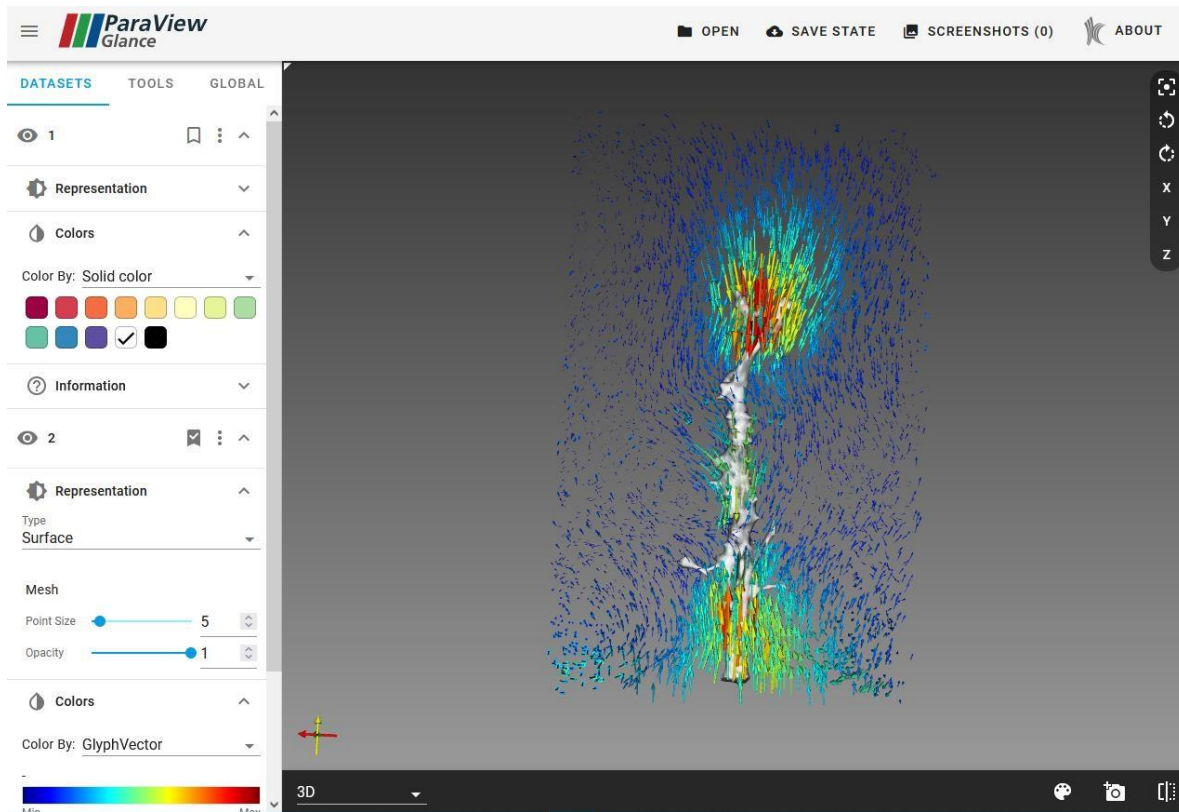


Figure 43. Results shown in ParaView.

6.7 Dataset – LVAD; Responsible partner - COVU

Dataset - LVAD	Responsible partner - COVU
-----------------------	-----------------------------------

The access to the Left Ventricular Assist Device (LVAD) belongs to the Cardiovascular disease modeling module⁹, on the SGABU platform is provided through the main dashboard as presented in Figure 44. LVAD is a type of mechanical pump that helps the left ventricle. This pump can't replace heart, but it increases function of sending blood to other body parts.

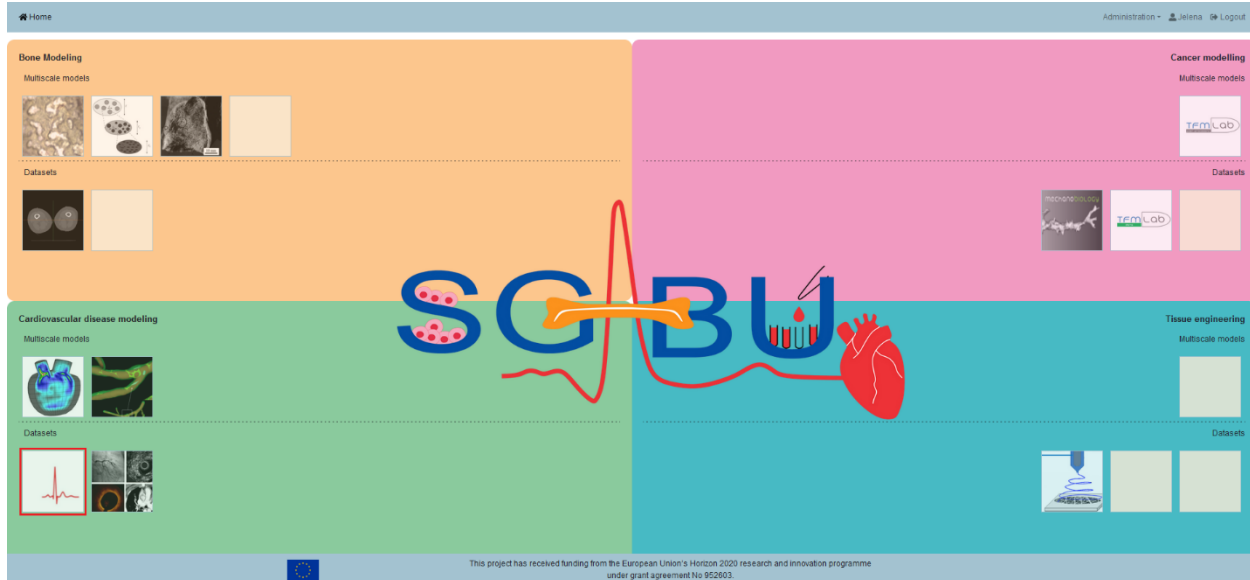


Figure 44. Main platform dashboard.

The importance of LVAD for a life of difficult patient has been studied in research and whether patients can achieve their results as healthy people by using LVAD and after its use combined with medical therapy. Figure 45 shows spreadsheet of Clinical Characteristics of Studied Population, only male patients were included in researching. Number of heart transplant candidates is 24, 18 men with implanted LVAD, LVAD was explanted in 16 patients and at the end healthy controls in 94 men. Criteria for selection of candidates were ability to solve test on a treadmill, exercises above the anaerobic threshold, symptomatic exercises and consent form.

⁹ Jakovljević, Đ. G., Yacoub, M. H., Schueler, S., MacGowan, G. A., Velicki, L., Seferovic, P. M., . . . Tan, L.-B. (2017). Left Ventricular Assist Device as a Bridge to Recovery for Patients With Advanced Heart Failure. *JOURNAL OF THE AMERICAN COLLEGE OF CARDIOLOGY*, 69(15), 1924-1933. doi:<https://doi.org/10.1016/j.jacc.2017.02.018>

Home

Left Ventricular Assist Device

Data Plot 1 Plot 2 Plot 3 Plot 4

TABLE 1: Clinical Characteristics of Studied Population

	Heart Transplant Candidates (n = 24)	LVAD Implanted (n = 18)	LVAD Explanted (n = 16)	Healthy Controls (n = 97)
Male/female	24/0	18/0	16/0	97/0
Age, yrs	46.50 ± 12.47	39.33 ± 13.03	40.94 ± 13.46	43.73 ± 18.08
Height, m	1.76 ± 0.08	1.78 ± 0.06	1.79 ± 0.07	1.77 ± 0.07
Body weight, kg	78.90 ± 11.50	79.30 ± 14.40	85.40 ± 13.20	81.10 ± 1.06
Body mass index, kg/m ²	25.60 ± 3.80	25.10 ± 4.10	26.70 ± 4.00	26.00 ± 3.10
Body surface area, m ²	1.94 ± 0.16	1.96 ± 0.17	2.04 ± 0.17	1.98 ± 0.15
Left ventricular ejection fraction, %	19.80 ± 8.3*	50 ± 8	58 ± 14	63 ± 12
Etiology of heart failure				
Idiopathic dilated cardiomyopathy	16	16	15	–
Coronary heart disease	8	2	1	–
Medical therapy				
Diuretic agents	24 (100)	16 (89)	–	–
Aldosterone antagonists	–	–	–	–
ACE inhibitors	9 (38)	13 (72)	12 (75)	–
Angiotensin II antagonists	12 (50)	3 (17)	6 (38)	–
Beta-blockers	16 (67)	15 (83)	13 (81)	–
Digoxin	15 (63)	11 (61)	13 (81)	–
Antiarrhythmic agents	5 (21)	4 (22)	6 (38)	–

Values are n, mean ± SD, or n (%). *p < 0.01 transplants vs. LVAD implanted, LVAD explanted, and controls.
ACE = angiotensin-converting enzyme, LVAD = left ventricular assist device

Figure 45. Clinical Characteristics of Studied Population.

For credible results, measurements during rest and maximum exercise were required. After main measuring weight and height, started test with loads. Measures arterial blood pressure and Innocor device was used with rebreathing system, additionally allowed estimation of cardiac output. One patients' group (heart transplant and LVAD implanted) performed a modified Bruce protocol, but second group (LVAD explanted patients and healthy controls) performed the Bruce protocol, heart rate and fatigue were measured. Figure 46 shows calculations and statistical analyses.

The cardiac power output was calculated by using the following form:

$$CPO = (QT \times MAP) \times K$$

where CPO is cardiac power output, QT is cardiac output in liters per min, MAP is mean arterial pressure in millimeters of mercury, and $K=2.22 \times 10^{-3}$ (the conversion factor). The second form is calculated form for mean arterial pressure:

$$SBP + 0.412 \times (SBP - DBP)$$

SBP is systolic blood pressure and DBP is diastolic blood pressure.

When the ratio between cardiac output and mean arterial pressure, multiplied by a factor 80, systemic vascular resistance was obtained. For testing differences between groups, a 1-way analysis of variance was used and to identify two groups with large differences a post hoc Tukey test was performed.

Home Administration SGABU Logout

TABLE 2: Resting and Peak Exercise Cardiac and Physical Function Variables in HTx, Implanted and Explanted LVAD Patients, and Healthy Controls

	Heart Transplant Candidates (n = 24)	LVAD Implanted (n = 18)	LVAD Explanted (n = 16)	Healthy Controls (n = 97)
Sitting rest				
Heart rate, beats/min	76.7 ± 19.7	72.6 ± 13.3	73.3 ± 6.2	65.7 ± 10.6
Stroke volume, ml	49.1 ± 12.3*	76.7 ± 17.0	71.1 ± 11.3	73.7 ± 18.0
Systolic BP, mm Hg	94.5 ± 17.5	95.3 ± 21.1	105.2 ± 15.8	123.3 ± 11.7
Diastolic BP, mm Hg	61.4 ± 10.3	63.3 ± 17.9	70.9 ± 12.7	76.3 ± 9.1
Mean arterial BP, mm Hg	74.4 ± 12.1	72.8 ± 15.6	85.5 ± 12.6	95.7 ± 8.98
Cardiac output, l/min	3.53 ± 0.66*	5.5 ± 1.4	5.2 ± 0.8	4.87 ± 1.20
Cardiac power output, W	0.59 ± 0.16*	0.89 ± 0.23	0.94 ± 0.20	1.02 ± 0.22
Vascular resistance, dyn/cm	1.735 ± 357*	1.143 ± 433	1.351 ± 293	14.85 ± 509
Oxygen consumption, ml/min	314.4 ± 54.2	371 ± 47	407 ± 35	374 ± 43
Oxygen consumption, ml/kg/min	4.32 ± 0.92	4.74 ± 0.56	4.88 ± 0.09	3.63 ± 0.66
Peak exercise				
Heart rate, beats/min	101.9 ± 21.6*	142.3 ± 26.0§	162.8 ± 12.9	173.9 ± 16.7
Stroke volume, ml	82.9 ± 22.2	88.9 ± 16.8	90.6 ± 15.2§	116.9 ± 18.5
Systolic BP, mm Hg	94.9 ± 16.3*	115.6 ± 25.0§	140.1 ± 21.9§	199.1 ± 18.4
Diastolic BP, mm Hg	59.4 ± 10.1	72.0 ± 14.5	78.1 ± 12.6§	66.0 ± 14.3
Mean arterial BP, mm Hg	74.0 ± 11.8*	86.9 ± 17.9§	103.5 ± 18.2§	120.8 ± 11.0
Cardiac output, l/min	8.12 ± 1.52*	12.4 ± 1.9§	14.7 ± 2.37§	20.3 ± 3.9
Cardiac power output, W	1.31 ± 0.31*	2.37 ± 0.47§	3.45 ± 0.72§	5.36 ± 0.94
Vascular resistance, dyn/cm	750 ± 195	569 ± 110	583 ± 159§	495 ± 116
Oxygen consumption, ml/min	916 ± 227*	1.814 ± 422§	2.511 ± 420§	3.090 ± 740
Oxygen consumption, ml/kg/min	12.0 ± 2.2*	20.5 ± 4.3§	29.8 ± 5.9§	36.4 ± 10.3
Arterial-venous oxygen difference, ml O ₂ /100 ml of blood	11.3 ± 2.2*	15.1 ± 4.1§	17.2 ± 2.3	18.2 ± 3.7
Respiratory exchange ratio	1.10 ± 0.15	1.13 ± 0.07	1.11 ± 0.07	1.11 ± 0.08

Values are mean ± SD. *p < 0.05 transplants vs. LVAD implanted, LVAD explanted, and controls. †p < 0.05 controls vs. transplants, LVAD implanted, LVAD implanted, ‡p < 0.05 controls vs. transplants and LVAD implanted. §p < 0.05 LVAD implanted vs. LVAD explanted, and controls. ¶p < 0.05 LVAD explanted vs. controls. BP = blood pressure; HTx = heart transplant candidate; LVAD = left ventricular assist device.

This project has received funding from the European Union's Horizon 2020 research and innovation programme under grant agreement No 952603.

Figure 46. Resting and Peak Exercise Cardiac and Physical Function Variables in HTx, Implanted and Explanted LVAD Patients, and Healthy Controls.

Some results are shown graphically, and they are accessible in different sections (Plot 1, Plot 2, Plot 3, Plot 4). A significant percent of LVAD explanted patients achieved a level of peak exercise cardiac power output equivalent to that of healthy controls. Number of these patients is 6. Chart on Figure 47 shows peak exercise cardiac power output.

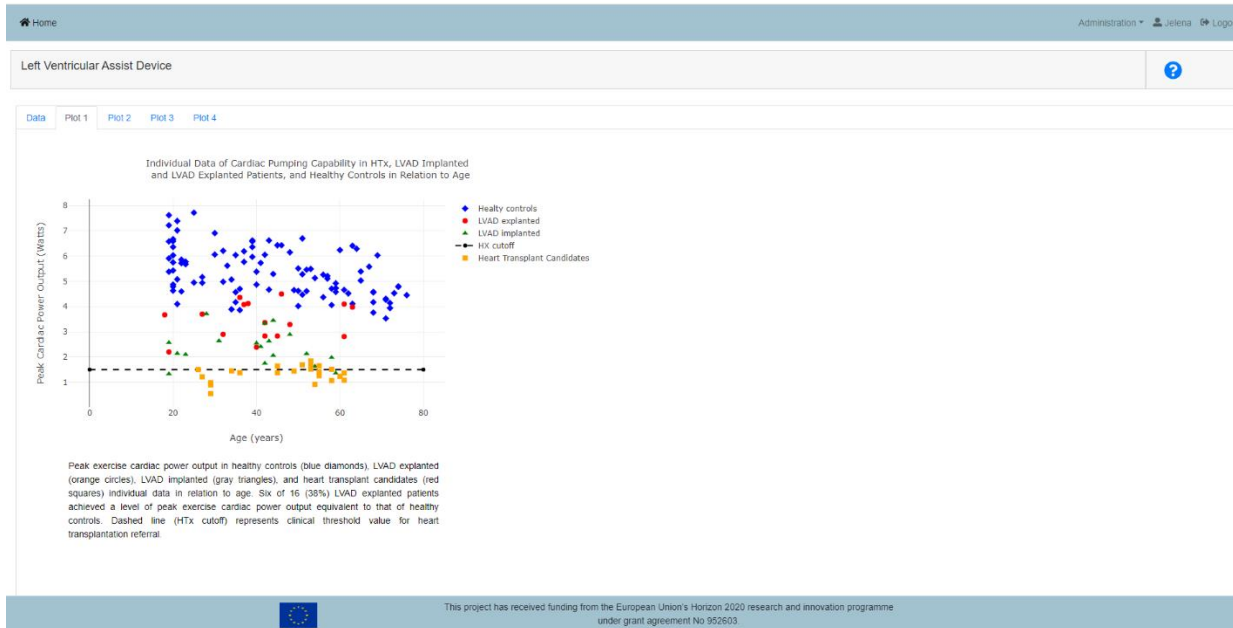


Figure 47. Individual Data of Cardiac Pumping Capability in HTx, LVAD Implanted and LVAD Explanted Patients, and Healthy Controls.

The Figure 48 shows peak oxygen consumption, on chart we can see that eleven patients achieved a level of peak exercise oxygen consumption. This is 69% of summary number of LVAD explanted patients. Dashed line (HTx cutoff) represents clinical threshold value for heart transplantation referral.

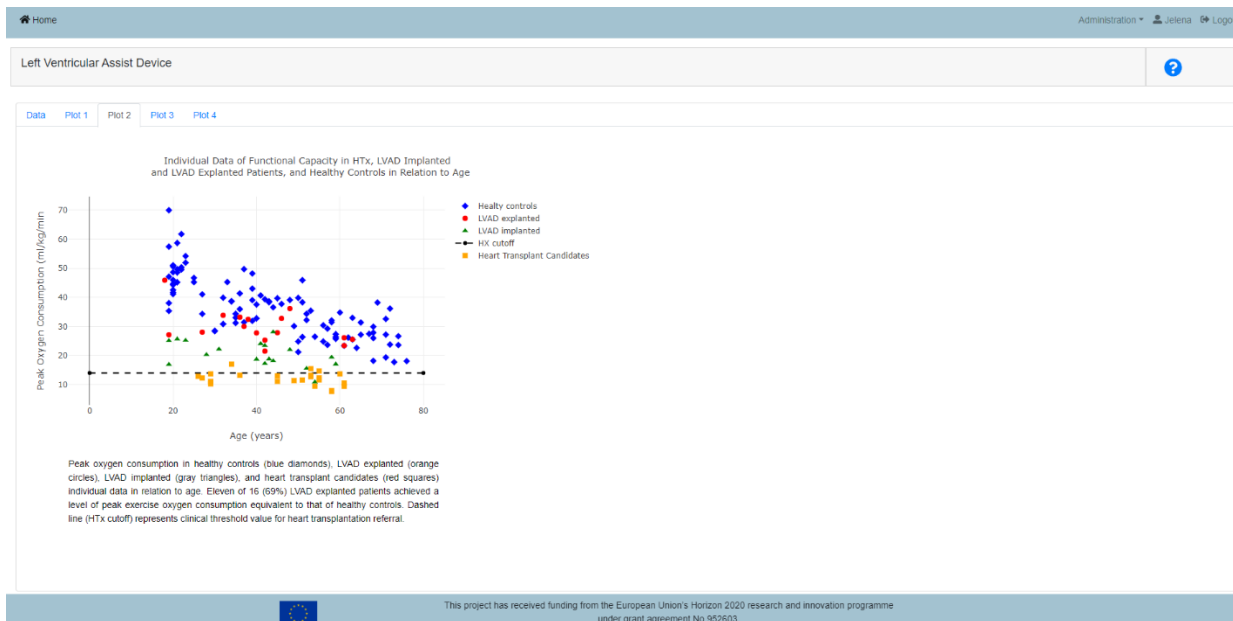


Figure 48. Individual Data of Functional Capacity in HTx, LVAD Implanted and LVAD Explanted Patients, and Healthy Controls in Relation to Age.

The important information for results is the time of LVAD explantation. An assessment was performed the relationship between this time and relationship of cardiac power and oxygen consumption at peak exercise. The important information for results is the time of LVAD explantation. An assessment was performed the relationship between this time and relationship of cardiac power and oxygen consumption at peak exercise. User can be included in calculation linear regression by clicking any point. When user clicks on a point, that point is exclude from the linear regression calculation (Figure 49).

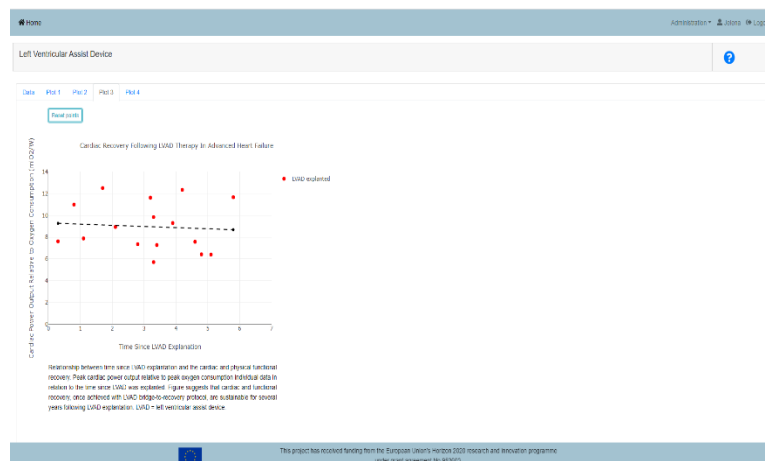


Figure 49. Cardiac Recovery Following LVAD Therapy In Advanced Heart Failure.

HTx group is group with most marked the pronounced decrease in cardiac functional capacity from 100% to $25.6 \pm 4.6\%$, and peak oxygen consumption is reduced to $33.7 \pm 8.5\%$. Every group was subject to

change, and peak cardiac power output is more disturbed than peak oxygen consumption. For clear chart user can turn off one parameter by clicking on its name (Figure 50).

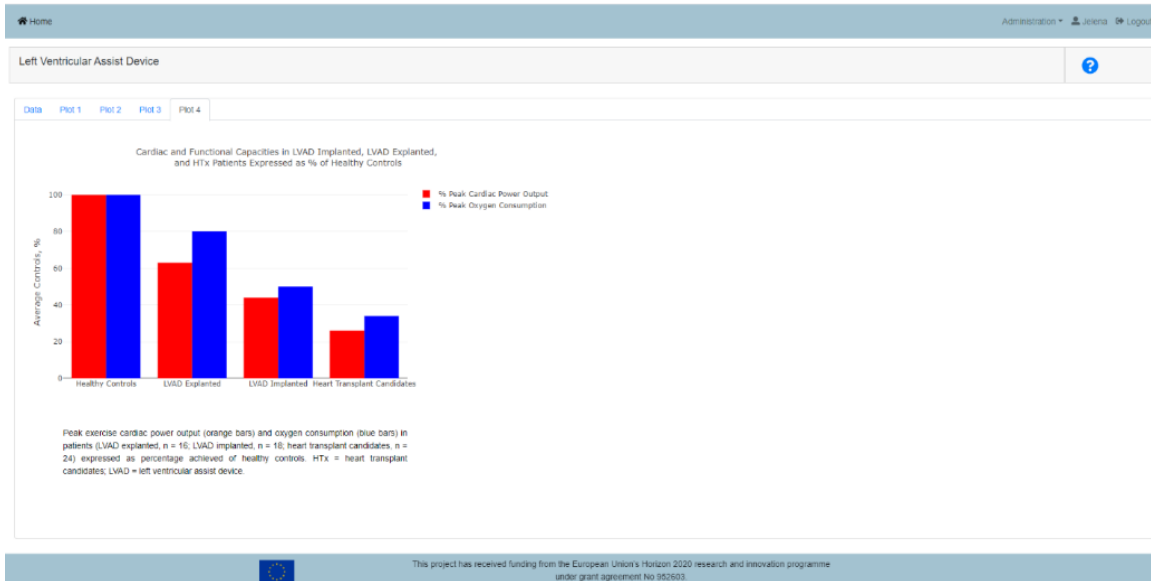


Figure 50. Cardiac and Functional Capacities in LVAD Implanted, LVAD Explanted, and HTx Patients Expressed as % of Healthy Controls.

6.8 Dataset – CORS; Responsible partner - COVU

Dataset - CORS	Responsible partner - COVU
-----------------------	-----------------------------------

The CORS dataset¹⁰ can be accessed by the end user through the Cardiovascular disease modeling module, which lies on the main dashboard of the SGABU platform, as presented in Figure 51.

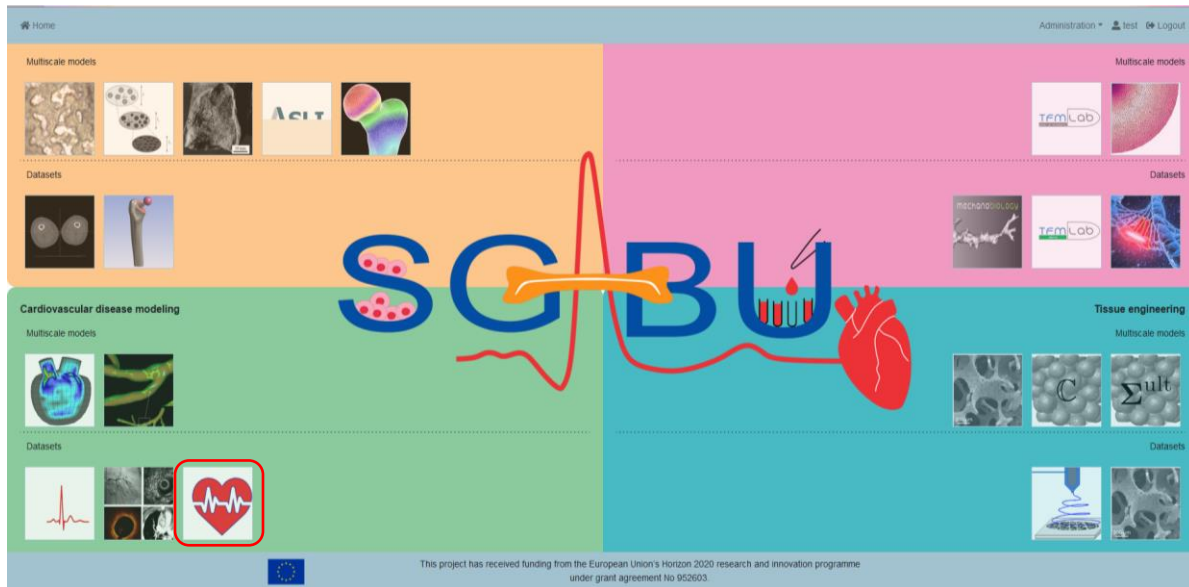


Figure 51. Main platform dashboard.

Heart failure is a complex clinical syndrome associated with structural and functional cardiac abnormalities, which lead to reduced cardiac output at rest and/or stress. Heart failure increases with age and in the presence of comorbidities and is a leading cause of hospitalization in people over 65 years of age. The prevalence of cardiac dysfunction and associated heart failure is >10% in people ≥ 70 years of age and rises to >20% in those with multi-morbidities including diabetes, coronary artery disease, metabolic syndrome, hypertension, and rheumatoid arthritis. Heart failure is associated with poor prognosis, poor quality of life for patients, and high healthcare costs.

In order for the user to see the results, the user needs to select the patient on SGABU platform. First tab is Demographic. The prospective observational study recruited 32 consecutive primary care patients (14 men and 18 women; mean age 63 ± 9 years). The demographic parameters are: Age, Alcohol, Confirmed History, DOB, Date of Test, Diagnosis, Estimated LVEF, Gender, Height, LVEF, Meds, NTproBNP, Smoker and Weight.

For the purposes of the study, people were instructed to abstain from vigorous exercise and alcohol consumption 24h prior to the study visit.

¹⁰ Charman, S. J., Okwose, N. C., & Stefanetti, R. J. (2018). A novel cardiac output response to stress test developed to improve diagnosis and monitoring of heart failure in primary care. ESC HEART FAILURE, 703-712. doi:10.1002/ehf2.12302

How Cardiac output was measured continuously using the bioelectance method in supine and standing positions and during two 3 min stages of a step-exercise protocol (10 and 15 steps per minute) using a 15 cm height bench, users of SGABU platform can see results for both positions (Figure 52).

The CORS test includes measurements at rest and in response to stress (short exercise, i.e. step test). The CORS consists of four phases: 3 min rest (supine), 3 min challenge (standing), and two 3 min step-exercise test stages (i.e. Stage 1 step exercise, 10 steps/minute followed by Stage 2 step exercise, 15 steps/minute) using a 15 cm height bench.

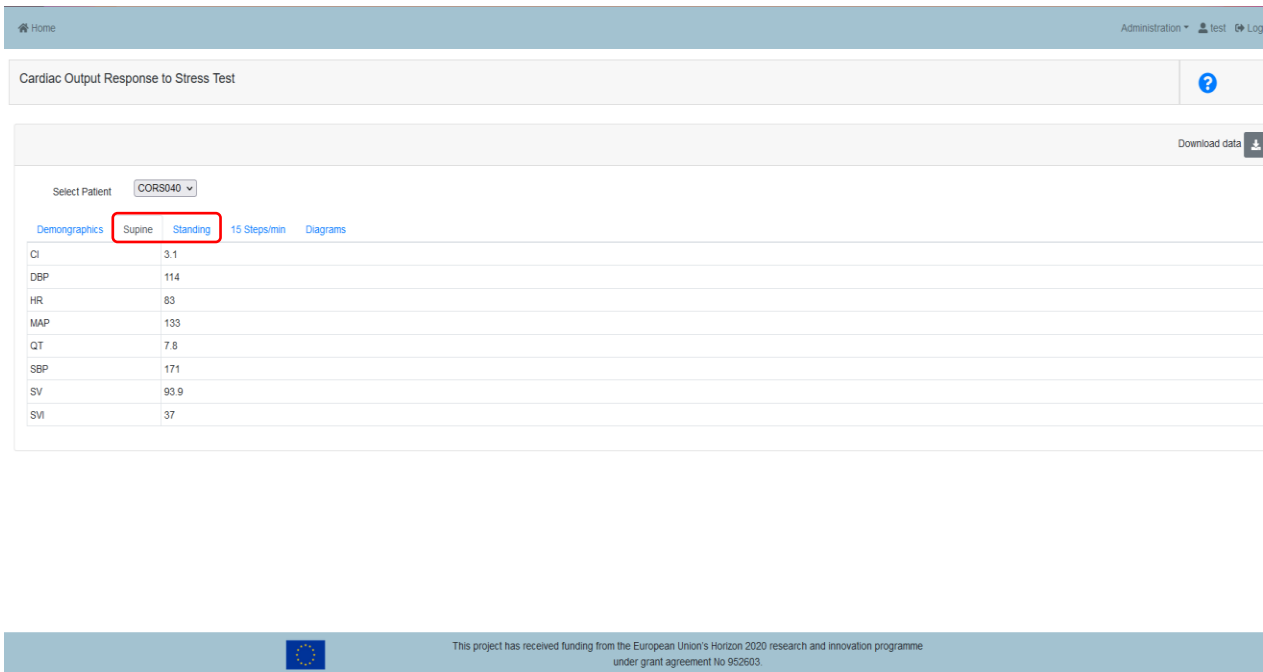


Figure 52. The results

The tab “Diagrams” provides pictorial representation of results. User can select graph type (Figure 53):

- CI- cardiac index;
- CV- coefficient of variation;
- DBP- diastolic blood pressure;
- HR- heart rate;
- MAP- mean arterial pressure;
- QT- cardiac output;
- R- correlation coefficient;
- SBP- systolic blood pressure;
- SV- stroke volume;
- SVI- stroke volume index



Figure 53. Diagram: user can select graph type.

Major findings suggest acceptable reproducibility of the CORS test, which is developed to potentially improve diagnosis and monitoring of heart failure in primary care.

6.9 Dataset – Hip joint; Responsible partner - UKG

Dataset - Hip joint	Responsible partner - UKG
----------------------------	----------------------------------

The access to the Hip joint with femoral implant dataset^{11,12,13,14} belongs to the Bone Modeling module on the SGABU platform is provided through the main dashboard as presented in the following Figure 54.

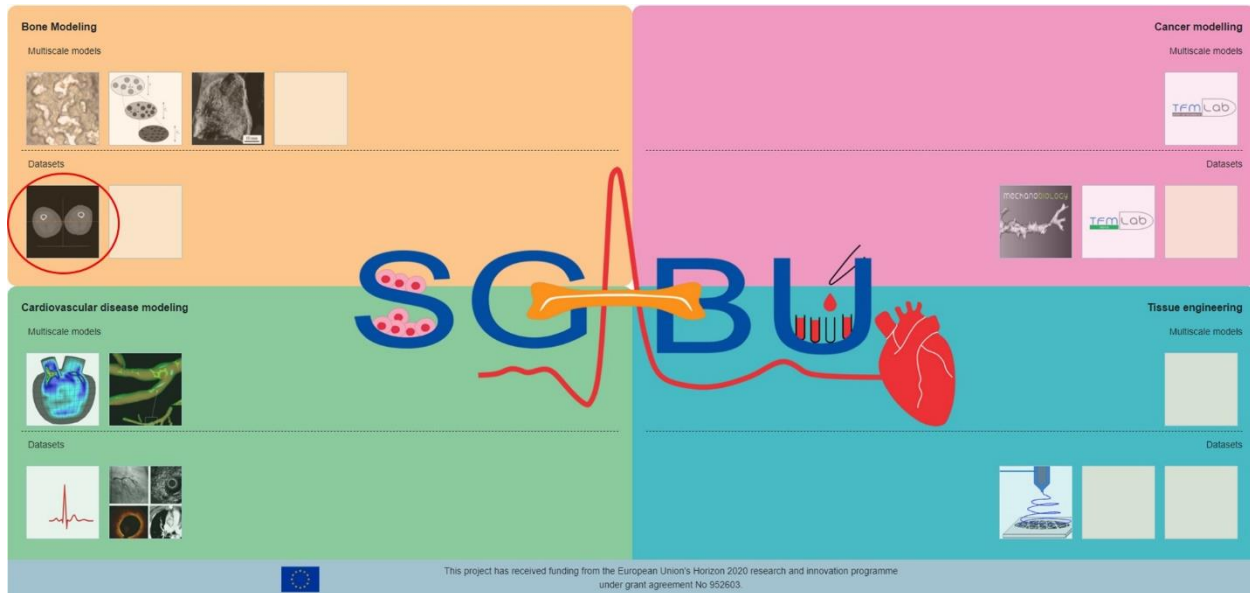


Figure 54. Main platform dashboard.

This dataset contains 301 DICOM images, obtained from a CT scanner. The scans include one hip joint with artificial femoral prosthesis (left) and one healthy hip joint (right).

User interface for this dataset is shown in Figure 55.

¹¹ Vulović, A., & Filipovic, N. (n.d.). Computational analysis of hip implant surfaces., 13, pp. 109-119. doi: 10.24874/jsscm.2019.13.01.0

¹² Vulović, A., & Filipović, N. (2020). Effect of Hip Implant Surface Modification on Shear Stress Distribution. Eight International Conference on Computational Bioengineering ICCB. Belgrade

¹³ Vulović, A., & Filipović, N. (2021). Numerical analysis of hip implant surfaces. ICIST, (pp. 128-130). Kopaonik

¹⁴ Vulović, A., Warchomicka, F., Ramskogler, C., Sommitsch, C., & Filipović, N. (2018). Simulation of the Interlocking Capacity of the Modified Hip Implant Surface. ICIST 2018. Kopaonik, Serbia.

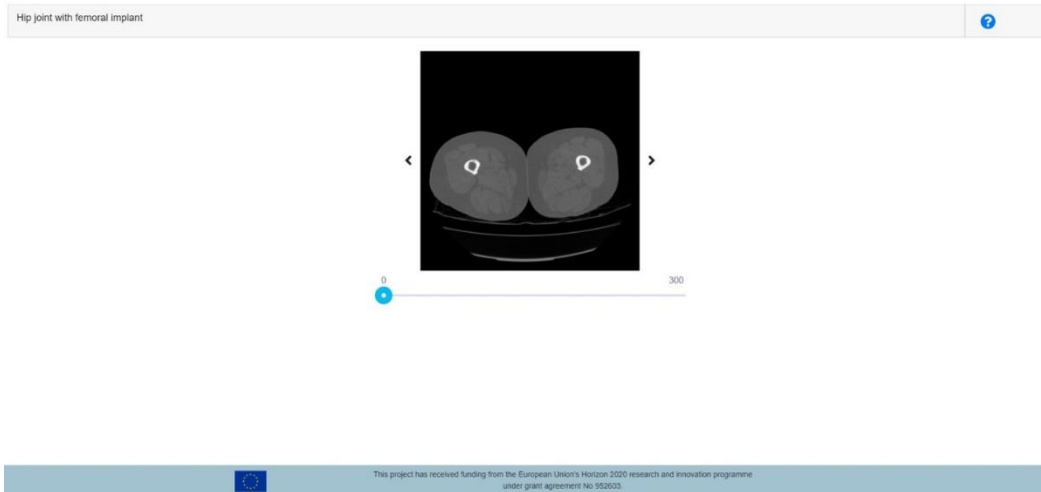


Figure 55. User Interface for Hip joint with femoral Implant dataset.

A user can move through the dataset by clicking on left or right arrows next to the image, or by using the slider function below the image.

The image 0 (default image after dataset is opened) represents the shaft of the femoral bone. As the number of the image increases the user will be able to see upper segments of the femoral bone and hip implants as well as the pelvic region (Figure 56).



Figure 56. Different dataset sections.

6.10 Dataset – Electrospinning; Responsible partner - UKG

Dataset - Electrospinning	Responsible partner - UKG
----------------------------------	----------------------------------

The access to the Electrospinning¹⁵ belongs to the Tissue engineering module, on the SGABU platform is provided through the main dashboard as presented in the following figure (Figure 57).

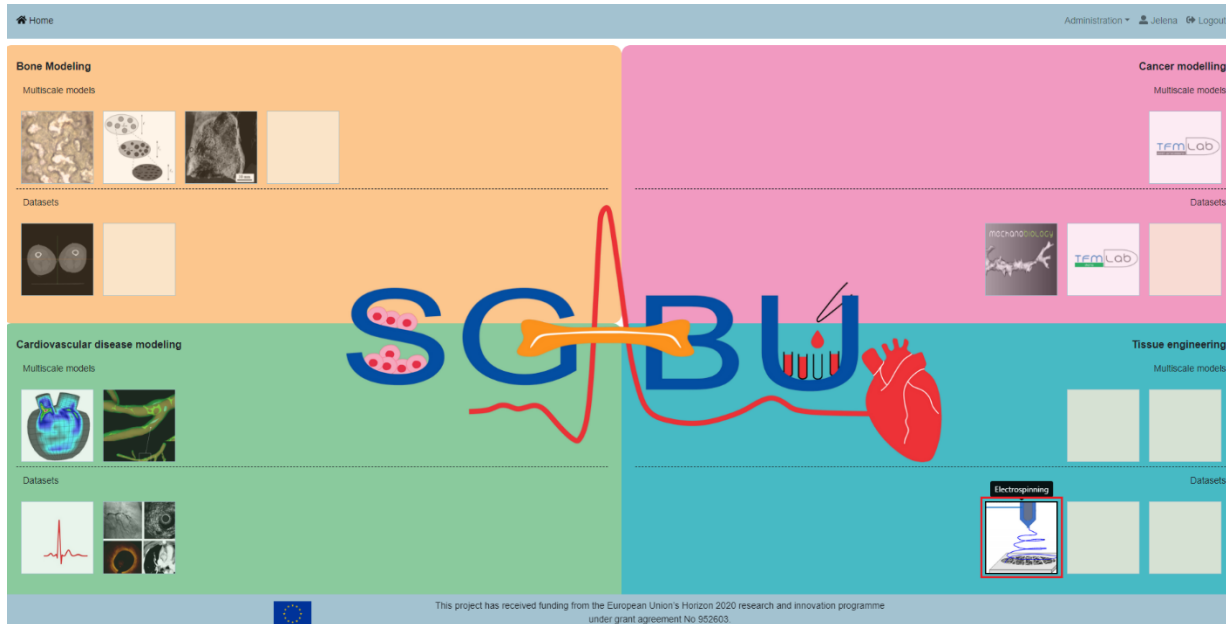


Figure 57. Main platform dishoard.

Electrospinning is technique for creating fibers, and it includes electrohydrodynamic process and high voltage electricity. During Electrohydrodynamic process, a jet is created by using liquid solution. Electrospinning is technique for creating fibers, and it includes electrohydrodynamic process and high voltage electricity. During Electrohydrodynamic process, a jet is created by using liquid solution. The deposition of solid fiber on the collector is product of stretching the charged jet. It was necessary to make gelatin scaffolds with micro / nano scale which they use to regenerate wound tissue.

Electrospinning is the selected method for scaffold development in this project, as fibre production can be modified based on the combination of parameters in use. Fibres are formed from a polymer and solvent solution, and the properties of these materials reflect the fibre production. The solution is passed through a positive needle electrode toward a negative collector electrode, with a large electric field between the two. The negative electrode can either be a flat collector for initial fibre testing, as seen in Figure 58.

¹⁵ K. Virijević, J. Grujić, M. Jovanovic, N. Kastratović, A. Mirić, D. Nikolić, M. Živanović and N. Filipović, "Electrospun gelatin nanofibrous scaffolds – applications intissue engineering," 1st International Conference on Chemo and Bioinformatics, pp. 251-254, 2021. doi:10.46793/ICCB121.251V

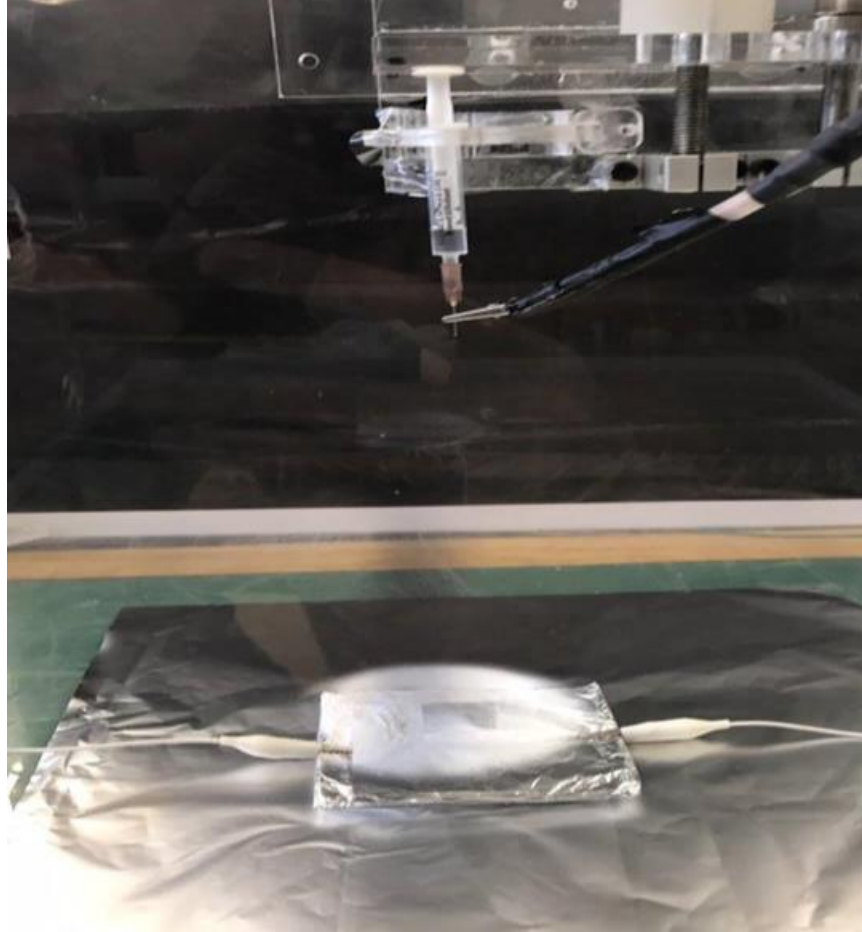


Figure 58. Electrospinning setup with flat negative electrode.

The distance between the electrodes and the voltage applied will determine the strength of the electric field through which the solution passes. At the suitable solution flow rate and applied voltage, the solution forms a Taylor cone, where enough positive charges are accumulated at the needle's tip, to which a fibre stream is formed. As the solution is electrically conductive, the Taylor cone is achieved when the dielectric constant value and surface tension is overcome. In an ideal case, where all electrospinning parameters are working harmoniously, a spiral cone is formed, as represented in Figure 59, hence the importance to consider all parameters.

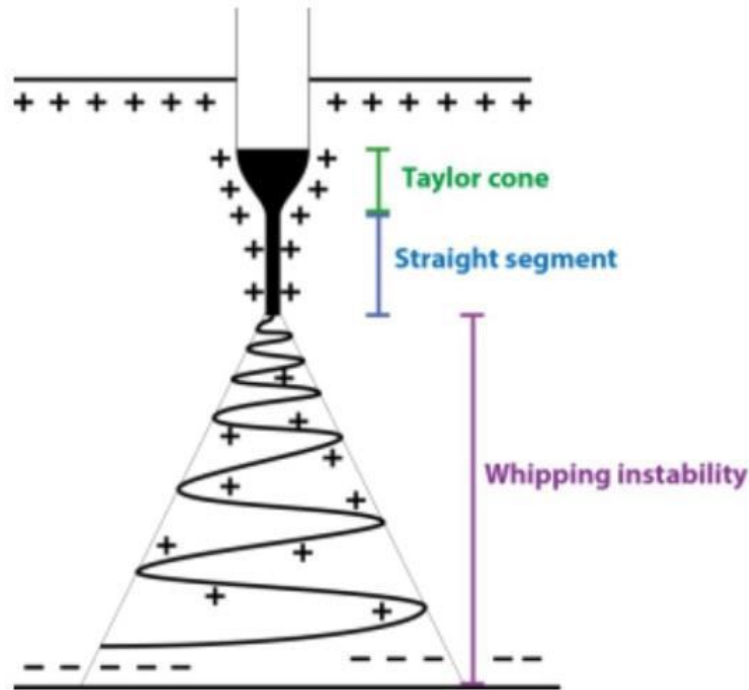


Figure 59. Representation of fiber cone formation.

Establishing Electrospinning Parameters

The first parameter for consideration is the solution viscosity, as it cannot be altered once testing commences. If polymers and solvents types are maintained, with increase to the polymer concentration, the viscosity would also increase. If the solution has a viscosity too high, it may be too difficult to pass through the needle, particularly if the needle has a thin inner diameter. Alternatively, a solution with a viscosity too low may cause drips before fibres can even form.

Secondly, voltage should be applied slowly to suit the selected flow rate and until fibre production is constant. Voltages too high may cause the fibres to dry out considerably before they even reach the collector. With a consistent voltage, decreasing electrode distance increases the electric field, which also needs to be considered. In the case that scaffolds are being built on a rotational collector, the rotational speed of the collecting rod should be also recorded.

The best analysis of flat collected fibres is done through a standard microscope.

For good stimulation of tissue regeneration necessary is projecting biomaterials with the best characteristic. This result is gotten by determining relations between properties of materials. The following image (Figure 60) shows tabular display of testing data with different relation between materials. All parameters can be sorted and downloaded on user's computer.

Home Administration Jekena Logout

Electrospinning ?

slozeni_ulazi.csv Download slozeni_ulazi.csv

PCL %	PEG %	Hloroform 0-1	DMF 0-1	U kV	Output
27	0	0.5	0.5	13	?
26	0	0.5	0.5	13	?
25	0	0.5	0.5	13	?
25	0	1	0	20	?
24	0	0.5	0.5	15	?
24	0	1	0	18	?
23	0	0.5	0.5	15	?
23	0	1	0	18	?
22	0	0.5	0.5	10	?
22	0	1	0	12	?
21	0	0.5	0.5	12	?
21	0	0.75	0.25	13	?
21	0	1	0	19	?
20.25	6.75	0.75	0.25	15	?
20	0	0.5	0.5	11	?
20	0	0.75	0.25	10	?
20	0	1	0	17	?
19.5	6.5	0.5	0.5	12	?
19	0	0.5	0.5	11	?
19	0	0.25	0.75	13	?
19	0	0.75	0.25	12	?
19	0	1	0	20	?
18.75	6.25	0.75	0.25	13	?

This project has received funding from the European Union's Horizon 2020 research and innovation programme under grant agreement No 952603.

Figure 60. Parameters for electrospinning process.

In this table shows percentage attendance of PCL, PEG, Hloroform, DMF, U kV for creating biomaterials. PCL is polycaprolactone, material for biomedical and it is important for fiber to be without beads. PEG is polyethylene glycol is a polymer to improve the wetting of nanofibers. DMF is dimethylformamide can improve electrospinning, lead to extensive jet splaying. DC and AC voltages can be applied.

6.11 Model – BonePoreDense; Responsible partner - TUW

Model - BonePoreDense	Responsible partner - TUW
------------------------------	----------------------------------

The access to the “BonePoreDensApp” on the SGABU platform is provided through the third icon in the main dashboard as presented in Figure 61. The model is based on the model published in Vass et al¹⁶.

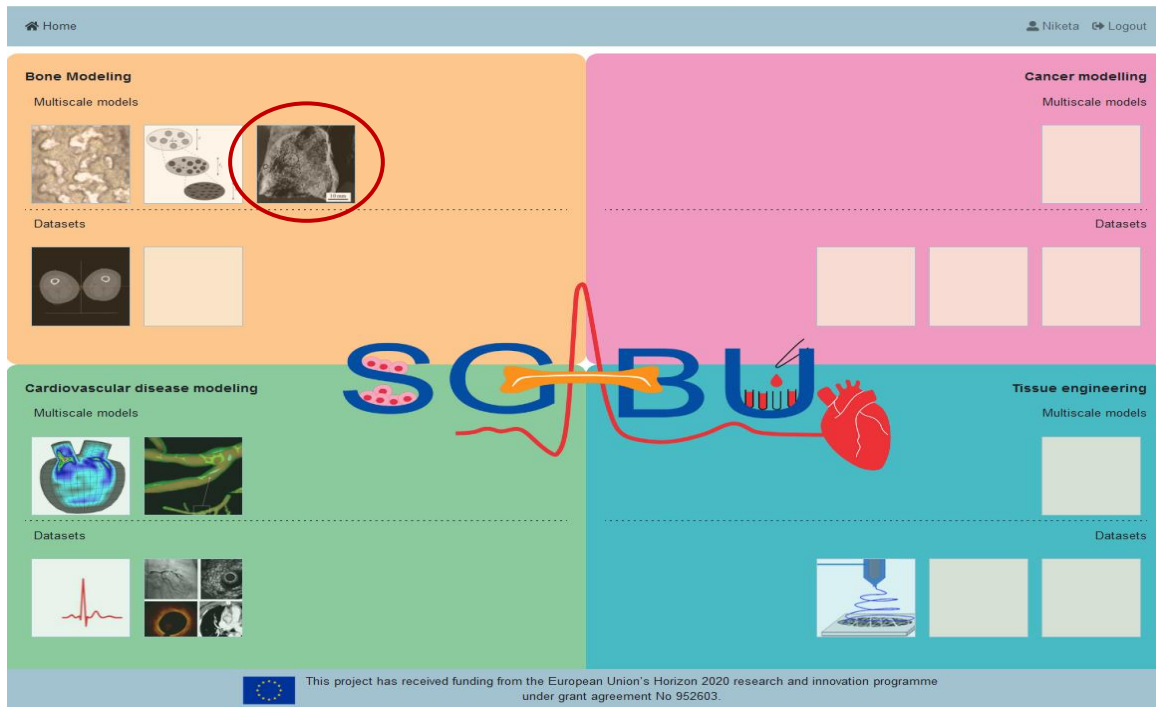


Figure 61. Main platform dashboard; icon for BonePoreDens.

(extracted from Figure 1(b) in A. Fritsch, C. Hellmich¹⁷)

After clicking the respective icon, a new window appears. The basic execution unit in SGABU is a workflow. In the left section of the window, users are able to see names and status of the workflows. Possible statuses of the workflow are:

- Not yet executed
- Terminated
- Running
- Finished OK
- Finished Error

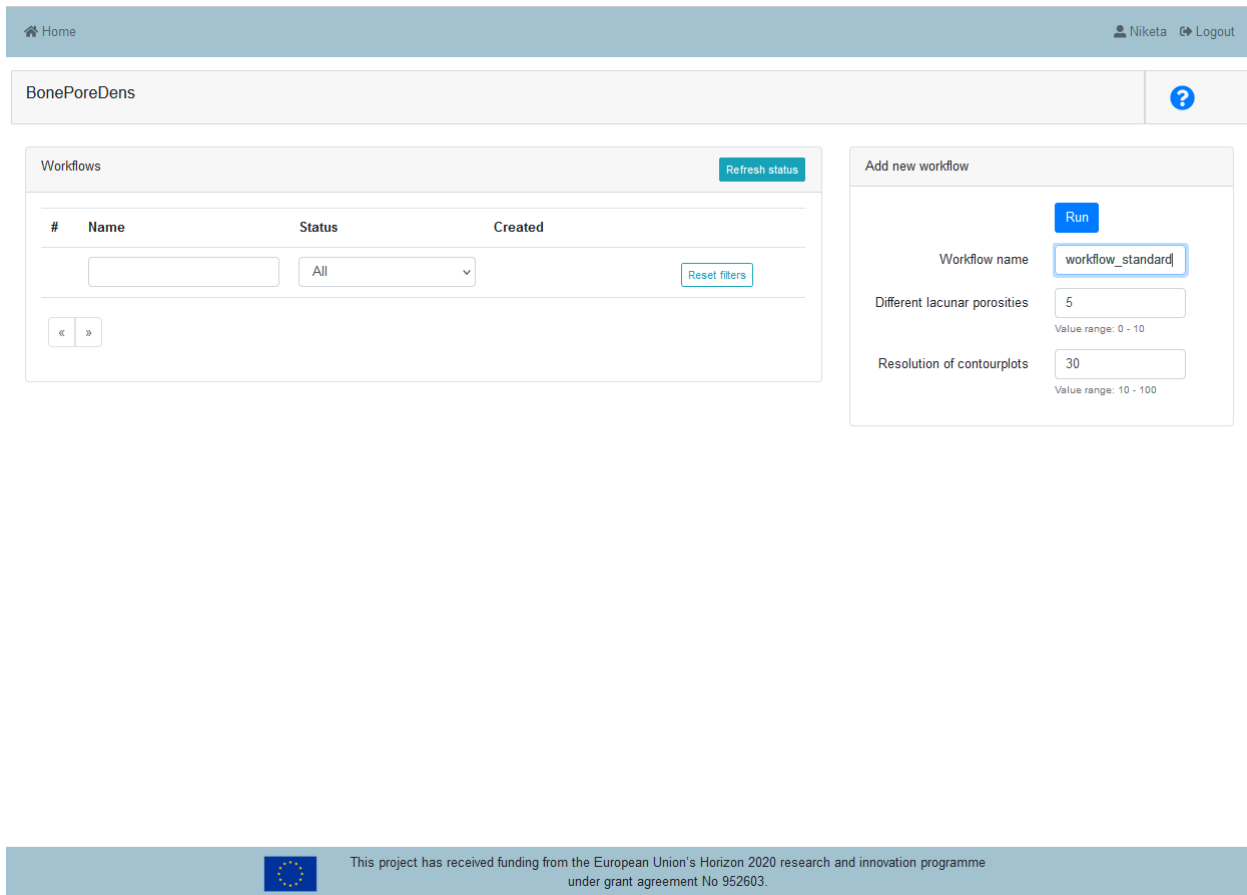
¹⁶ Vass V., Morin C., Scheiner S., Hellmich C. (2018) Review of “Universal” Rules Governing Bone Composition, Organization, and Elasticity Across Organizational Hierarchies. In: Pivonka P. (eds) Multiscale Mechanobiology of Bone Remodeling and Adaptation. CISM International Centre for Mechanical Sciences (Courses and Lectures), vol 578. Springer, Cham. https://doi.org/10.1007/978-3-319-58845-2_4

¹⁷ Fritsch A, Hellmich C. 'Universal' microstructural patterns in cortical and trabecular, extracellular and extravascular bone materials: micromechanics-based prediction of anisotropic elasticity. J Theor Biol. 2007 Feb 21;244(4):597-620. doi: 10.1016/j.jtbi.2006.09.013. Epub 2006 Sep 17. PMID: 17074362.

In the right section of the window, users can create new workflows for this submodule (Figure 62). Each of the forms needs to be filled out in order for the simulation to run.

Users are expected to fill out the following forms:

- Workflow name
- Different lacunar porosities
- Resolution of contourplots



The screenshot shows the BonePoreDens user interface. At the top, there is a navigation bar with 'Home' and user information 'Niketa Logout'. Below this, the main content area is titled 'BonePoreDens' and contains two main sections:

- Workflows:** A table with columns for '#', 'Name', 'Status', and 'Created'. There is a search bar, a status filter dropdown set to 'All', and a 'Reset filters' button. A 'Refresh status' button is also present.
- Add new workflow:** A form with a 'Run' button. It includes:
 - 'Workflow name' input field with the value 'workflow_standard'.
 - 'Different lacunar porosities' input field with the value '5', with a note 'Value range: 0 - 10'.
 - 'Resolution of contourplots' input field with the value '30', with a note 'Value range: 10 - 100'.

At the bottom of the interface, there is a footer with the European Union logo and the text: 'This project has received funding from the European Union's Horizon 2020 research and innovation programme under grant agreement No 952603.'

Figure 62. User Interface for BonePoreDens module.

All forms except for the Workflow name are numerical and value ranges are provided for the users. The workflow name can be freely chosen. For the “Different lacunar porosities” a value between 1 and 100 should be entered. It stands for the number of different values considered for the lacunar porosity ϕ_{lac} , evenly distributed between 0 and 10%¹⁸ - thereby, ϕ_{lac} refers to the volume of lacunar (and canalicular) pores divided by the volume of a macroscopic piece of bone. Secondly, the “Resolution of contourplots” stands for the number of considered values for the vascular porosity and extracellular mass density each.

¹⁸ Luis Zelaya-Lainez, Hawraa Kariem, Winfried Nischkauer, Andreas Limbeck, Christian Hellmich, “Variances” and “in-variances” in hierarchical porosity and composition, across femoral tissues from cow, horse, ostrich, emu, pig, rabbit, and frog, Materials Science and Engineering: C, Volume 117, 2020, 111234, ISSN 0928-4931, <https://doi.org/10.1016/j.msec.2020.111234>.

A value between 10 and 100 should be entered. The exception handling is integrated into the user interface (UI) of the SGABU platform, see Figure 63.

Once everything is correctly filled, the workflow can be started. The user can monitor the current status of the workflow in the left section of the window. Table 4 shows the summarized information for the input parameters. For each of the aforementioned datasets, the following steps are performed: (a) computation of all the volume fractions of all micromechanical phases occurring in Figure 15 of Vass et al¹⁶; (b) computation of the corresponding macroscopic stiffness tensor components; (c) computation of the Young's moduli and Poisson's ratios at the macroscopic level.

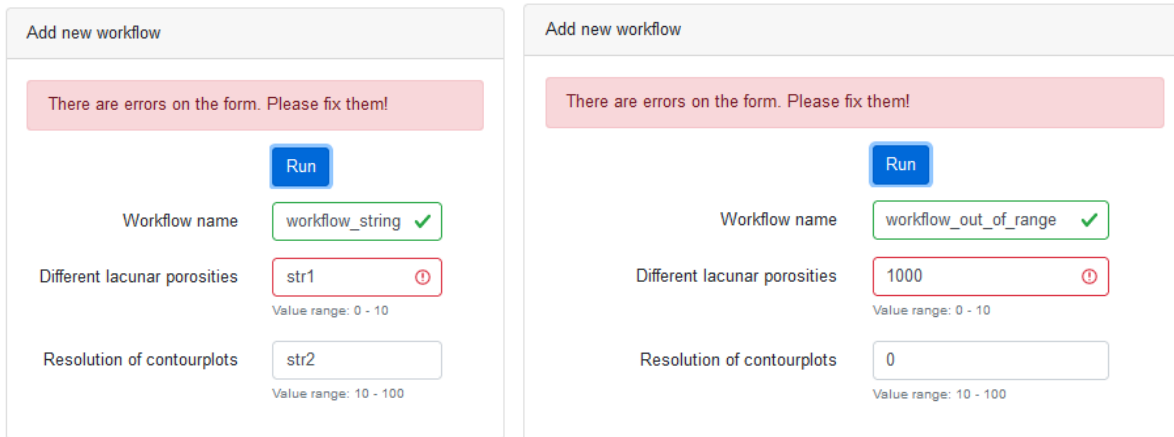


Figure 63. Exception handling.

Table 4. Inputs for the BonePoreDensApp.

Name of the parameter	Label	Explanation	Unit	Range	Default value
Different lacunar porosities	N	Number for different values considered for the lacunar porosity, evenly distributed between 0 and 10%	/	1-100	5
Resolution of contourplots	R	Number of considered values for the vascular porosity and extracellular mass density each	/	10-100	30

Results are displayed in the form of images. By clicking on the eye-icon a new window pops up, where the entered input parameters are shown in a table, see Figure 64 (a). By switching to „Figs“, images showing five contour plots and corresponding numeric results appear, see Figure 64 (b). These five plots are shown for each lacunar porosity. By clicking on the arrows, see red circles in Figure 64 (b), the user can switch through the plots.

These plots show the following elastic properties: (a) Longitudinal Young's modulus, (b) Transverse Young's modulus, (c) Poisson's ratio quantifying transverse strain under longitudinal loading, (d) Poisson's ratio quantifying longitudinal strain under transverse loading, (e) Poisson's ratio quantifying transverse strain under transverse loading. Each of these properties will be shown as function of the vascular porosity ranging from 0 to $100 \cdot (1 - \phi_{lac})\%$ and of the extracellular mass density ranging from 1.1 g/cm³ to 2.6 g/cm³, according to Figure 3 found in Vass et al¹⁶. Furthermore, in (f) numeric results are given: the value of the

respective lacunar porosity and the corresponding values of the minima and maxima of the Young's Modules and the Poisson's ratios shown in figures (a) to (e).

These results can also be downloaded, see blue circles in Figure 64, in form of figures and csv files containing all the calculated values. Users can find more details in additional relevant references for this model.^{19,20,21,22,23,24}

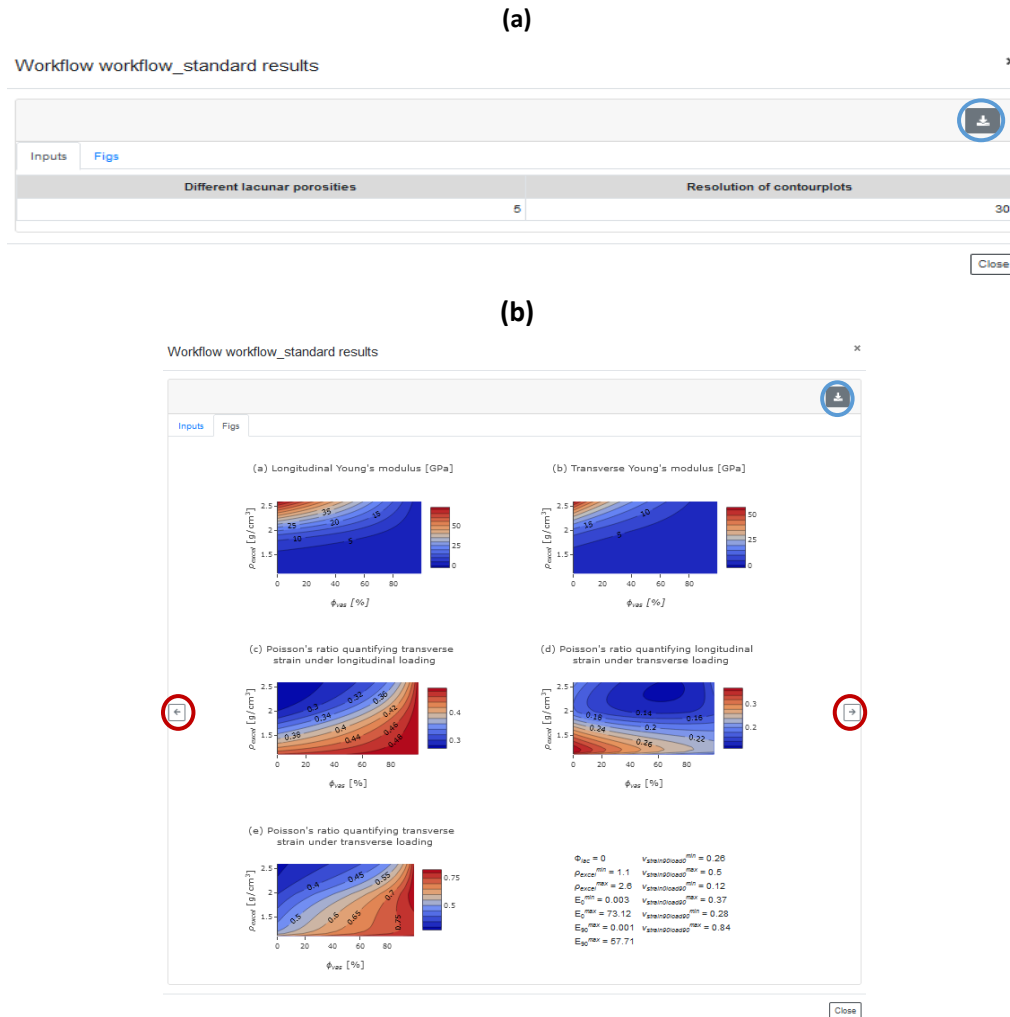


Figure 64. Results section: (a) Overview of input parameters, (b) figures.

¹⁹ Badel, P. B., & Leblond, J. B. (2004). A note on integration schemes for the microplane model of the mechanical behaviour of concrete. COMMUNICATIONS IN NUMERICAL METHODS IN ENGINEERING, 75–81. doi:10.1002/cnm.658

²⁰ Fritsch, A., Hellmich, C., & Dormieu, L. (2009). Ductile sliding between mineral crystals followed by rupture of collagen crosslinks: Experimentally supported micromechanical explanation of bone strength. Journal of Theoretical Biology, 230-252. doi:10.1016/j.jtbi.2009.05.021

²¹ Morin, C., & Hellmich, C. (2013). Mineralization-driven bone tissue evolution follows from fluid-to-solid phase transformations in closed thermodynamic systems. Journal of Theoretical Biology, 335, 185-197. doi:https://doi.org/10.1016/j.jtbi.2013.06.018.

²² Morin, C., & Hellmich, C. (2014). A multiscale poromicromechanical approach to wave propagation and attenuation in bone. Ultrasonics, 54, 1251-1269. doi:https://doi.org/10.1016/j.ultras.2013.12.005

²³ Morin, C., Hellmich, C., & Henits, P. (2013). Fibrillar structure and elasticity of hydrating collagen: A quantitative multiscale approach. Journal of Theoretical Biology, 317, 384-393. doi:https://doi.org/10.1016/j.jtbi.2012.09.026

²⁴ Morin, C., Vass, V., & Hellmich, C. (2017). Micromechanics of elastoplastic porous polycrystals: Theory, algorithm, and application to osteonal bone. International Journal of Plasticity, 91, 238- 267. doi:10.1016/j.ijplas.2017.01.009

6.12 Model – BoneMinOrg; Responsible partner - TUW

Model - BoneMinOrg	Responsible partner - TUW
--------------------	---------------------------

The access to the “BoneMinOrgApp” on the SGABU platform is provided through the second icon in the main dashboard as presented in Figure 65. The model is based on the model published in Vass et al¹⁶.

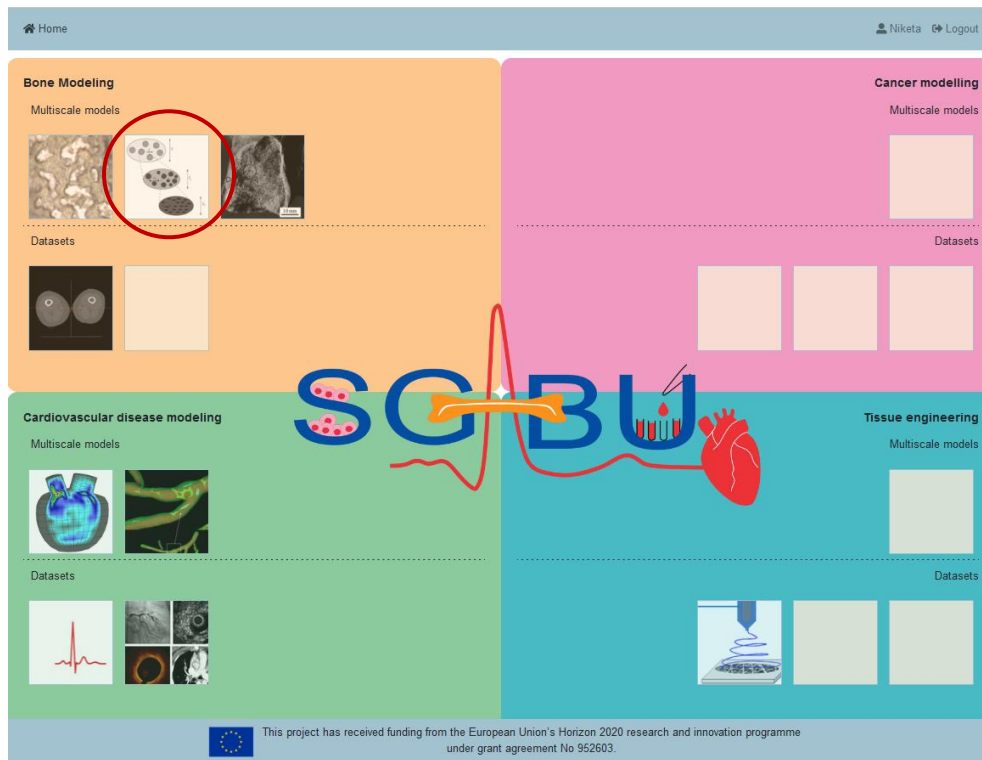


Figure 65. Main platform dashboard; icon for BoneMinOrg.

(extracted from Figure 2 of: A. Fritsch, C. Hellmich, L. Dormieu¹⁷)

After clicking the respective icon, a new window appears (see Figure 66). The basic execution unit in SGABU is a workflow. In the left section of the window, users are able to see names and status of the workflows. Possible statuses of the workflow are:

- Not yet executed
- Terminated
- Running
- Finished OK
- Finished Error

In the right section of the window, users can create new workflows for this submodule. Each of the forms needs to be filled out in order for the simulation to run.

Users are expected to fill out the following forms:

- Workflow name
- Lacunar porosity in [%]
- Different vascular porosities
- Resolution of contourplots

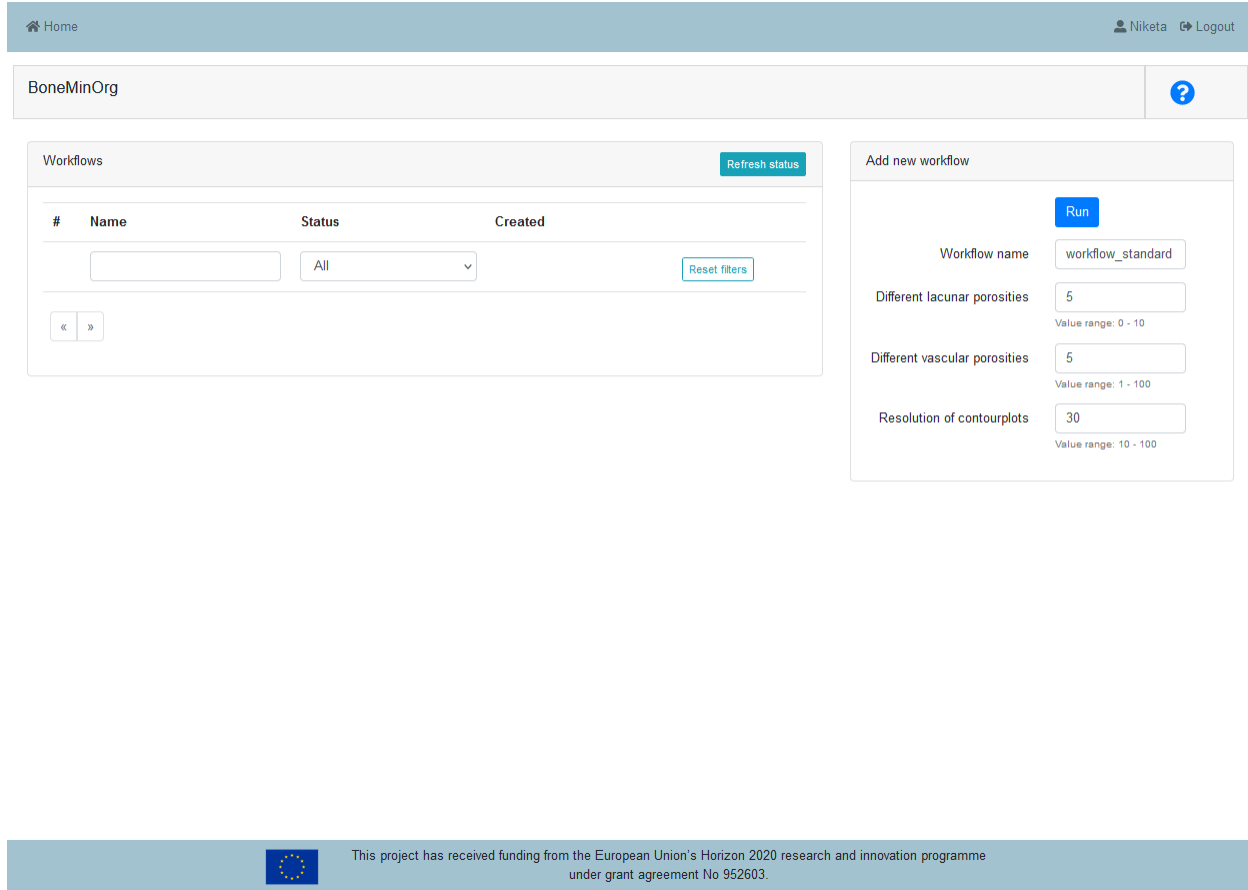


Figure 66. User Interface for BoneMinOrg module.

All forms except for the Workflow name are numerical and value ranges are provided for the users. The workflow name can be freely chosen. For the “Lacunar porosity in [%]” a value between 0 and 10 should be entered. It stands for the real value of the lacunar porosity ϕ_{lac} in %. The “Different vascular porosities” refers to the number of different values considered for the vascular porosity ϕ_{vas} , evenly distributed between 0 and $100 \cdot (1 - \phi_{lac})\%$ - again, ϕ_{lac} refers to the volume of lacunar (and canalicular) pores divided by the volume of a macroscopic piece of bone – and the “Resolution of contourplots” stands for the number of considered values for the apparent organic mass density and the apparent mineral mass density each. A value between 10 and 100 should be entered.

The exception handling is integrated into the user interface (UI) of the SGABU platform, see Figure 67.

Once everything is correctly filled, the workflow can be started. The user can monitor the current status of the workflow in the left section of the window. Table 5 shows the summarized information for the input parameters. For each of the aforementioned data triplets, the following steps are performed: (a)

computation of all the volume fractions of all micromechanical phases occurring in Figure 15 of Vass et al¹⁶; (b) computation of the corresponding macroscopic stiffness tensor components; (c) computation of the Young’s moduli and Poisson’s ratios at the macroscopic level.

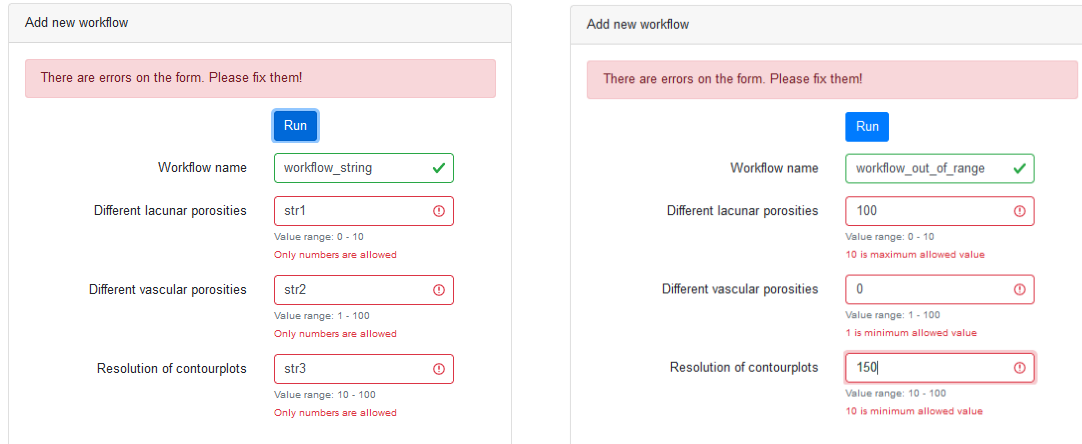


Figure 67. Exception handling.

Table 5. Inputs for the BoneMinOrgApp.

Name of the parameter	Label	Explanation	Unit	Range	Default value
Lacunar porosity in [%]	ϕ_{lac}	The real value of the lacunar porosity ϕ_{lac} in %.	%	0-10	5
Different vascular porosities	N	number of different values considered for the vascular porosity ϕ_{vas} , evenly distributed between 0 and $100*(1-\phi_{lac})\%$	/	1-100	5
Resolution of contourplots	R	Number of considered values for the vascular porosity and extracellular mass density each	/	10-100	30

Results are displayed in the form of images. By clicking on the eye-icon a new window pops up, where the entered input parameters are shown in a table, see Figure 68(a). By switching to „Figs“, images showing five contour plots and corresponding numeric results appear, see Figure 68(b). These five plots are shown for each lacunar porosity. By clicking on the arrows, see red circles in Figure 68(b) , the user can switch through the plots.

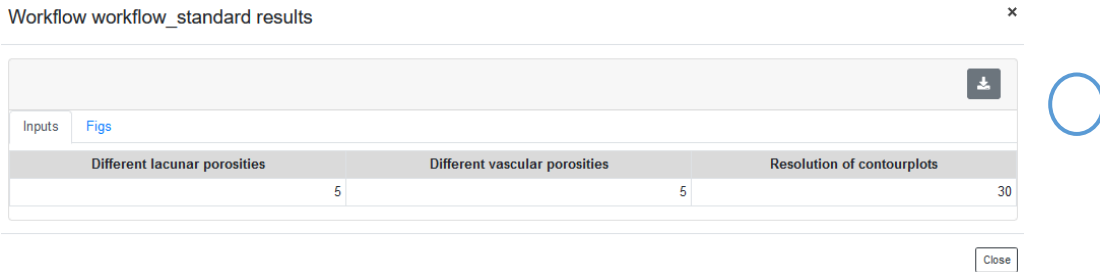
These plots show the following elastic properties: (a) Longitudinal Young’s modulus, (b) Transverse Young’s modulus, (c) Poisson’s ratio quantifying transverse strain under longitudinal loading, (d) Poisson’s ratio quantifying longitudinal strain under transverse loading, (e) Poisson’s ratio quantifying transverse strain under transverse loading. Each of these properties will be shown as function of the apparent organic mass density ranging from 0.3 to 0.6 g/cm³ and of the apparent mineral mass density ranging from 0.5 to 2 g/cm³, motivated by Figure 2a of Vass et al¹⁶. Furthermore, in (f) numeric results are given: the value of

the lacunar porosity, the value of the respective vascular porosity, and the corresponding values of the minima and maxima of the Young's Modules and the Poisson's ratios shown in the figures (a) to (e).

These results can also be downloaded, see blue circles in Figure 68, in form of figures and csv files containing all the calculated values.

Users can find more details in additional relevant references for this model.^{19,20,21,22,23,24}

(a)



(b)

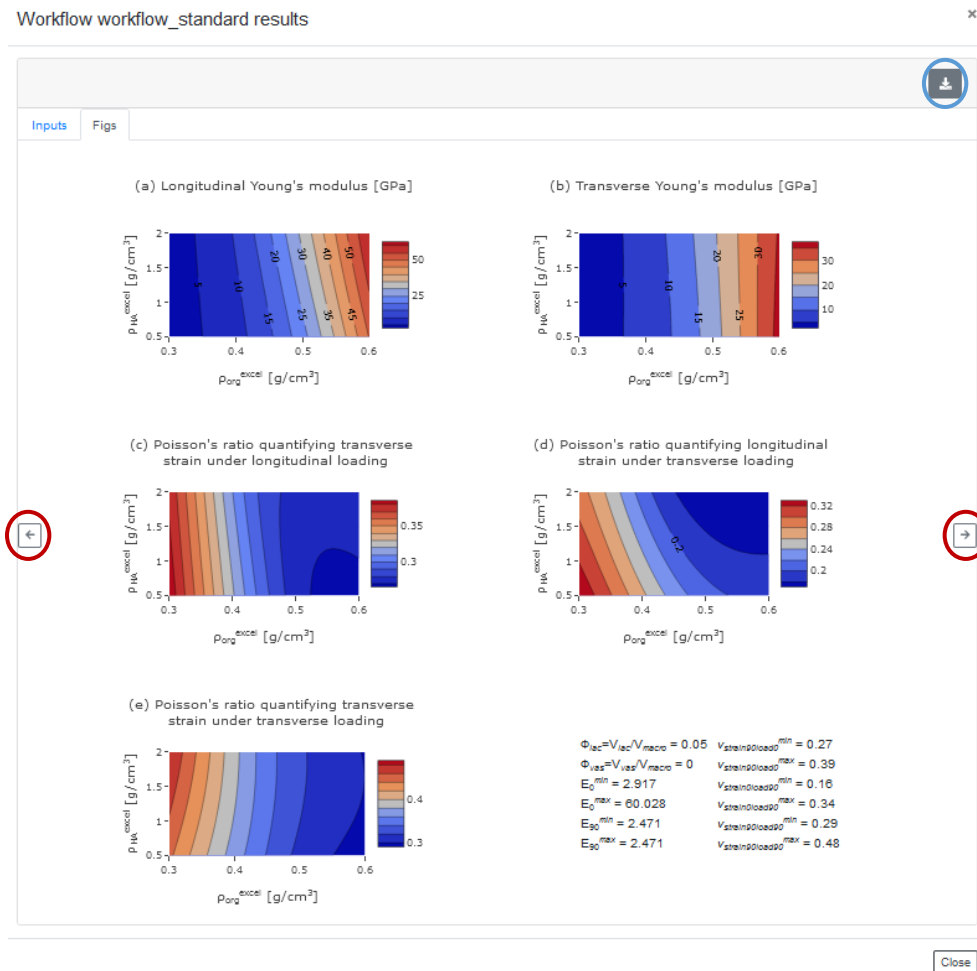


Figure 68. Results section: (a) Overview of input parameters, (b) figures.

6.13 Model – TissueEngUlt + TissueEngElast; Responsible partner - TUW

Model – TissueEngUlt+ TissueEngElast	Responsible partner - TUW
---	----------------------------------

There are two models integrated regarding “Micromechanics scaffold” on the SGABU platform (TissueEngElast, TissueEngUlt) which can be accessed through the third and fourth icon in the main dashboard for Tissue engineering as presented in Figure 69.

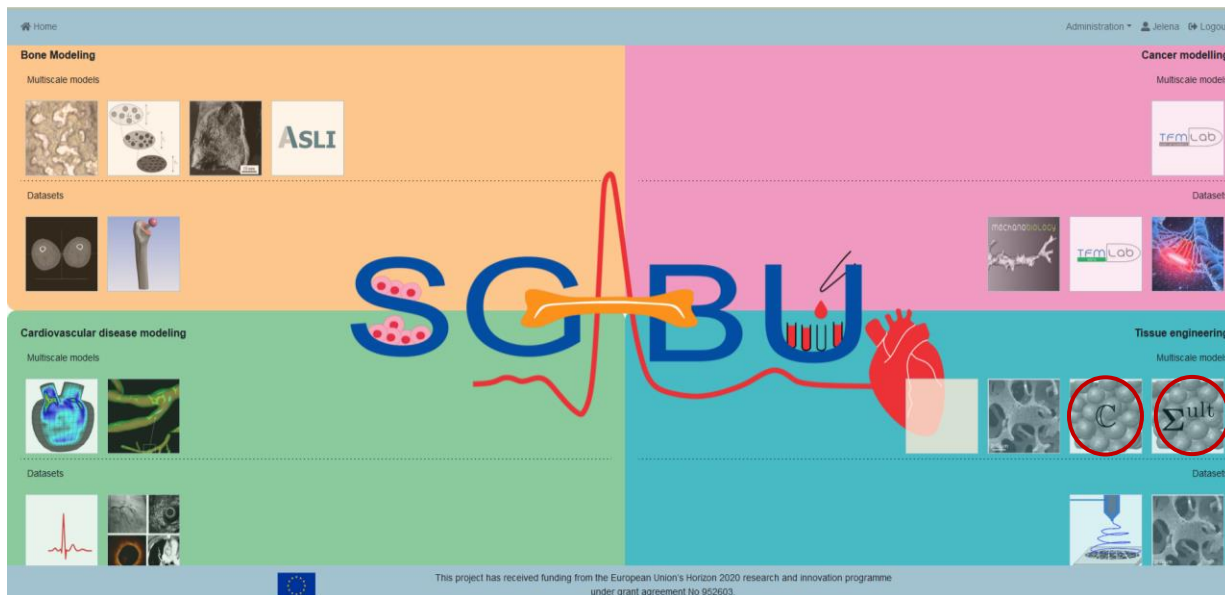


Figure 69. Main platform dashboard.

(icon for Micromechanics Scaffold adapted from Figure 1 from S. Scheiner, V. Komlev, A. Gurin, and C. Hellmich²⁵)

After clicking the respective icon, a new window appears (see Figure 70). The basic execution unit in SGABU is a workflow. In the left section of the window, users are able to see names and status of the workflows. Possible statuses of the workflow are:

- Not yet executed
- Terminated
- Running
- Finished OK
- Finished Error

²⁵ Scheiner, S., Komlev, V. S., Gurin, A. N., & Hellmich, C. (2016). Multiscale Mathematical Modeling in Dental Tissue Engineering: Toward Computer-Aided Design of a Regenerative System Based on Hydroxyapatite Granules, Focussing on Early and Mid-Term Stiffness Recovery. *Frontiers in Physiology*. doi:<https://doi.org/10.3389/fphys.2016.00383>

In the right section of the window, users can create new workflows for this submodule. Each of the forms needs to be filled out in order for the simulation to run. For both models, users are expected to fill out the following forms:

- Workflow name
- Crack density
- Filling degrees
- Mass density

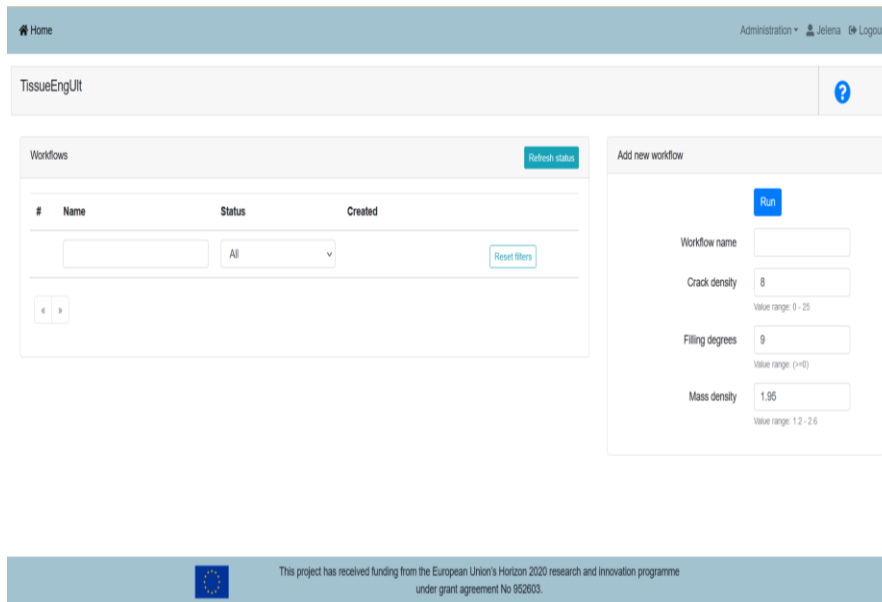


Figure 70. User Interface for TissueEngUlt model.

All forms except for the workflow name are numerical. The workflow name can be freely chosen. For “Crack density” a value between 0 and 25, for “Filling degrees” a value ≥ 0 , for “Mass density” a value between 1.2 and 2.6 should be entered. The exception handling is integrated into the user interface (UI) of the SGABU platform, see Figure 71.

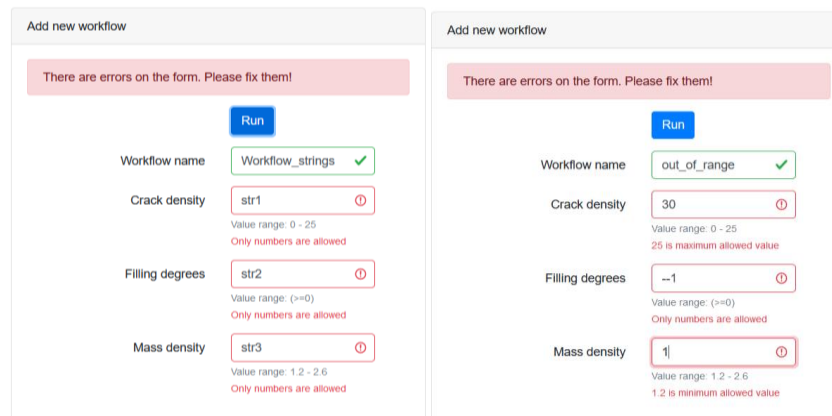


Figure 71. Exception handling.

Once everything is correctly filled, the workflow can be started. The user can monitor the current status of the workflow in the left section of the window. Table 6 shows the summarized information for the input parameters.

Table 6. Inputs for the TissueEng workflows.

Name of the parameter	Label	Explanation	Unit	Range	Default value
Crack density	ϵ	The resolution of the crack density parameter relating to the cracks pervading the granules, quantified in terms of the number of intermediate values, distributed equidistantly between the lower limit of the crack density parameter (i.e., 0), and the upper limit (i.e., 25).	/	0-25	8
Filling degrees	BFD	A further resolution value, again quantified in terms of the number of intermediate values between lower and upper limits of parameters that are varied in the computations. This concerns the macroscopic porosity of the material, which is varied between 0.1 and 0.9; and the so-called bone filling degree BFD, varied between 0 and 1, quantifying how much of the macroscopic pore space is filled with newly deposited extracellular bone tissue.	/	≥ 0	9
Mass density	ρ_{mass}	The mass density of the extracellular bone tissue, which is micromechanically translated into a corresponding stiffness, see the bone apps for more details	g/cm ³	1.2-2.6	1.95

On this basis, respective plots are generated. In particular, TissueEngElast generates contour plots showing the macroscopic Young's modulus and Poisson's ratio as functions of the macroscopic porosity and the BFD, for the selected values of the crack density parameter, see Figure 72. Furthermore, TissueEngUlt generates contour plots of the elastic limits (or ultimate loading) of the macroscopic materials, also as functions of the macroscopic porosity and the BFI, for the selected values of the crack density parameter, see Figure 73. User can find additional details in references.^{25,26}

²⁶ Scheiner, S., Komlev, S. V., & Hellmich, C. (2016). Strength increase during ceramic biomaterial-induced bone regeneration: a micromechanical study. *Int J Fract* 202, 217–235. doi:<https://doi.org/10.1007/s10704-016-0157-z>

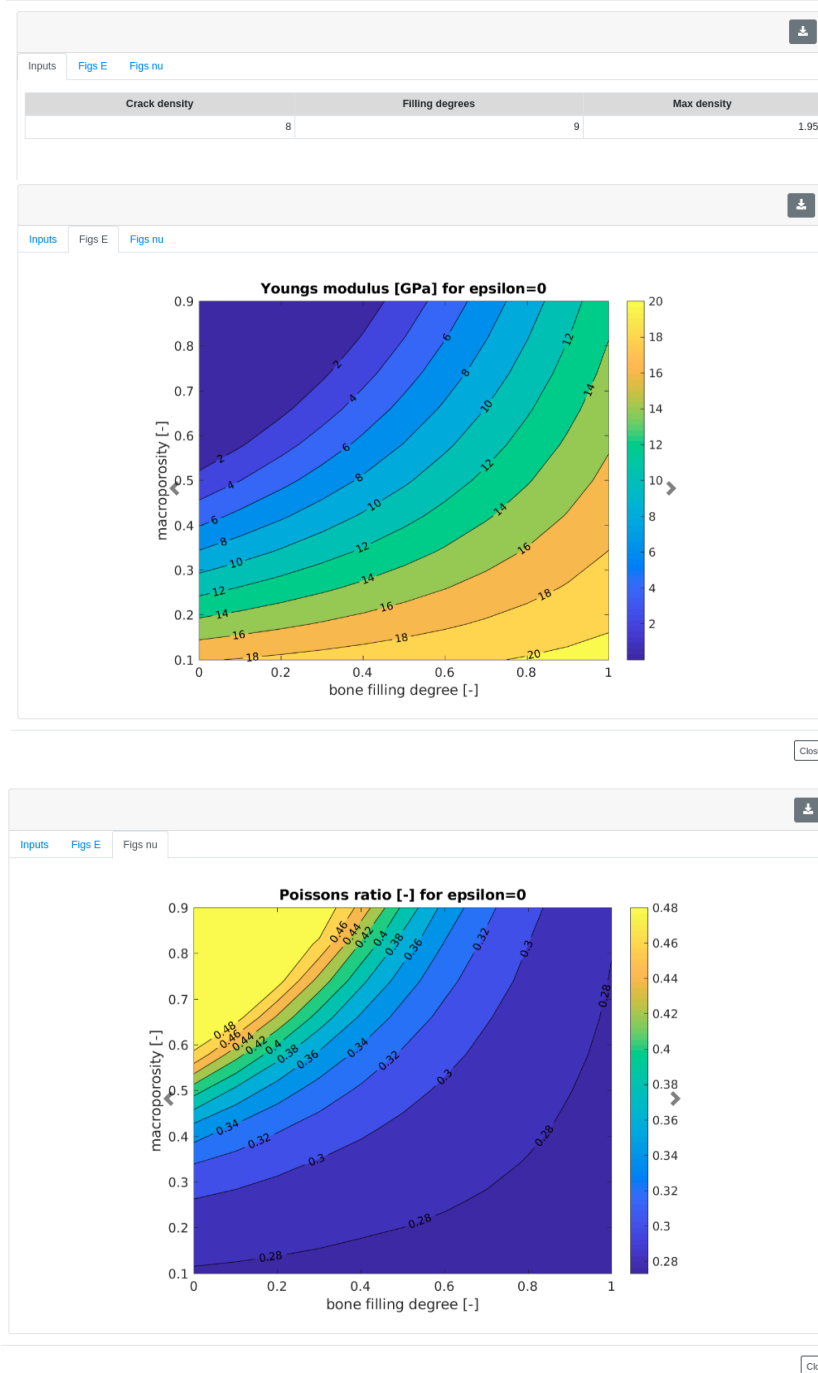


Figure 72. Displayed results for the TissueEngElast model.

Crack density	Filling degrees	Max density
8	9	1.95

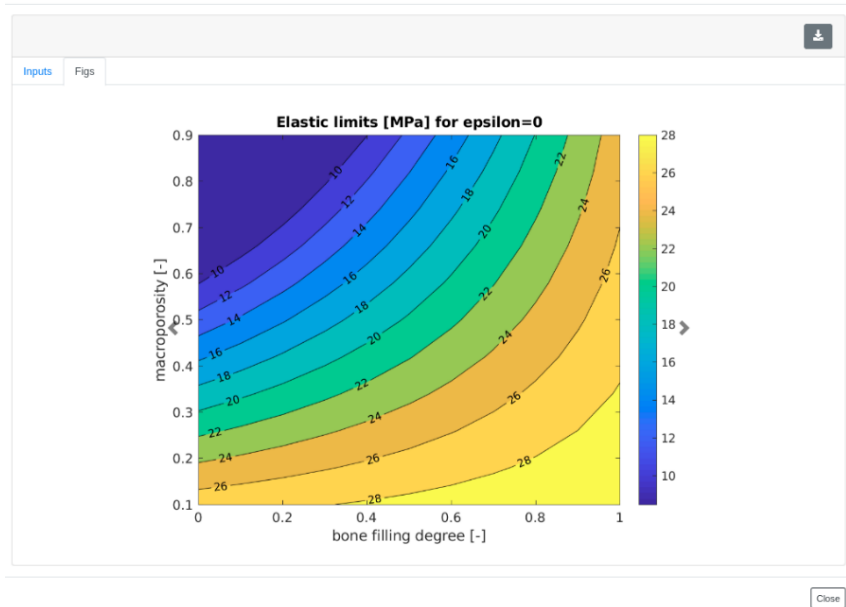


Figure 73. Displayed results for the TissueEngUlt model.

6.14 Model – Plaque progress; Responsible partner - UOI

Model - Plaque progress	Responsible partner - UOI
--------------------------------	----------------------------------

The plaque growth workflow can be accessed in the cardiovascular disease modeling module through the main dashboard of the SGABU platform (Figure 74).

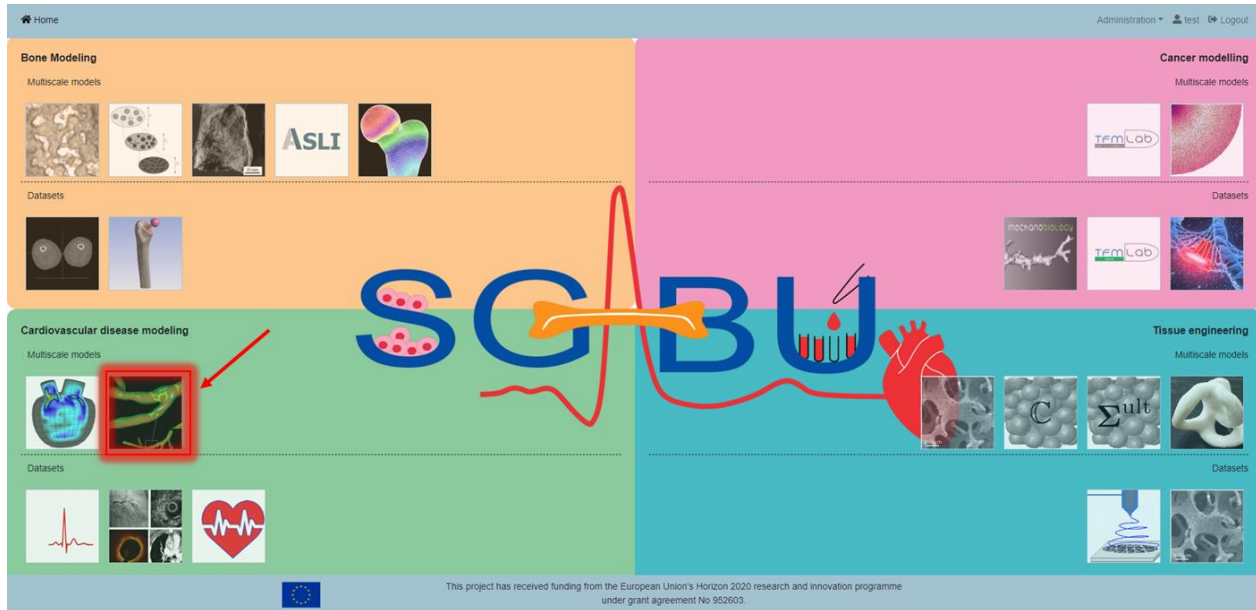


Figure 74. Locating the plaque growth workflow in the SGABU platform.

Upon accessing the plaque growth workflow, a user will observe two sections, namely the “Workflows” and “Add new workflow”, which are depicted in Figure 75. The workflows section includes a collection of simulation runs along with their current status and the date in which they were created. Namely possible status states include: “NOT_YET_EXECUTED”, “TERMINATED”, “RUNNING”, “FINISHED_OK” and “FINISHED_ERROR”.

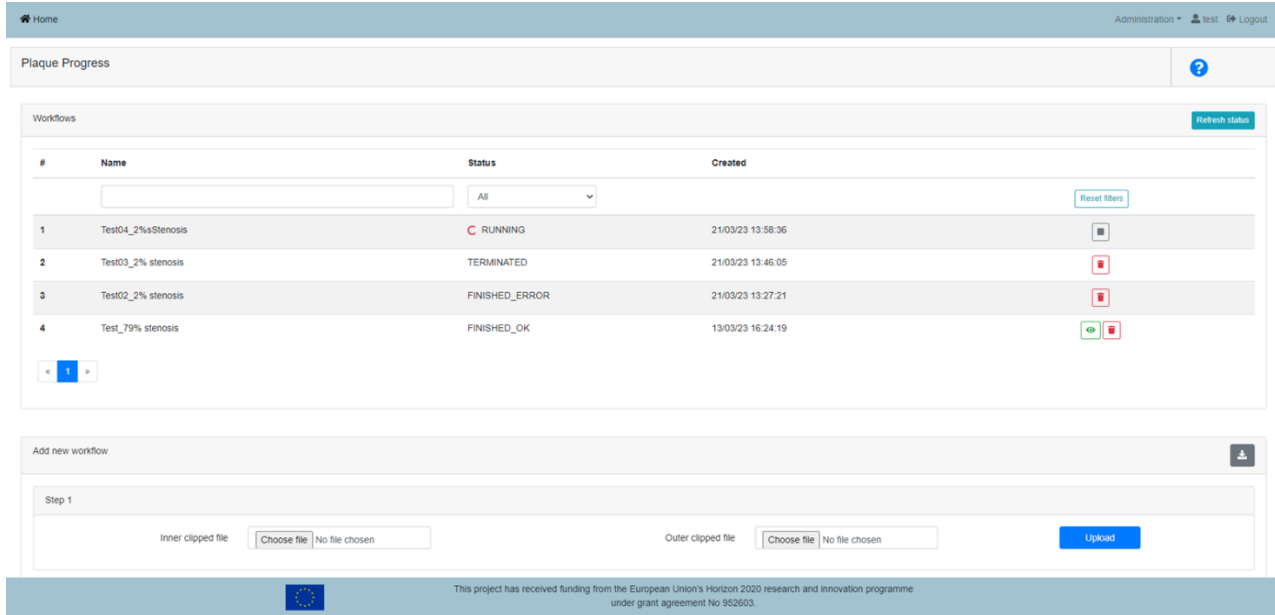


Figure 75. The dashboard of the plaque growth workflow.

The finished-ok status corresponds to a simulation run which has run successfully. The finished-error status corresponds to a simulation run which could not run successfully due to an error. The running status corresponds to an analysis which is still running in the background. The terminated status corresponds to an analysis which has been paused by the user, and lastly the not-yet-executed status corresponds to an analysis which has not been initiated by the user.

The add-new-workflow section enables the user to upload in STL format the geometries of the lumen and the intima-media boundary. Although STL format constitutes the outer surface of a body, the preprocessing algorithms inside the plaque growth workflow are able to construct the mesh that corresponds to the full volume of the lumen and the intima wall. The feature “Inner clipped file” allows the user to upload the outer surface of the lumen, while the feature “Outer clipped file” allows the user to upload the outer surface of the intima. Upon successful uploading of both geometries the platform allows the user with the provision of two “Show” features to visualize them with the help of the in-browser Paraview Glance (Figure 76).

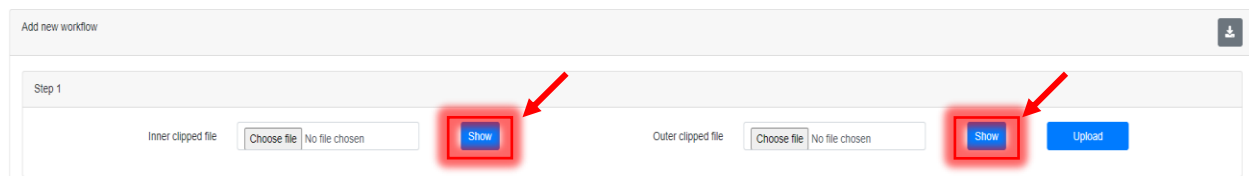


Figure 76. Provision of show features upon successful uploading of the geometries.

The visualization of the geometry enables the user to verify that the geometry he/she uploaded is correct. Inside Paraview Glance several features can be found on the left of the screen which control the representation type of the geometry, the mesh, the color of the geometry or the background, the type of system orientation axis, etc. (Figure 77).

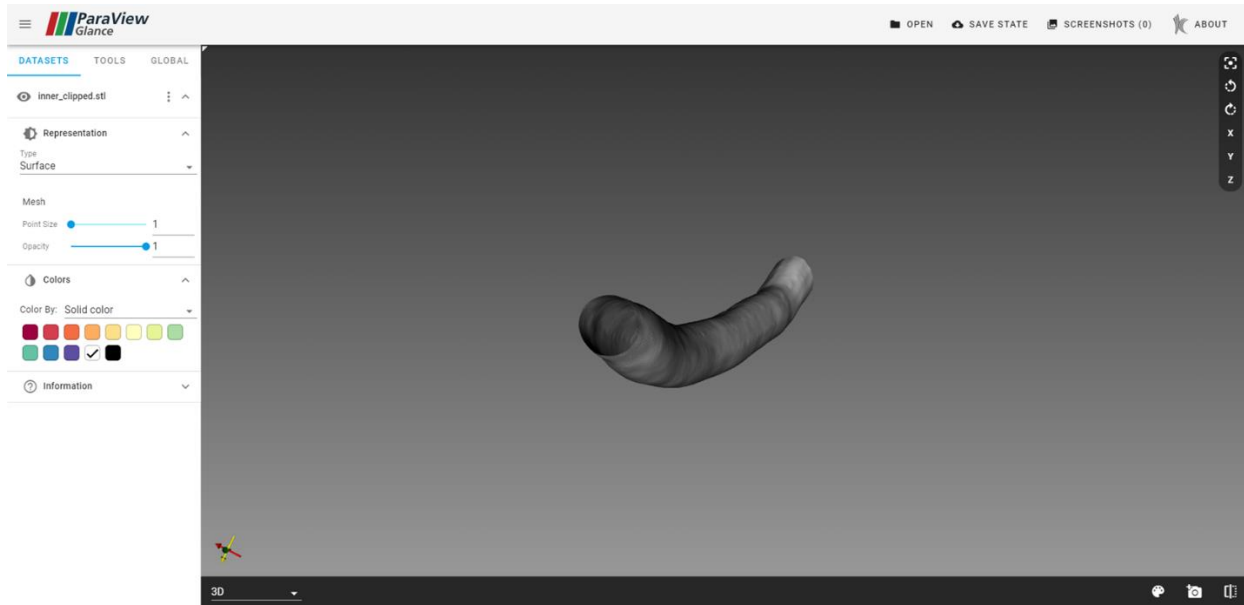


Figure 77. Visualization of the lumen geometry inside Paraview Glance.

After successful uploading of the lumen and intima wall, a template shows up with different input parameters that control the mesh and the physics of the simulation analysis (Figure 78).

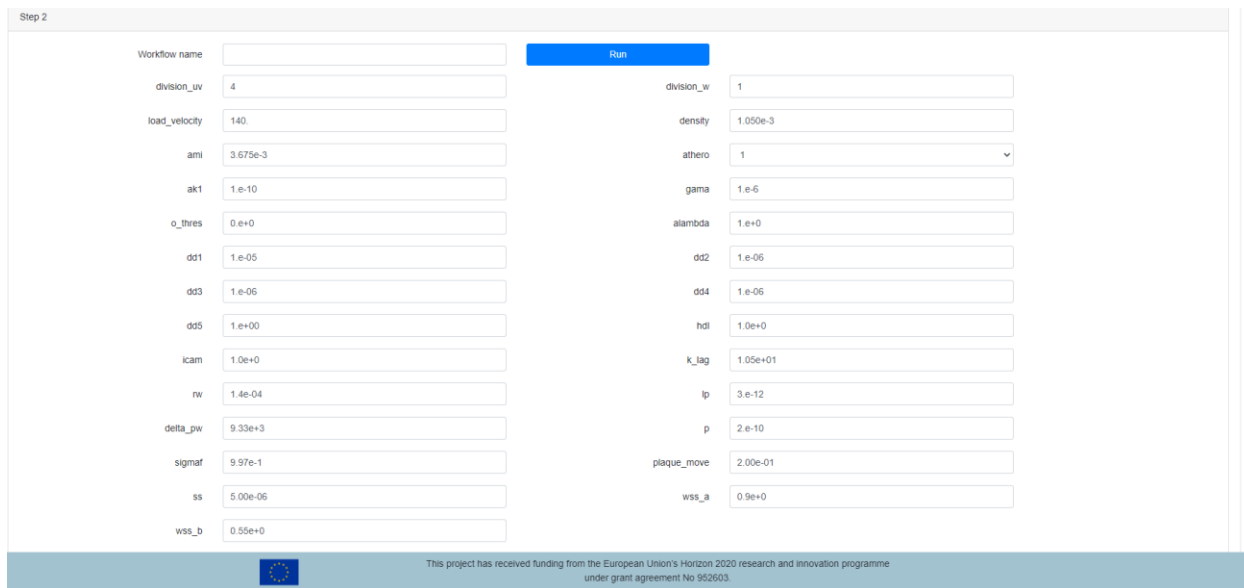


Figure 78. The template of the input parameters.

In brief, the plaque growth problem^{27,28} is modeled by the Navier-Stokes and continuity equations for the motion of the fluid flow inside the lumen:

²⁷ Filipovic, Nenad, et al. "ARTreat project: three-dimensional numerical simulation of plaque formation and development in the arteries." IEEE Transactions on Information Technology in Biomedicine 16.2 (2011): 272-278.

²⁸ Filipovic, N., et al. "ARTREAT project: Computer, experimental and clinical analysis of three-dimensional plaque formation and progression in arteries." J Serb Soc Comput Mech 5 (2011): 129-146.

$$-\mu \nabla^2 u_l + \rho(u_l \cdot \nabla) + \nabla p_l = 0, \quad (1)$$

$$\nabla u_l = 0, \quad (2)$$

where μ and ρ is the dynamic viscosity and density of the blood, respectively, u_l is the velocity vector of blood inside the lumen and p_l is the pressure of blood inside the lumen. For fluid flow inside porous materials like the intima wall the Navier-Stokes equations take the form of the Darcy's formula, while the continuity equations remain the same:

$$u_w - \frac{\kappa_w}{\mu} \nabla p_w = 0, \quad (3)$$

$$\nabla u_w = 0, \quad (4)$$

where u_w is the velocity vector of blood inside the intima wall, p_w is the pressure of blood inside the intima wall and κ_w is the Darcian permeability of blood in the intima wall. The transport of LDL inside the lumen is modeled with diffusion-convection equations:

$$\nabla \cdot (D_l \nabla c_l + c_l u_l) = 0, \quad (5)$$

where D_l is the LDL diffusion coefficient inside the lumen and c_l is the concentration of LDL inside the lumen. The transport of LDL inside the intima is modeled with diffusion-convection-reaction equations:

$$\nabla \cdot (D_w \nabla c_w + K_{lag} c_w u_w) = r_w c_w, \quad (6)$$

where D_w is the LDL diffusion coefficient inside the intima wall, c_w is the concentration of LDL inside the intima wall, K_{lag} is the LDL lag coefficient and r_w is the consumption rate of LDL which is oxidized and transforms to oxidized LDL (OxLDL). The equations that model the fluid motion and LDL transport in the lumen and the wall are coupled with the Kedem-Katchalsky equations that model the transport of LDL and blood through the endothelium membrane. These equations take the form:

$$J_v = L_p (\Delta p - \sigma_d \Delta \pi), \quad (7)$$

$$J_s = P \Delta c + (1 - \sigma_f) J_v \bar{c}, \quad (8)$$

where J_v is the transmural velocity, L_p is the hydraulic conductivity, Δp is the pressure drop through the endothelium, $\Delta \pi$ is the osmotic pressure difference, J_s is the LDL flux through the endothelium, P is the LDL endothelial permeability, Δc is the LDL concentration difference, \bar{c} is the mean concentration, and σ_d and σ_f represent reflection coefficients. Note that for the modeling of this problem osmotic gradients across the endothelium are neglected, and thus we have that $\Delta \pi = 0$.

The inflammation process that describes the evolution of plaque growth in the wall is modelled with three extra partial differential equations:

$$\partial_t O_x = d_1 \Delta O_x - k_1 O_x \cdot M, \quad (9)$$

$$\partial_t M + \text{div}(v_w M) = d_2 \Delta M - k_1 O_x \cdot M + S / (1 + S), \quad (10)$$

$$\partial_t S = d_3 \Delta S - \lambda S + k_1 O_x \cdot M + \gamma (O_x - O_x^{thr}), \quad (11)$$

where O_x , M , S are the oxidized LDL, the macrophages and cytokines concentration in the wall, respectively, d_1, d_2, d_3 are their corresponding diffusion coefficients, k_1 is the plague growth coefficient, λ is the cytokine degradation rate, γ is the OxLDL detection rate and O_x^{thr} is the threshold upon which

cells sense the presence of OxLDL and start to produce cytokines. A more detailed description of the above-mentioned model and equations can be found in the following work.^{27,28}

After successful completion of a simulation run, a green eye button will appear in the workflows section which allows the user for viewing the results. Upon pressing the green eye, a pop-up window appears which allows the user to review the values of the input parameters and view the results in 3D animation. The results are classified into three categories, namely the lumen, the shell and the wall results. In Figure 79 the shear stress in the lumen has been prompted.

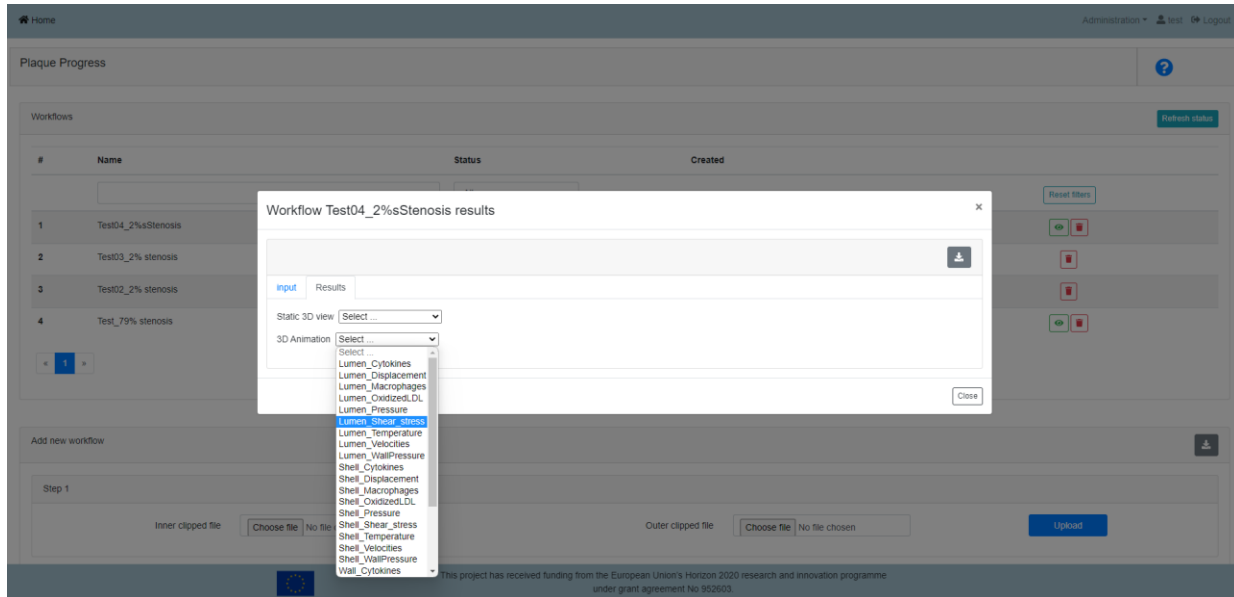
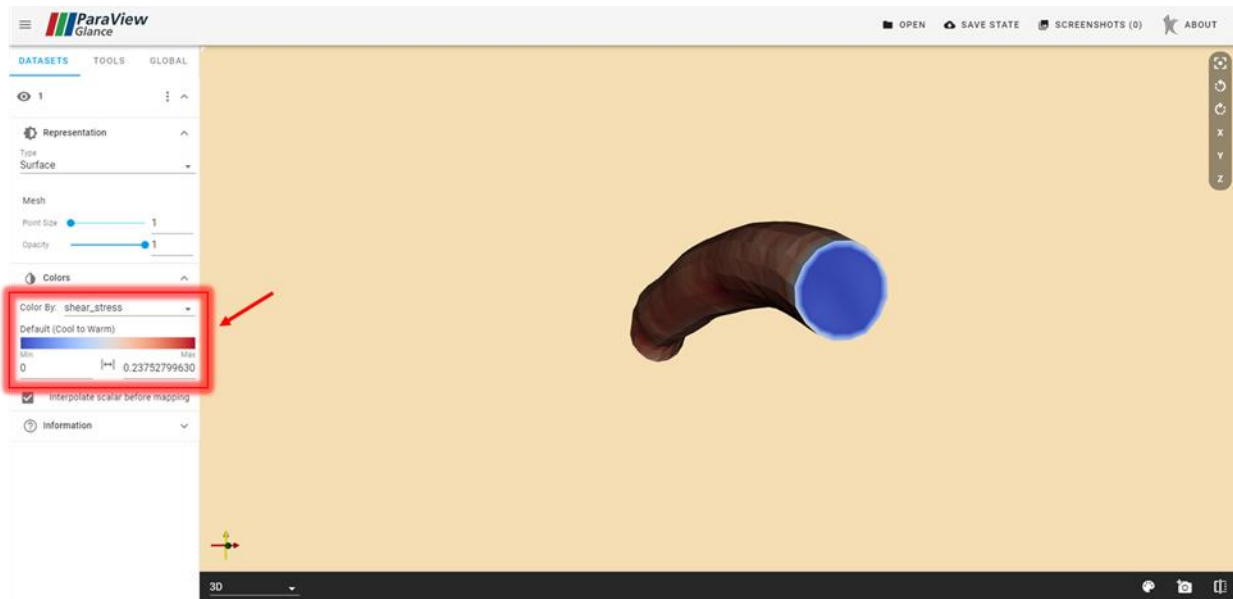
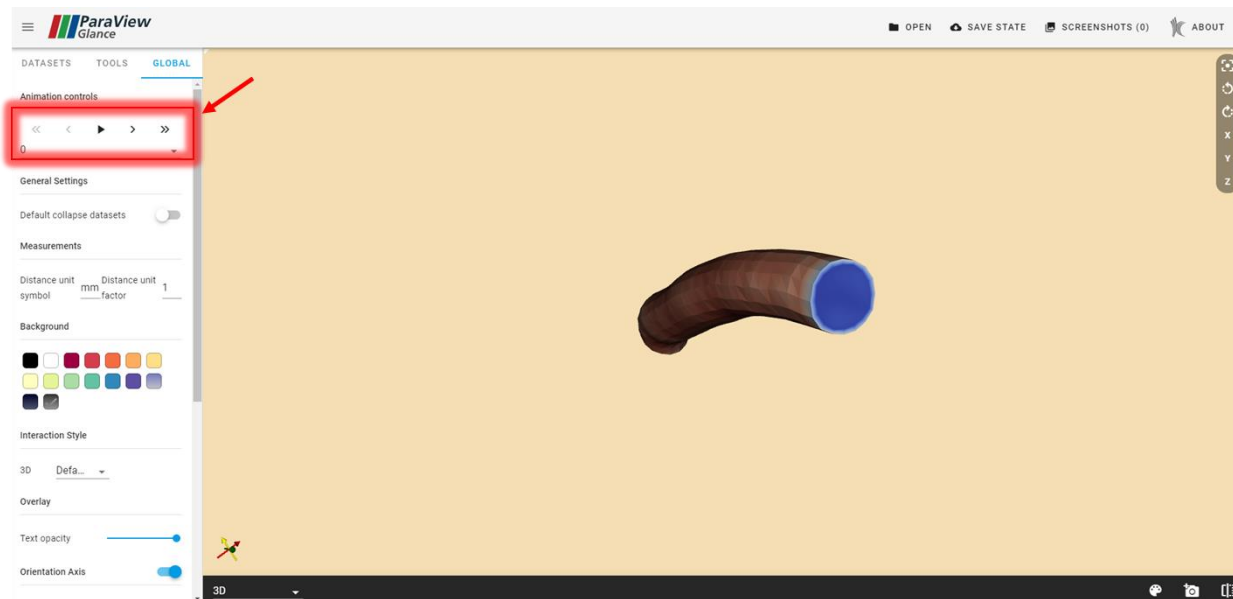


Figure 79. Prompting to view the 3D animated results of the shear stress in the lumen.

A window inside Paraview Glance opens which allows for the visualization of the results. In this case, the results of the shear stress in the lumen are shown as color-coded values imprinted upon the geometry of the body. The color-coded range that corresponds to the minimum and maximum values of the shear stress in the lumen is located in the datasets tab under the colors settings (Figure 80a). In the Global settings the user can find the animation controls, which include the play/stop options and extra options that allow to view the results between consecutive or more time frames (Figure 80b).



(a) The red frame shows the color range of the lumen shear stress results in the datasets tab.



(b) The red frame shows the animation controls in the global tab.

Figure 80. Viewing the results of the lumen shear stress inside Paraview Glance.

Mediators of the plague progression are the oxidized LDL, the cytokines and the macrophages which transform into foam cells (which represent the plague) after digesting the oxidized LDL. Figure 81 shows the selection of the oxidized LDL in the wall.

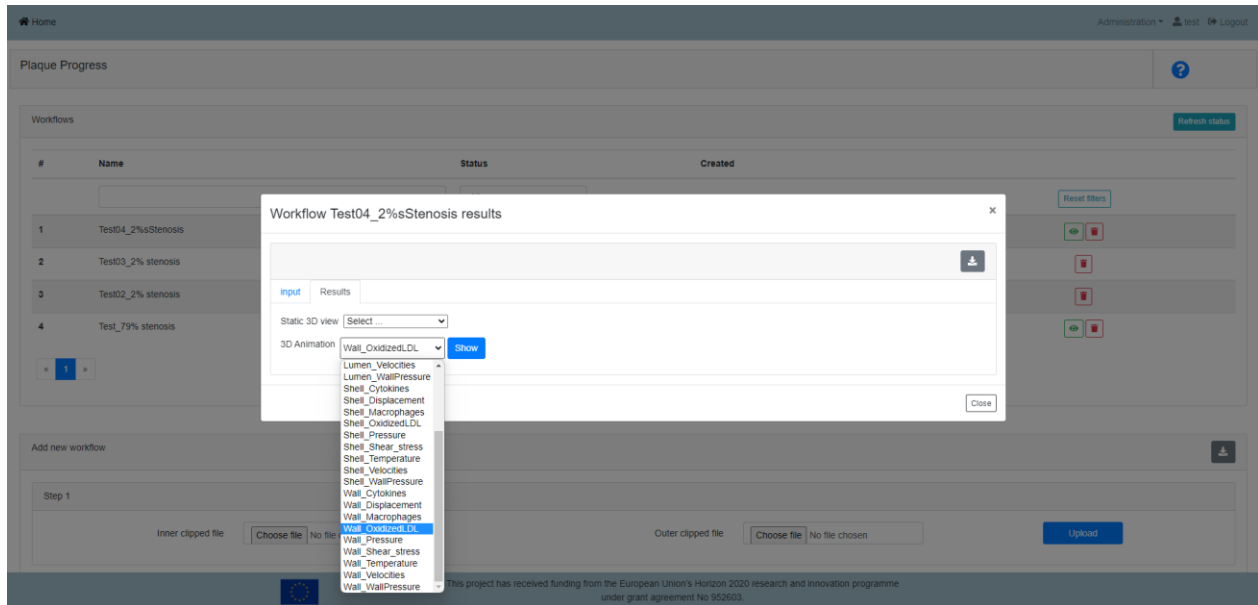
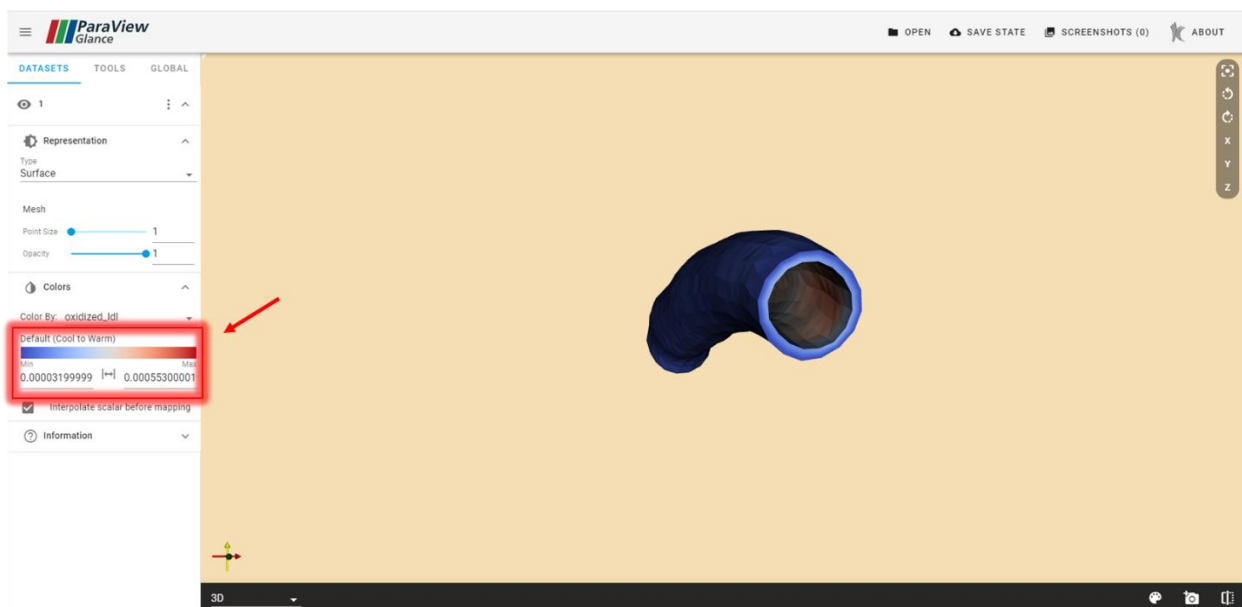
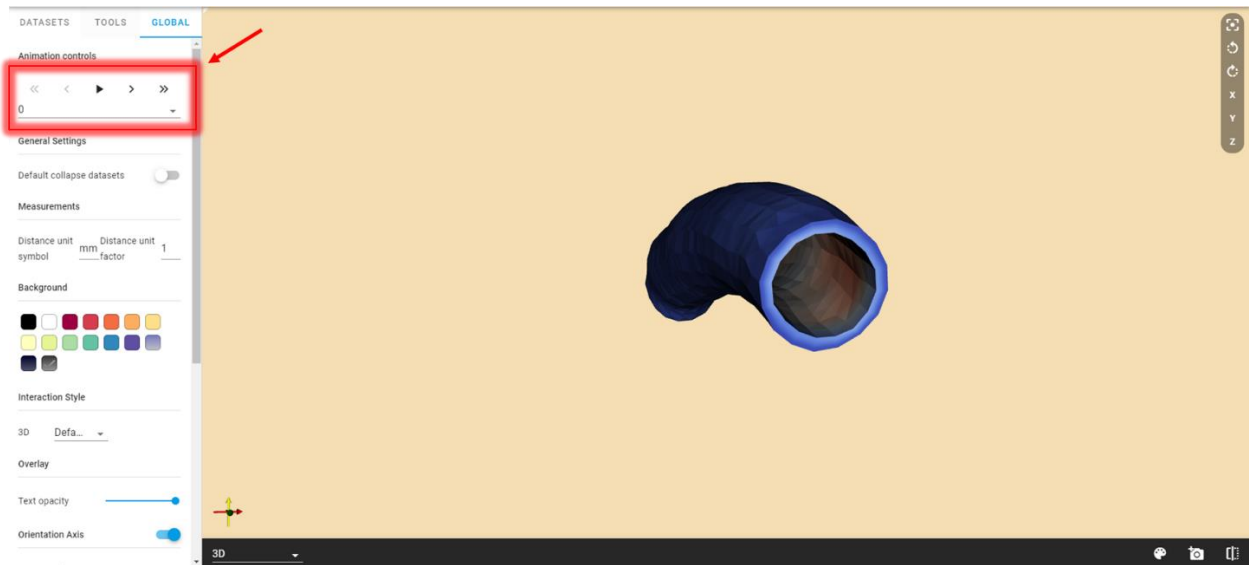


Figure 81. Prompting to view the results of the oxidized LDL in the wall.

Similarly, the window inside Paraview Glance allows for the visualization of the OxLDL results. The distribution of the OxLDL is shown in color coded values imprinted upon the geometry of the intima wall. Figure 82a shows encapsulated in a red frame the color spectrum that corresponds to the minimum and maximum values of the OxLDL in the wall. The evolution of the OxLDL can be viewed in different solution time steps with the animation controls located in the global settings tab (Figure 82b).



(a) The red frame shows the color range of the OxLDL results in the datasets tab.



(b) The red frame shows the animation controls in the global tab.

Figure 82. Viewing the results of the OxLDL in the wall inside ParaView Glance.

6.15 Model – ASLI; Responsible partner - KUL

Model - ASLI	Responsible partner - KUL
--------------	---------------------------

Access to ASLI²⁹ (A simple lattice infiller) on the SGABU platform is provided through the main dashboard shown in Figure 83. ASLI is a tool that gives users the ability to provide functionally graded lattice infills to 3D geometries. The provided infill is constructed out of unit cells, described by implicit functions, whose type, size and feature can be varied locally based on user provided inputs. The resulting geometries can be 3D printed or used to create FE-models for computational analysis.

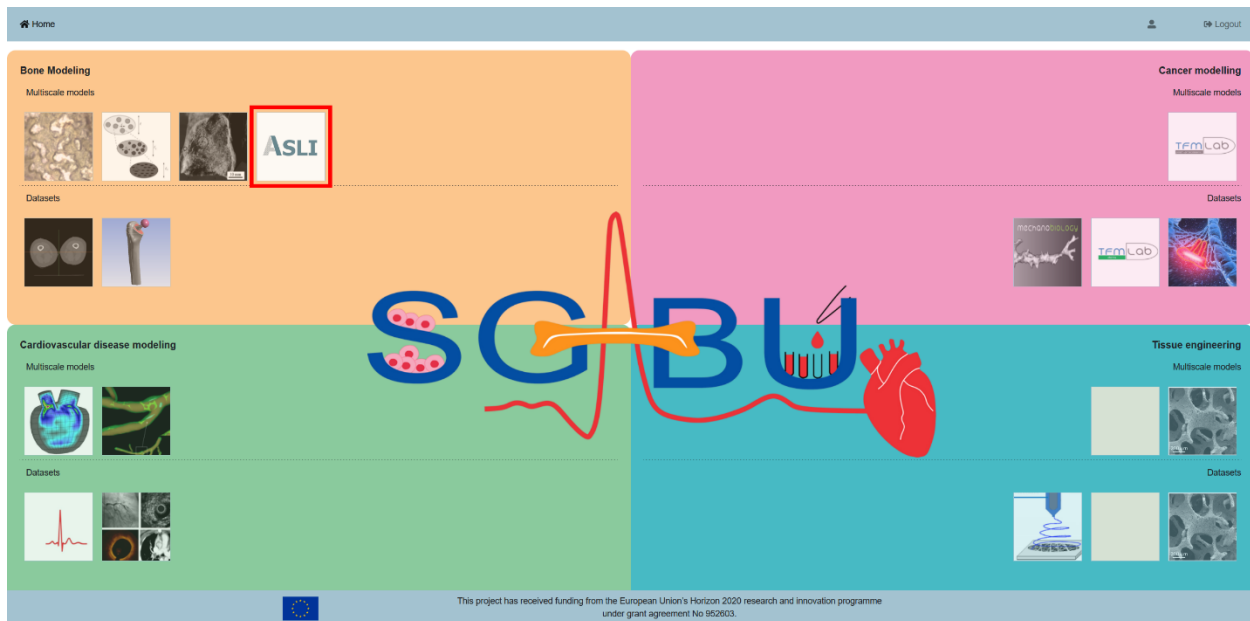


Figure 83. Main platform dashboard.

The user interface of ASLI on the SGABU platform can be seen in Figure 84. The interface is divided in two sections: *Workflows* and *Add new workflow*. In the *Workflows* section users can find the status of previously initiated workflows. The possible statuses of the workflows are:

- Not yet executed
- Terminated
- Running
- Finished OK
- Finished Error

In the *Add new workflow* section users can create a new workflow. To this end users are required to fill in the following fields:

²⁹ Perez-Boerema, F., M. Barzegari and L. Geris (2022) A flexible and easy-to-use open-source tool for designing functionally graded 3D porous structures, *Virtual and Physical Prototyping*, 17:3, 682-699, DOI: 10.1080/17452759.2022.2048956

D6.3 - Materials for teaching and learning purposes



- Workflow name
- STL file (geometry)
- YML file (Yaml configuration file)

Depending on the specifications given in the configurations file, one or more of the following optional fields may also be required:

- SAP file (Unit cell size specification)
- TAP file (Unit cell type specification)
- FAP file (Unit cell feature specification)

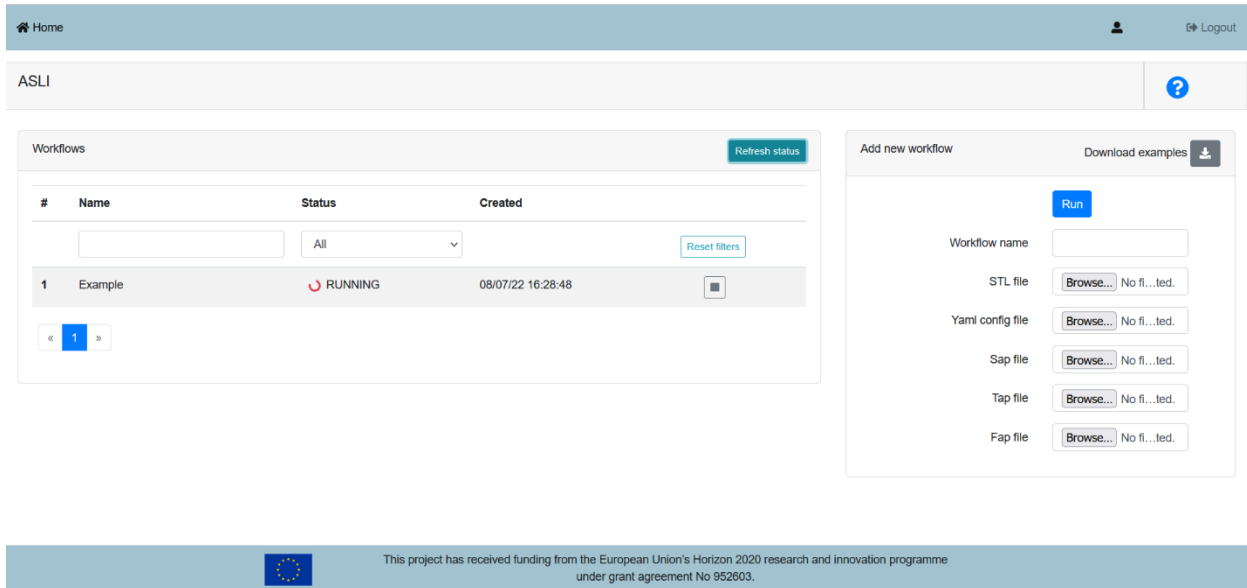


Figure 84. User Interface of the ASLI module.

Except for the field where the workflow name is defined, all fields require input files to be specified. The STL file should contain the surface³⁰ of the geometry that is to be provided of an infill while the YML file is the text document used to pass to ASLI the user settings. A template of the YML file is given in Table 7 and a detailed description of the parameters is given in Table 8. The remaining 3 file types, i.e. SAP, TAP and FAP, all have the same structure. Specifically, they are comma separated files where the first three columns correspond to the x, y and z coordinate and the fourth column correspond to the size, type or feature specified.

Table 7. Configuration file template.

```
# ---- CONFIGURATION FILE ---- #
# Input & output files
files:
  stl: _.stl
  tap: _.tap
```

³⁰ The surface must be at the watertight closed surface.


```
sap: _.sap
fap: _.fap
output: outputs/

# Lattice settings
lt_type: gyroid
lt_type_filterRadius: 1.0
lt_type_correctionFactor: 0.25
lt_size: 0.5
lt_feature: isovalue
lt_feature_val: 0.5
lt_feature_mode: relative

# Mesh settings
me_mesher: CGAL
me_side: scaffold
me_volumeMesh: FALSE
me_nThreads: 1

# Mesh settings (CGAL)
me_facetAngle: 0
me_facetSize: 0
me_facetDistance: 0.015
me_cellRadiusEdgeRatio: 0
me_cellSize: 0
me_preserveEdges: TRUE
me_poissonOffset: 0

# Mesh settings (MMG)
me_hvol: 0
me_hinitial: 0
me_hmin: 0
me_hmax: 0
me_hausd: 0.42
me_hgrad: 0
```

In order to help users become acquainted with the workflow and file formats, four data sets have been made available through the SGABU platform. These datasets can be downloaded by clicking on the download button  at the top of the *Add new workflow* section in the ASLI module. When clicking on

the download button a ZIP file containing four folders will be downloaded. Each folder contains one data set with varying number of input files. The data sets and corresponding input files are:

- **Cylindrical specimen** with varying unit cell type.
 - cylinder/cylinder.stl, cylinder/config.yml, cylinder/cylinder.tap
- **Tensile specimen** with constant infill.
 - tensile/tensile_specimen.stl, tensile/config.yml, tensile/tensile_specimen.fap
- **Acetabular cup** with varying unit cell size.
 - cup/cup.stl, cup/config.yml, cup/cup.sap
- **Femoral stem** with varying unit cell type, size and feature (normalized isovalue).
 - femur/femoral_implant.stl, femur/config.yml, femur/femoral_implant.sap, femur/femoral_implant.tap, femur/femoral_implant.fap

The geometries that the provided datasets will generate are shown in Figure 85.

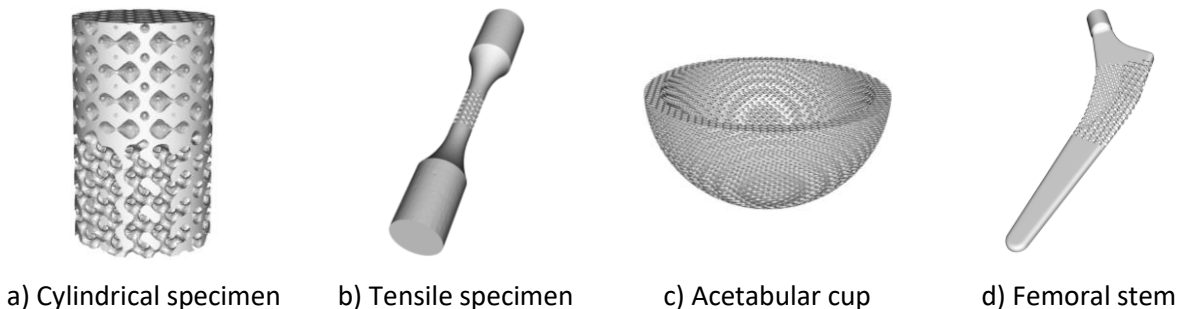


Figure 85. Geometries generated by the four sample data sets.

To run the provided examples on the SGABU platform start by downloading and decompressing the previously mentioned ZIP file. Next, go to the *Add new workflow* section in the ASLI module of the SGABU platform, give the new workflow a name and use the buttons of the STL and YML file fields to locate the STL and YML configuration file of the example you would like to run. If the example in question also includes a SAP, TAP and/or FAP file, also specify it/them using the corresponding button(s). Once all relevant input files have been selected the workflow can be started by clicking on . The current status of the workflow can be followed in the *Workflows* section of ASLI's module.

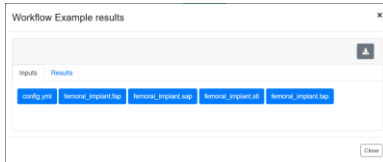
After the workflow has been successfully executed users can open the results window by clicking on the eye-icon (Figure 86a)). The results window is divided in two tabs: *Inputs* and *Outputs*. Under *Inputs* (Figure 86b)) users will find back the provided inputs while under *Outputs* (Figure 86c)) users will find the STL file containing the geometry generated by ASLI. The generated geometry can be visualized within the SGABU platform by clicking on its filename in the *Outputs* tab. The file will be displayed by ParaView in a new browser tab (Figure 86d)).

Workflows Refresh status

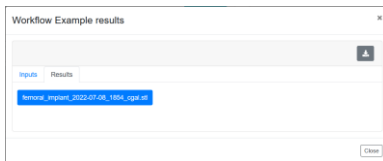
#	Name	Status	Created
<input type="text"/>		All v	Reset filters
1	Example	FINISHED_OK	08/07/22 20:33:58

« 1 »

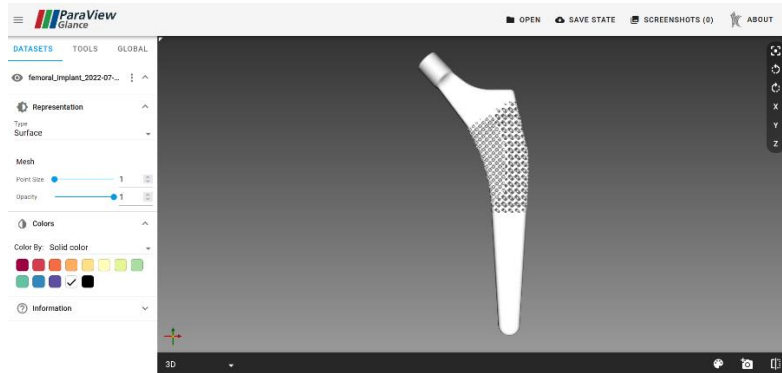
a)



b)



c)



d)

Figure 86. Result section of the ASLI module: a) *Workflows* section of the ASLI module with a successfully completed run, b) *Inputs* tab of the results window, c) *Results* tab of the results window and d) output visualization.

Table 8. Description of the input parameters found in the configuration file.

	Parameter	Default Value	Description
Inputs/Outputs	stl	Should be provided	STL file containing the object to be provided of an infill.
	tap	Should be provided	Type at point file containing local unit cell type specifications
	sap	Should be provided	Size at point file containing local unit cell size specifications.
	fap	Should be provided	Feature at point file containing local unit cell feature specifications.
	output	outputs/	Location where the output file(s) will be stored.
Infill settings	lt_type	Should be provided	Parameter specifying the unit cell type, i.e. gyroid, sheet_gyroid, diamond, sheet_diamond, primitive, sheet_primitive, IWP or sheet_IWP. To specify multiple unit cell types set to hybrid and provide a .tap.
	lt_type_filterRadius	1.0	Radius specifying the size of hybrid regions. The radius scales automatically with local unit cell size.
	lt_type_correctionFactor	0.25	Correction factor to compensate for the thinning effect of hybridization.
	lt_size	Should be provided	Parameter specifying the unit cell size. Set to a value larger than 0 for a constant unit cell size. To prescribe a variable unit cell size set to 0 and provide a .sap file.
	lt_feature	Should be provided	Parameter specifying the unit cell feature that will be specified, i.e. isovalue, volumeFraction, wallSize or poreSize.
	lt_feature_val	Should be provided	Parameter specifying the unit cell feature value. Set to a value larger than 0 for a constant feature value. To prescribe a variable feature value set to 0 and provide a .fap file. If specifying an isovalue it should be specified as a normalized isovalue.
	lt_feature_mode	relative	Parameter specifying the feature size mode, i.e. absolute or relative. Only active if lt_feature is set to wallSize or poreSize. If set to relative, provide wall and pore sizes relative to a $1 \times 1 \times 1$ unit cell.
General mesh settings	me_mesher	Should be provided	Parameter specifying the mesh library to use, i.e. CGAL or MMG
	me_side	scaffold	Parameter specifying the side of the scaffold to discretize, i.e. scaffold or void.
	me_volumeMesh	FALSE	Parameter specifying if the volume should also be discretized. Set to TRUE to discretize the volume, otherwise only the surface mesh will be generated.
	me_nThreads	1	Number of threads to use. (Parallel mode is currently only available when me_mesher is set to CGAL)
CGAL settings	me_facetAngle	30	Surface facet shape, i.e. lower bound for the surface facets angle in degrees.
	me_facetSize	Local unit cell size	Surface facet size, i.e. upper bound for the radii of surface Delaunay balls. Scales with unit cell size.
	me_facetDistance	Should be provided	Surface approximation error, i.e. upper bound for the distance between the circumcenter of a surface facet and the center of the surface Delaunay ball of this facet. Scales with the unit cell size.

D6.3 - Materials for teaching and learning purposes



me_cellRadiusEdgeRatio	3.0	Tetrahedron shape quality measure, i.e. upper bound for the ratio between the circumradius of a mesh tetrahedron and its shortest edge. Only active if me_volumeMesh is set to TRUE.
me_cellSize	Local wall size	Tetrahedra size, i.e. upper bound on the circumradii of the mesh tetrahedra. Only active if me_volumeMesh is set to TRUE. Scales with wall size.
me_preserveEdges	TRUE	Set to TRUE to preserve the edges, otherwise set to FALSE.
me_poissonOffset	0.5	Poisson reconstruction offset. Scales with largest unit cell size in the design. Only active if me_preserveEdges is set to TRUE.

	me_hvol	1.5	Maximum volume constraint of the intermediate TetGen mesh. Scales with the smallest unit cell size in the design.
	me_hinitial	0.36	Mesh size of the mesh used to compute the level-set. Scales with the smallest feature size.
MMG settings	me_hmin	Inactive	Minimum edge size. Scales with the smallest feature size in the design.
	me_hmax	Inactive	Maximum edge size. Scales with the largest feature size in the design.
	me_hausd	Should be provided	Maximal Hausdorff distance for the boundaries approximation. Scales with the mean feature size.
	me_hgrad	1.3	Gradation value. Only active if me_volumeMesh is set to TRUE.

6.16 Model – TMFLAB; Responsible partner - KUL

Model - TMFLAB	Responsible partner - KUL
----------------	---------------------------

The field of mechanobiology has a special interest in studying cell force generation using in vitro models. A crucial process for the correct development of tissues in vitro is angiogenesis or the growth of blood vessels from pre-existing vasculature. The field has developed multiple in vitro models of sprouting angiogenesis, where the initial states of growth of a new blood vessel can be tracked³¹. Moreover, a very common methodology used to calculate cell forces is called **Traction Force Microscopy (TFM)**³².

Recently, the group of **Prof. Hans Van Oosterwyck of the KU Leuven (Belgium)** developed an open-source Matlab toolbox called TFMLAB that allows for an accurate calculation of cell-induced matrix displacements and cell-generated forces around angiogenic sprouts that invade a Polyethylene Glycol (PEG) hydrogel⁷. However, the results provided by TFMLAB often require further post-processing to allow for a proper interpretation. For example, in work of Vaeyens et al.,³³ 3D matrix displacements around angiogenic sprouts were calculated but also **graphs showing the evolution of displacements along the direction of growth of a sprout** were provided.

sproutBranchAnalysis is a toolbox that can be used to post-process the output from TFMLAB and generate such graphs. In this document, we provide step-by-step instructions to use this tool.

³¹ P. Carmeliet, R.K. Jain, Molecular mechanisms and clinical applications of angiogenesis, *Nature*. 473 (2011) 298–307. <https://doi.org/10.1038/nature10144>.

³² J. Barrasa-Fano, A. Shapeti, J. de Jong, A. Ranga, J.A. Sanz-Herrera, H. Van Oosterwyck, Advanced in silico validation framework for three-dimensional traction force microscopy and application to an in vitro model of sprouting angiogenesis, *Acta Biomater.* 126 (2021) 326–338. <https://doi.org/10.1016/j.actbio.2021.03.014>.

³³ M.M. Vaeyens, A. Jorge-Peñas, J. Barrasa-Fano, C. Steuwe, T. Heck, P. Carmeliet, M. Roeffaers, H. Van Oosterwyck, Matrix deformations around angiogenic sprouts correlate to sprout dynamics and suggest pulling activity, *Angiogenesis*. 23 (2020) 315–324. <https://doi.org/10.1007/s10456-020-09708-y>

Software description

Inputs

sproutBranchAnalysis performs a post-processing operation on the results provided by the software TFMLAB. One can access this software in this Gitlab repository (manual to use TFMLAB is included): https://gitlab.kuleuven.be/MAtrix/Jorge/tfmlab_public.

The SGABU platform includes an example dataset to be run in TFMLAB as well as the resultant output folders that it should generate.

sproutBranchAnalysis only requires an output folder generated by TFMLAB. These folders typically will have a structure such as the one depicted in Figure 87.

Name	Date modified	Type	Size
■ A_rawImagesTiff_xyres0.57_zres0.50	28/03/2022 13:53	File folder	
■ B_filteredImages	28/03/2022 13:53	File folder	
■ C_shiftCorrectedImages	28/03/2022 13:53	File folder	
■ D_1_calcElastix	28/03/2022 13:53	File folder	
■ D_2_displacements	28/03/2022 13:53	File folder	
■ D_3_postShiftCorrectedImages	28/03/2022 13:53	File folder	
■ E_resultsParaview	28/03/2022 13:53	File folder	

Figure 87. Folder structure of the output of TFMLAB.

The Graphical User Interface (GUI)

The GUI of *sproutBranchAnalysis* is simple (see Figure 88). The different items in the GUI are explained below:

- **Channel name** ('beads'/'fibers'): this parameter refers to the type of marker that was used to measure displacements using TFMLAB. For the example dataset provided by SGABU, this should always be 'beads'. If the user is not sure, he/she can open the folder D_2_displacements folder and see the name of the existing subfolder.
- **Voxel size in microns (XY, Z)**: this parameter asks the user to input the size of the image voxel in microns. This can be typically obtained from the name of the A folder. Example: an A folder name of 'A_rawImagesTiff_xyres0.57_zres0.50' indicates that the voxels have a size of 0.57 microns in the XY direction while 0.5 microns in the Z direction. It is important to fill in this parameter properly. For the dataset provided with SGABU this field should be filled with '0.57' and '0.5'.
- **Number of timepoints**: this parameter asks the user to input how many timepoints were acquired in the TFM experiment. For static TFM (the most common one, as well as the one provided with SGABU), this will be equal to 1.
- **Crop. Parameters**: this button asks the user to load a specific file provided with the outputs of TFMLAB called 'paraview_param.mat'. The user can easily find it within the 'E_resultsParaview' folder and in the marker ('beads'/'fibers') subfolder.
- **Cell segmentation**: this button asks the user to load the image-based segmentation of the cell. The user can easily find it within the 'D_3_postShiftCorrectedImages' folder, followed by the marker subfolder, followed by 'cellSeg'. In this folder, the user may see multiple .mat files. The

user is free to select any of them, depending of which time point is to be analysed. *Remark: Do not select `tp_R.mat` as this is the relaxed state and there are no displacements available.*

- **Displacement field:** this button asks the user to load the matrix displacements. The user can easily find it with the 'D_2_displacements' folder, followed by the marker folder. Again, the user is free to select any of the '.mat' files, depending of which time point is to be analysed. *Remark: please select the same time point as in Cell segmentation.*
- **RUN!:** this button initiates the data processing.
- **Sprout skeletonization:** this figure will display a 2D maximum projection of the cell segmentation overlaid with its skeleton and branch points and end points labelled in green. A specific path within the skeleton will be labelled in red, indicating the path that the program will follow to perform the analysis.
- **Displacement analysis progress:** this figure will display the cell segmentation in 3D, colored with a projection of the matrix displacements on its surface. While the program progresses it will paint black the part of the cell that has been already analyzed.
- **Displacements along sprout growth direction:** this figure will display the magnitude of the displacements along the growth direction of the sprout in a similar manner as shown in literature³³.

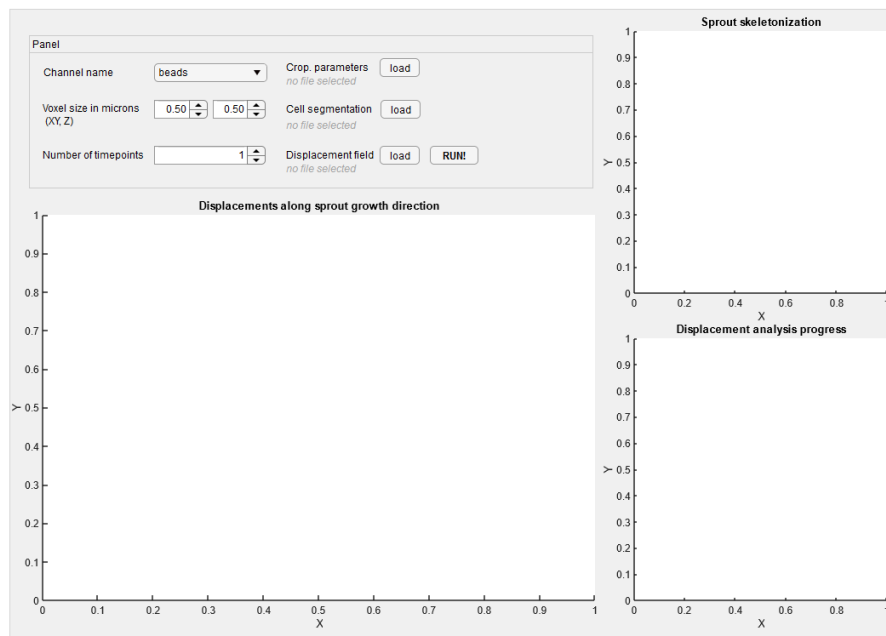


Figure 88. GUI.

Outputs

The software provides a file called `dispsAlongSprout.mat` as an output. The user can save this file in his/her local computer. Moreover, the user can save the resultant figures of the software although these can be reproduced using the data provided in `dispsAlongSprout.mat` by running the following code in Matlab:

```
load('dispsAlongSprout.mat');
```

figure

```
plot((0:length(dispsAlongSprout.disp.avgs_signed)-1)/(length(dispsAlongSprout.disp.avgs_signed)-1),dispsAlongSprout.disp.avgs_signed);
```

Within *dispsAlongSprout.mat* the user can find the values for the graphs to perform any further analysis.

Brief description of the code principles

The following description has been adapted from literature³³ with permission from the authors.

The principal direction of a sprout or protrusion – termed growth direction - was defined based on its mask and average displacement vectors in its vicinity were calculated as a function of the position along the growth direction and as a function of time (see Figure 89 – taken from literature³³).

For a given sprout the cellular mask of the first time point is skeletonized using MATLAB's function `bwskel`. The base and tip point of the sprout skeleton were automatically selected based on their position in the image. The base point is chosen from the branch points of the sprout and the cell layer skeletons. The top point is chosen from the endpoints of the sprout skeleton.

The path with the minimum geodesic distance within the 3D skeleton that connects both points, is automatically defined as the main branch of the sprout. The first eigenvector \mathbf{b}_{sprout} of the main branch is computed using principal component analysis and is defined as the sprout growth direction. In order to determine the regions in which displacements are averaged, a set of 1 μm spaced planes was defined perpendicular to \mathbf{b}_{sprout} and between tip and base of the main branch. The intersection between each plane and a 1 μm dilated version of the cellular mask is computed. Within each intersection j the average displacement vector \mathbf{u}_j is calculated as follows:

$$\mathbf{u}_j = \frac{\sum_{n=1}^N \mathbf{u}_{jn}}{N}$$

with \mathbf{u}_{jn} the displacement vector at the location n within the intersection j . The angle θ_j between \mathbf{b}_{sprout} and \mathbf{u}_j is computed using the following expression:

$$\theta_j = \text{atan2}(\|\mathbf{b}_{sprout} \times \mathbf{u}_j\|_2, \mathbf{b}_{sprout} \cdot \mathbf{u}_j)$$

where `atan2` is the four-quadrant inverse tangent, $\|\mathbf{u}\|_2$ is the L2- norm, \times is the cross product and \cdot is the dot product. An angle of 0° corresponds to an average displacement pointing from tip to base, while 180° corresponds to a displacement in the opposite direction. A signed displacement magnitude U_j was defined by multiplying the 2-norm of the displacement vector with the sign of the dot product $\mathbf{b}_{sprout} \cdot \mathbf{u}_j$:

$$U_j = \|\mathbf{u}_j\|_2 \text{sign}(\mathbf{b}_{sprout} \cdot \mathbf{u}_j).$$

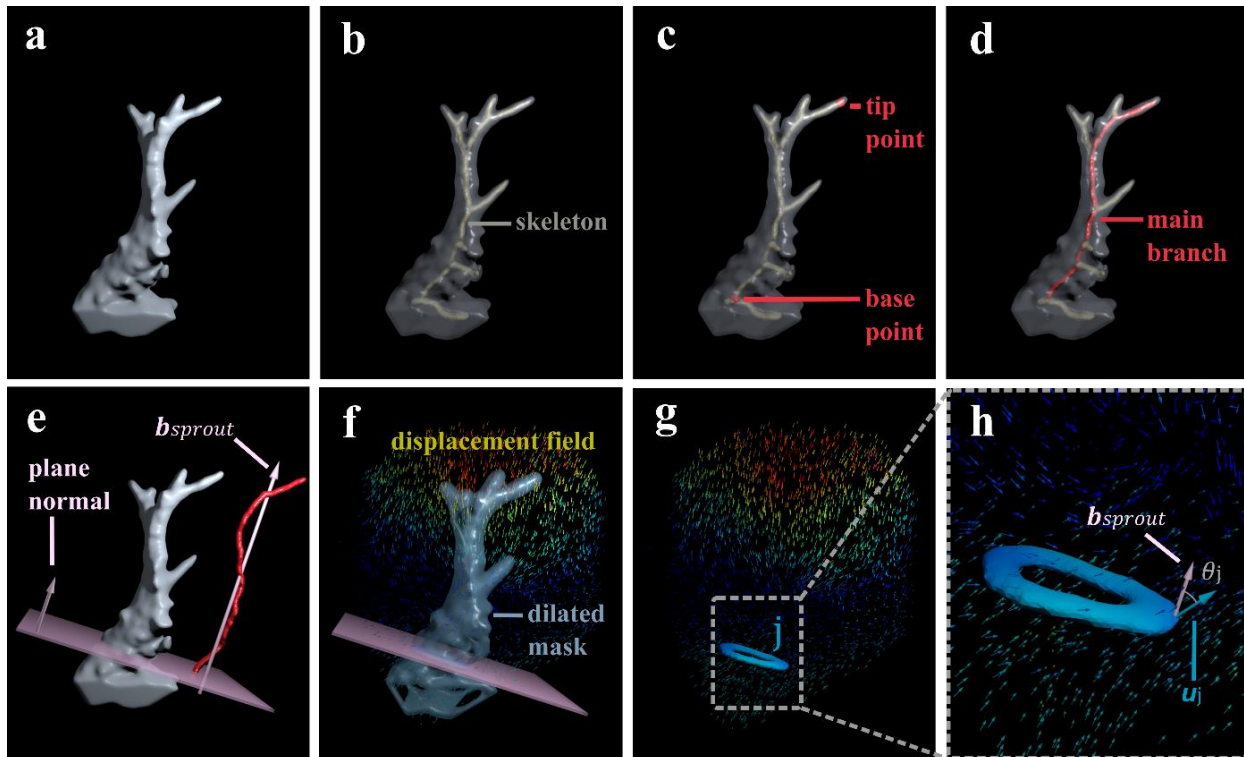


Figure 89. Illustration of procedures for calculating sprout growth direction and average displacements that are used to analyze directionality of displacements.

(a) Representative example of a 3D cellular mask of a sprout after segmentation. (b) Skeletonization of the cellular mask. Note that the opacity of the cellular mask has been modified to ease the visualization of the internal skeleton. (c) Manually selected tip and base points. (d) Calculated main branch or shortest path within the skeleton that connects the tip and base point. (e) Sprout growth direction \mathbf{b}_{sprout} (computed as the first eigenvector of the main branch) and the definition of a plane perpendicular to the growth direction. Note that the main branch has been placed outside of the cellular mask to ease its visualization. (f) Displacement around a dilated version of the cellular mask, which in combination with perpendicular planes generate intersection volumes. Note that the displacement field has been downsampled and the opacity of the dilated mask has been modified to ease visualization. (g) Representation of an intersection volume j for which the magnitude of the displacements within that volume has been projected onto its surface. (h) Close-up of the intersection volume, also showing its average displacement vector \mathbf{u}_j and angle θ_j with respect to \mathbf{b}_{sprout} .

6.17 Model – Biomaterial Corrosion; Responsible partner - UKG

Model - Biomaterial Corrosion	Responsible partner - UKG
--------------------------------------	----------------------------------

The access to the Biomaterial Corrosion model³⁴ on the SGABU platform is provided through the main dashboard as presented in the Figure 90. The model of corrosion has been developed based on Cellular Automata (CA) theory. Evolution of cell CA each occurs through a series of synchronous updates of all cells, governed by a set of rules. The computational modelling of multi-pit corrosion in medical implants based on cellular automata is divided into two sub-models - pit initiation and growth models. The state of each cell is represented by a predefined interval in the range of 0 – 255, where un-corroded cell has the value of 0 and totally corroded cell the value of 255. This means that we look at the surface as it is an image and prescribe certain rules to follow where the corrosion pit will appear (corrosion pit initiation) and then later how it will develop (corrosion growth model).

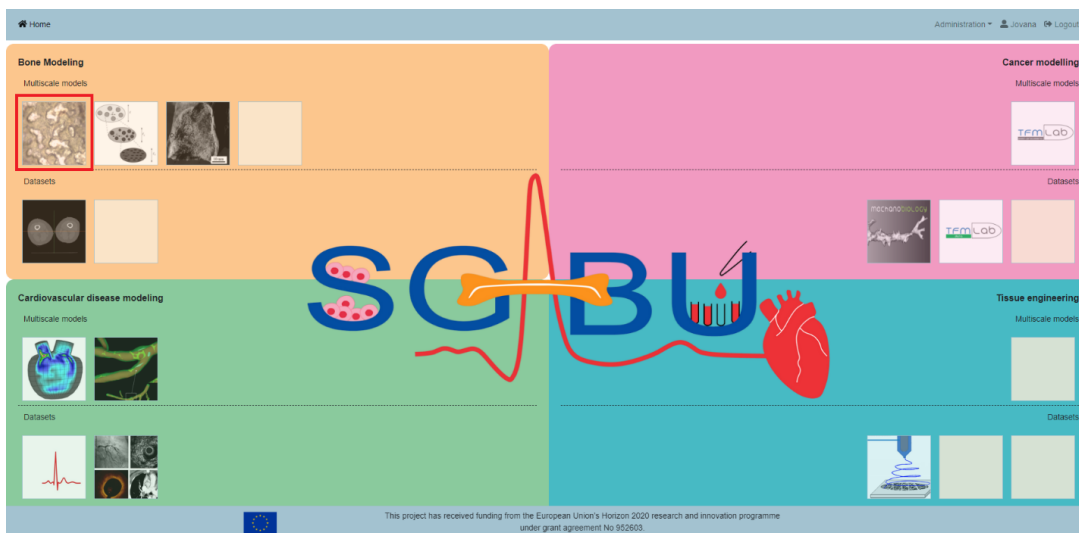


Figure 90. Main platform dashboard; marked CorrosionPit model.

User Interface for CorrosionPit example is shown in Figure 91. The window is divided into 2 sections. The basic execution unit in SGABU is a workflow. In the left section of the window, users are able to see names and status of the workflows. Possible statuses of the workflow are:

- Not yet executed
- Terminated
- Running
- Finished OK
- Finished Error

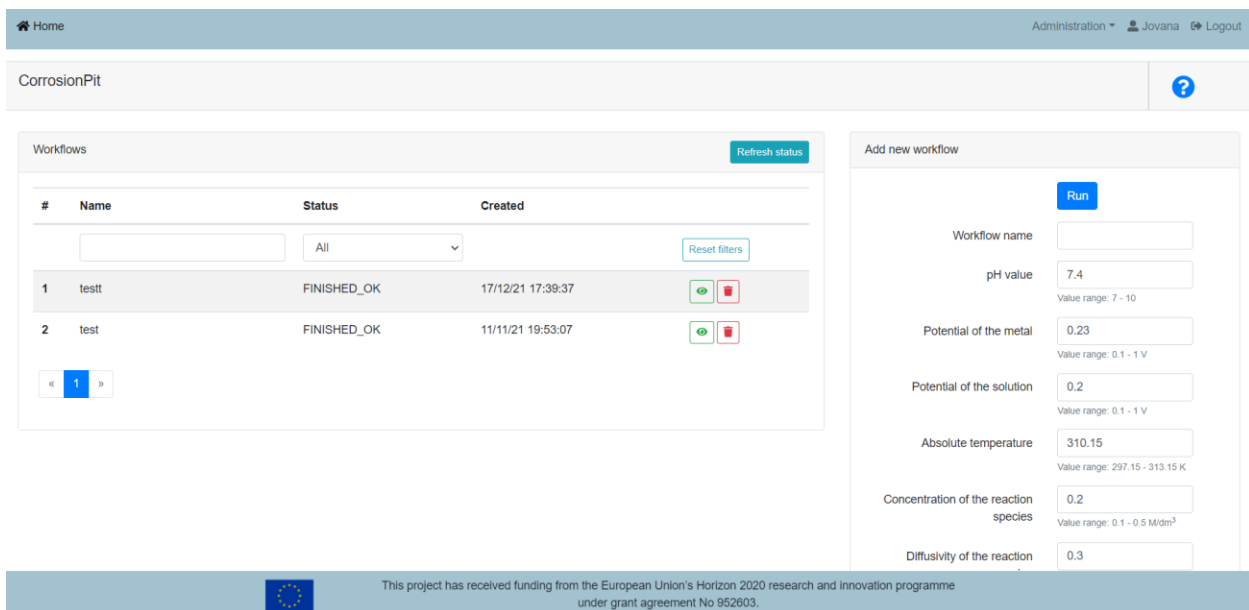
In the right section of the window, users can create new workflows for this submodule. Each of the forms

³⁴ T. Šušteršič, G. M. Simsek, G. G. Yapici, M. Nikolić, R. Vulović, N. Filipovic and N. E. Vrana, "An In-Silico Corrosion Model for Biomedical Applications for Coupling With In-Vitro Biocompatibility Tests for Estimation of Long-Term Effects," *Front. Bioeng. Biotechnol.*, vol. 9, 2021., doi: 10.3389/fbioe.2021.718026

needs to be filled out in order for simulation to run. Users are expected to fill out the following forms:

- Workflow name
- pH value
- Potential of the metal
- Potential of the solution
- Absolute temperature
- Concentration of the reaction species
- Diffusivity of the reaction species
- Charge of the reaction species
- Time of simulation

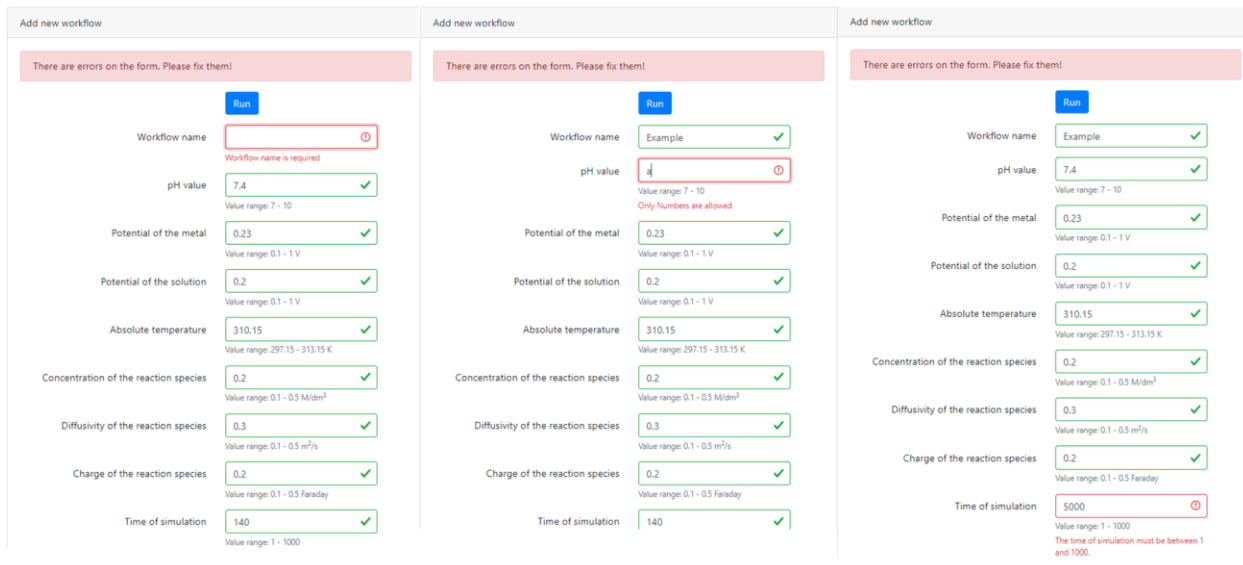
All forms except for Workflow name are numerical and value ranges are provided for the users.



The screenshot shows the CorrosionPit user interface. At the top, there is a navigation bar with 'Home', 'Administration', 'Jovana', and 'Logout'. Below this is a header for 'CorrosionPit' with a help icon. The main content is divided into two panels. The left panel, titled 'Workflows', contains a table with columns for '#', 'Name', 'Status', and 'Created'. It also includes a search bar, a status filter dropdown set to 'All', a 'Reset filters' button, and a pagination control showing '1'. The right panel, titled 'Add new workflow', features a 'Run' button and several input fields with numerical values and value ranges: Workflow name (empty), pH value (7.4, range 7-10), Potential of the metal (0.23, range 0.1-1 V), Potential of the solution (0.2, range 0.1-1 V), Absolute temperature (310.15, range 297.15-313.15 K), Concentration of the reaction species (0.2, range 0.1-0.5 M/dm³), and Diffusivity of the reaction species (0.3).

Figure 91. User Interface for CorrosionPit module.

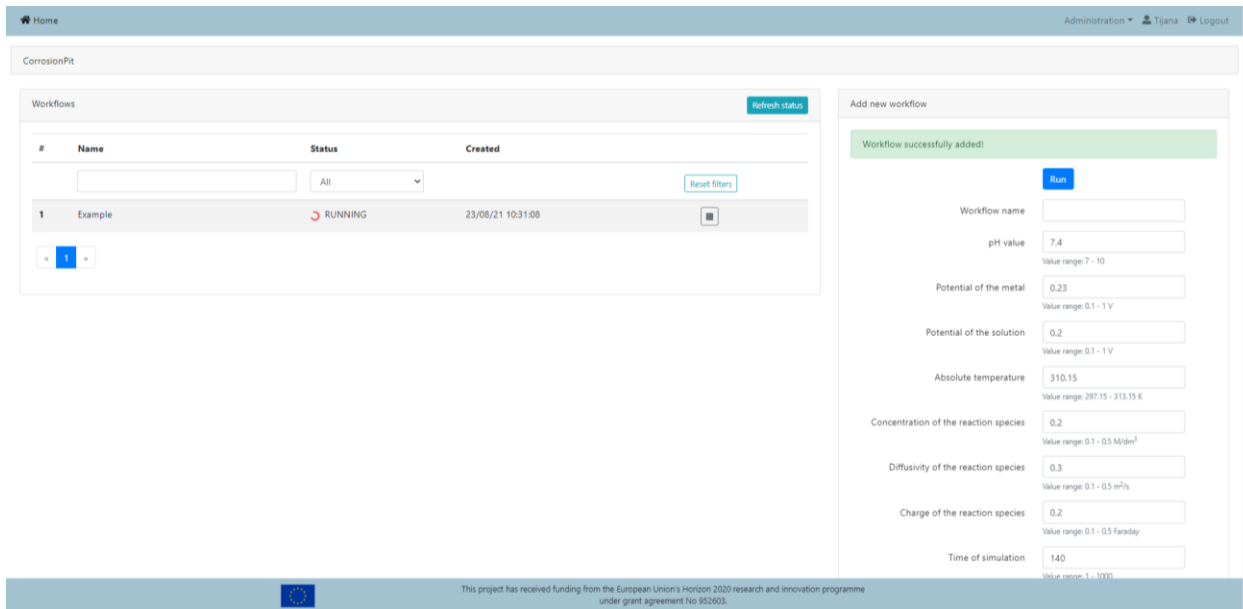
The exception handling is integrated into the user interface (UI) of the SGABU platform. Specific examples can be seen in Figure 92 (Empty forms, Non-numerical forms, Out of range values).



The figure shows three sequential screenshots of a web form titled 'Add new workflow'. Each screenshot has a red header bar that says 'There are errors on the form. Please fix them!'.
 - The first screenshot shows the 'Workflow name' field as empty with a red error message 'Workflow name is required'. Other fields like 'pH value' (7.4), 'Potential of the metal' (0.23), 'Potential of the solution' (0.2), 'Absolute temperature' (310.15), 'Concentration of the reaction species' (0.2), 'Diffusivity of the reaction species' (0.3), 'Charge of the reaction species' (0.2), and 'Time of simulation' (140) are all filled and have green checkmarks.
 - The second screenshot shows the 'Workflow name' field filled with 'Example' and a green checkmark. The 'pH value' field is now empty with a red error message 'Only Numbers are allowed'.
 - The third screenshot shows the 'pH value' field filled with '7.4' and a green checkmark. The 'Time of simulation' field is now empty with a red error message 'The time of simulation must be between 1 and 1000'.

Figure 92. Exception handling.

Once everything is correctly filled, the workflow can be started. The user can monitor the current status of the workflow in the left section of the window (Figure 93).



The screenshot shows the 'CorrosionFit' application interface. On the left, there is a 'Workflows' table with the following data:

#	Name	Status	Created
1	Example	RUNNING	23/08/21 10:31:08

 Below the table are navigation buttons and a 'Refresh status' button. On the right, the 'Add new workflow' form is shown with a green header 'Workflow successfully added!'. The 'Run' button is highlighted in blue. The form fields are filled with the same values as in Figure 92, and all have green checkmarks, indicating they are valid.

Figure 93. Running the workflow.

At the beginning we assume no corrosion, meaning the first step is the black image (all zeros). After that, in pit initiation model, each cell x is associated with an initial potential state $I(u, t) = I(u, t - 1) + \alpha$

at time t . For each un-corroded cell u , initiation potential state values in its Von Neumann neighbourhood together with its own is considered $I(u, t) + \sum I(u + \delta_i, t)$ and if that sum divided by 3 overcomes the threshold value (currently fixed at the value of 20), then a corrosion pit is initiated at cell u and its corrosion state $S(u, t)$ is set to a small positive number between 3 and 5.

For the next time steps, pit initiation model is applied on the uncorroded cells again, and at the same time pit growth model is applied on the cells where corrosion has been initiated with formula:

$$S(t + 1, x) = S(t, x) + k_1 f[S(t, x)] + k_2 \sum_i f[S(t, x + c_i)] + k_3 \sum_j f[S(t, x + d_j)] + k_4 \Delta$$

where $c_i = (0, -1), (1, 0), (0, 1), (-1, 0), d_j = (1, 1), (1, -1), (-1, -1), (-1, 1)$ for $i = 1, 2, 3, 4, j = 1, 2, 3, 4$. This means that we use Moore neighborhood to describe how the surrounding cells influence the cell of interest (Figure 94).

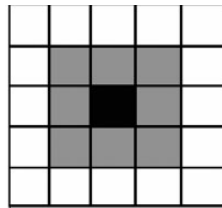


Figure 94. Moore neighborhood is used to describe the effect of surrounding cells on the cell of interest.

Coefficient k_1 is described as:

$$k_1 = \lambda \times (pH - 7)^2 \times \text{step}(4, 8.5) \times e^{\varphi_M - \varphi_S} \times (1/T) \times C \times D \times z$$

In these eq. λ is a discount factor ranges from 1 to 3; pH is the pH value of the solution; $\text{step}(4, 8.5)$ is a function with value 0 between 4 and 8.5, and 1 otherwise; φ_M and φ_S are the potentials of the metal and solution, respectively; T is the absolute temperature; C is the concentration of the reaction species; D is the diffusivity of the reaction species; z is the charge of the reaction species. The parameters k_2, k_3 and k_4 are in similar forms as k_1 , but with different discount factors.

Different environmental factors are included in the model to describe their effect on the corrosion. Inputs to the corrosion pit model with allowed ranges and default values, as well as adequate unites are given in Table 9.

Table 9. Inputs for the corrosion pit model.

Name of the parameter	Label	Explanation	Unit	Range	Default value
pH value	pH	pH value of the solution	/	7-10	7.4
Potential of the metal	φ_M	change in a corrosion system of the metal	V	0.1 - 1	0.23
Potential of the solution	φ_S	change in a corrosion system of the solution	V	0.1 - 1	0.2

Absolute temperature	T	Absolute temperature of the environment	K	297.15 - 313.15 (24°C – 40°C)	310.15
Concentration of the reaction species	C	Concentration of one of the species participating in a corrosion reaction	M/dm ³	0.1-0.5	0.2
Diffusivity of the reaction species	D	The rate of diffusion-controlled corrosion of reaction species	m ² /sec	0.1-0.5	0.3
Charge of the reaction species	z	Charge resulting from the reaction of species	Faraday	0.1-0.5	0.2
Time of simulation	t	Number of time steps to run the simulation (number must be divisible by 20, as every 20 steps are plotted)	/	1000	100

Results are displayed in the form of images and analysis of the resulted images that represent the corrosion in time. The model describes adequately the multi-pit corrosion pit initiation and growth. Figure 95 shows the corrosion states at four different time steps, where black indicates uncorroded cells and white indicates fully corroded cells.

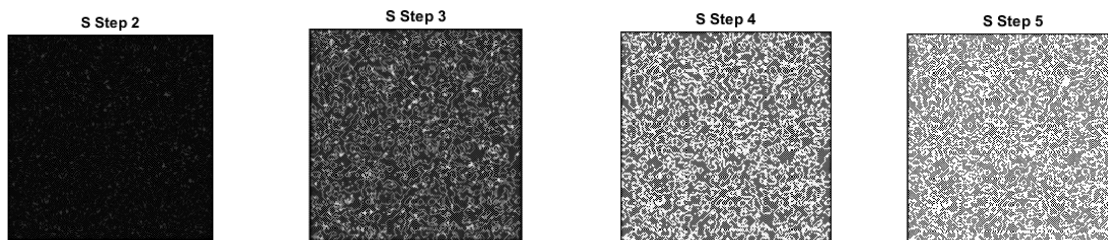


Figure 95. Corrosion state $S(u, t)$ at time steps $t = 2, 3, 4, 5$.

After the workflow has been successfully executed, a user can visualize the results on the platform itself. The results window, includes the following sections:

- Overview of the input parameters (Figure 96)
- Results in the table form (Figure 97),
- Results in the form of figures, following corrosion steps in time (Figure 98).

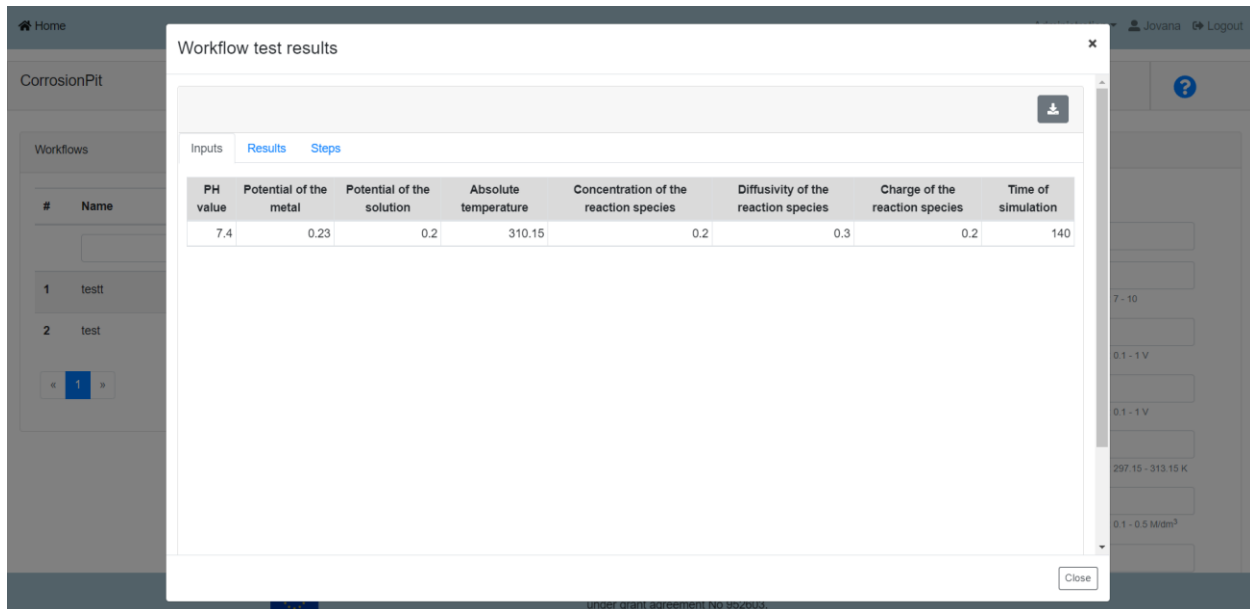


Figure 96. Inputs section – table form.

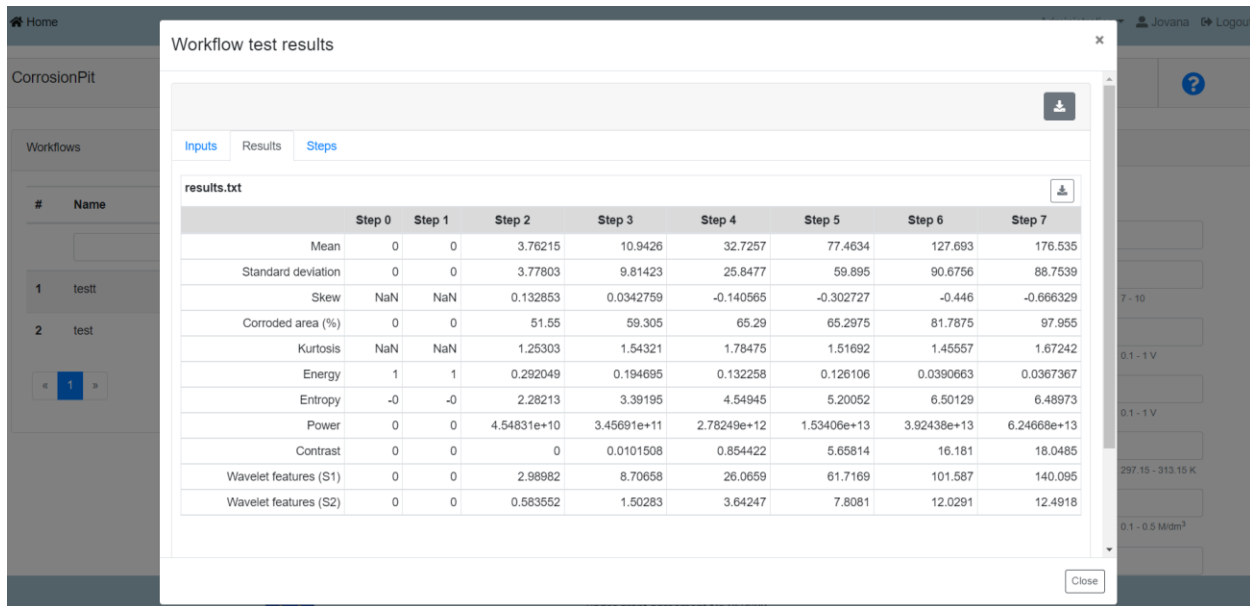


Figure 97. Results section – table form.

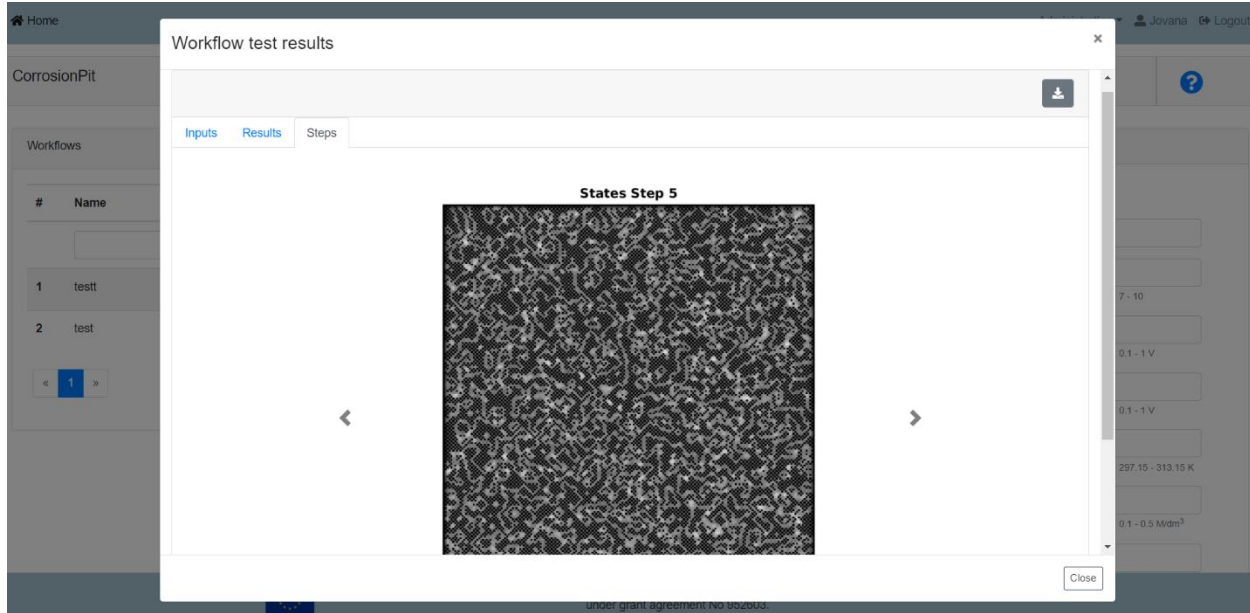


Figure 98. Steps section – figures.

The results can also be downloaded in the form of figures and txt files (Figure 99). In order to estimate quantitatively how the corrosion has progressed in time, we calculate statistical measures presented in textual file:

- Mean corrosion (calculated based on histogram probability as the average grey value)
- Standard deviation (describes the spread in the data, which is related to the contrast)
- Skew (measures the asymmetry about the mean value in the distribution)
- Percentage of corroded material (sum of the corroded pixels (all non-zero values) divided by number of pixels and multiplied by 100)
- Kurtosis (shows whether the data are peaked or flat relative to a normal distribution)
- Energy (indicates something about how the pixel intensities are distributed in the region under consideration. In the case of corrosion image, this feature indicates the degree of corrosion at the pit level)
- Entropy (entropy of each sub-band provides a measure of the image characteristics in that sub-band, indicates the number of bits we need to code the image data)
- Power (indicates the texture property in an image and in this case, the level of corrosion itself. The higher the power value, the texture change will be higher)
- Contrast (difference between maximum and minimum pixel intensity in an image)
- Wavelet features (calculated through the processes of singular values decomposition (SVD) and first two eigenvalues are reported)

Resulted matrix will be of size 11 x number of simulated time steps. Each row will represent one statistical measure in the order given in Table (Figure 97). First column will always be the same, as starting image is assumed to be totally uncorroded material (all zeros). If one wants to extend the time of the simulation, he/she has to change the last input parameter and run the simulation again.



Figure 99. Downloading of results.

6.18 Model – FEA of Femoral Bone; Responsible partner - UKG

Model - FEA of Femoral Bone	Responsible partner - UKG
------------------------------------	----------------------------------

The access to the Finite Element Analysis of Femoral Bone^{35,36,37} belongs to the Bone Modeling module on the SGABU platform is provided through the main dashboard as presented in Figure 100.

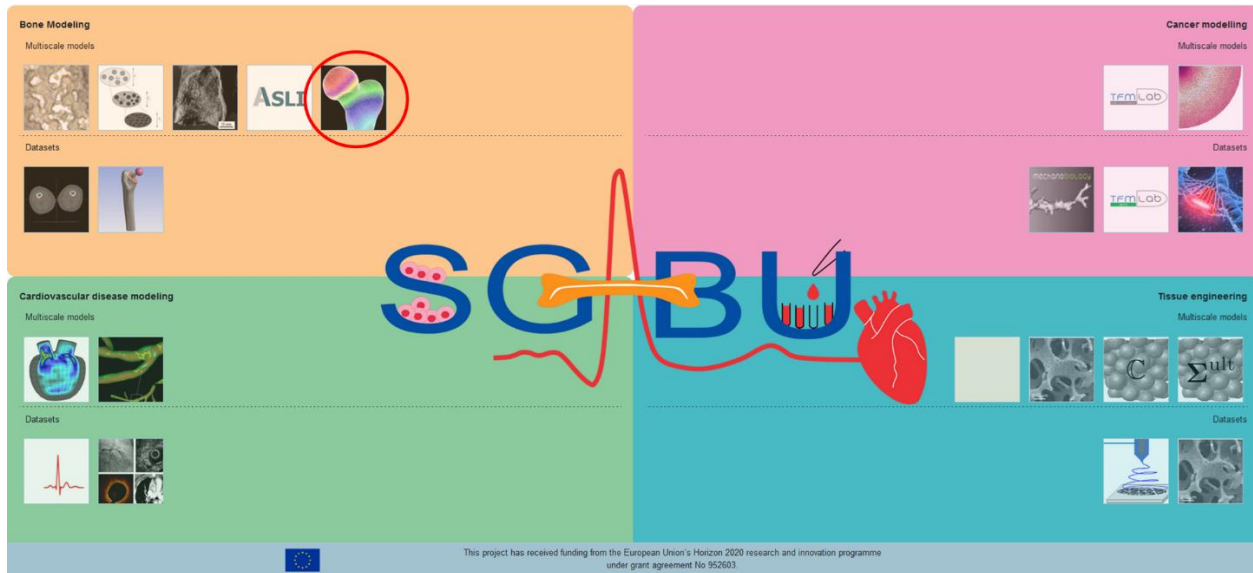


Figure 100. Main platform dashboard.

In order to execute the workflow, the user needs to input several parameters (Figure 101), located in the right section of the screen.

³⁵ Vulović, A., & Filipovic, N. (2019). Computational analysis of hip implant surfaces. *Journal of the Serbian Society for Computational Mechanics*, 13, 109-119. doi:DOI: 10.24874/jsscm.2019.13.01.0

³⁶ Vulović, A., & Filipović, N. (2019). Effect of the femoral bone material properties on the numerical simulation results. In *The 7th International Congress of Serbian Society of Mechanics*. Sremski Karlovci, Serbia. doi:978-86-909973-7-4

³⁷ Vulović, A., Šušteršič, T., & Filipović, N. (2017). Finite Element Analysis of Femur During Gait. In *4th South-East European Conference on Computational Mechanics - SECCM 2017* (pp. 61-66). Kragujevac. doi:978-86-921243-0-3

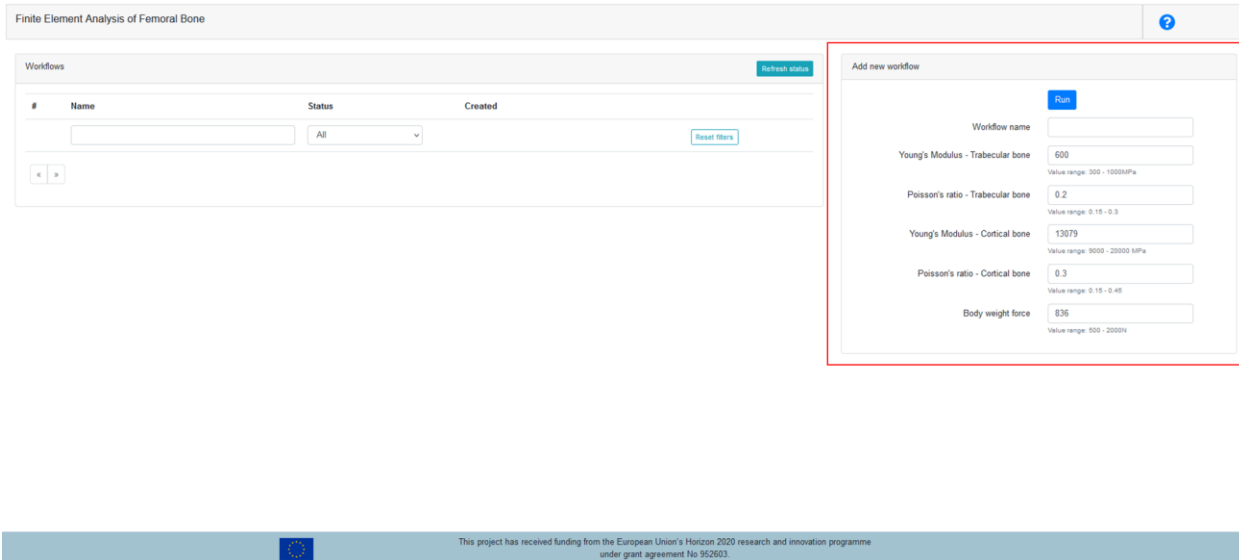


Figure 101. Input parameters.

Default values for parameters are already predefined as it can be seen in Figure 102. The value range for each parameter has been given. User can run simulation using default values or can change one or more of the parameters. “Workflow name” is necessary to run the simulation.

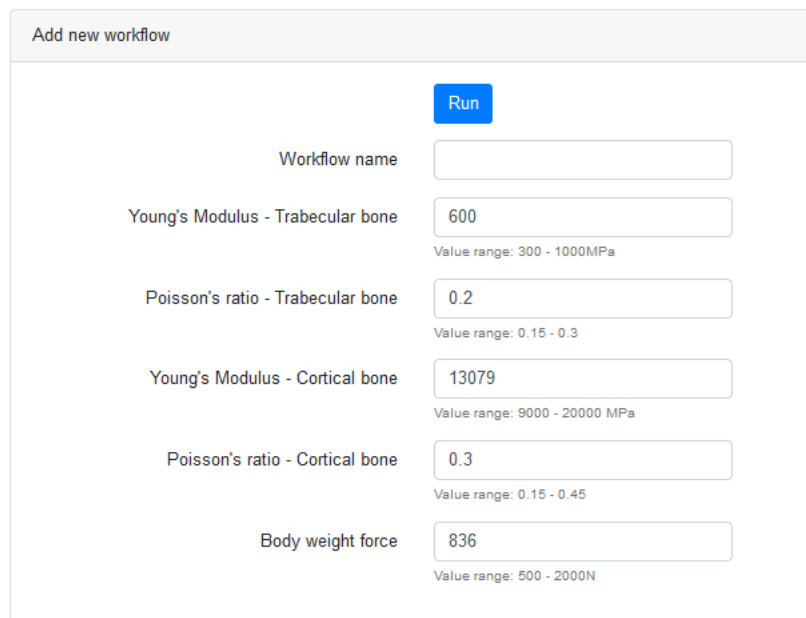


Figure 102. Default values and value ranges.

Once the “Run” button is pressed, the execution of the created workflow will start, and it will appear in the list on the left side of the screen with status “RUNNING” (Figure 103).

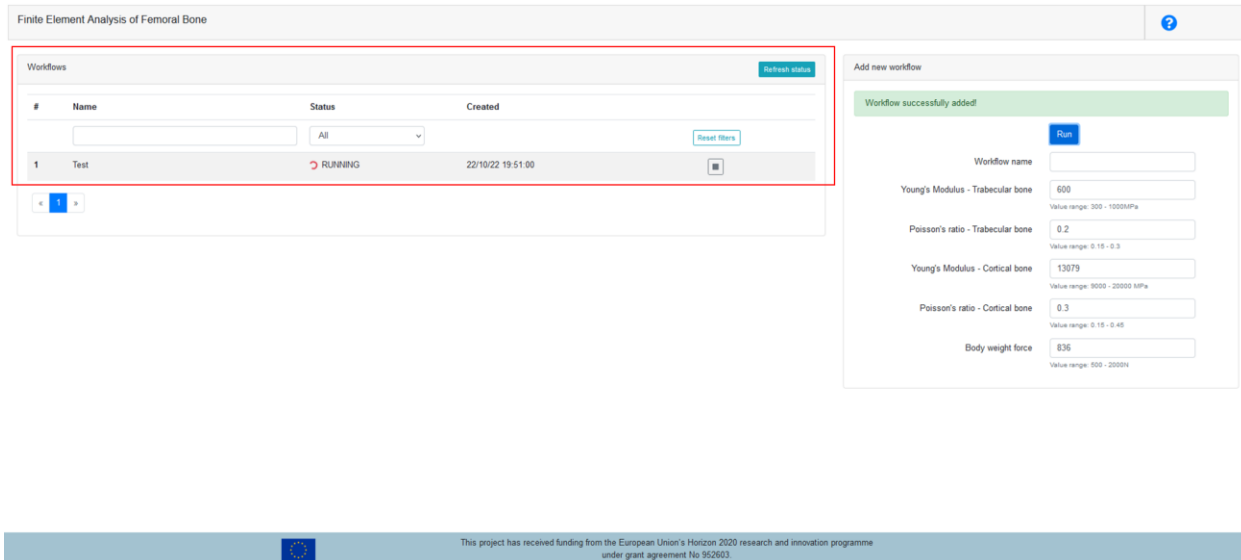


Figure 103. Workflow execution.

The workflow takes a few minutes to execute. If it takes longer, refresh the webpage to see if the workflow finished execution. When the execution is done, the status will be changed from “RUNNING” to “FINISHED_OK” (Figure 104).

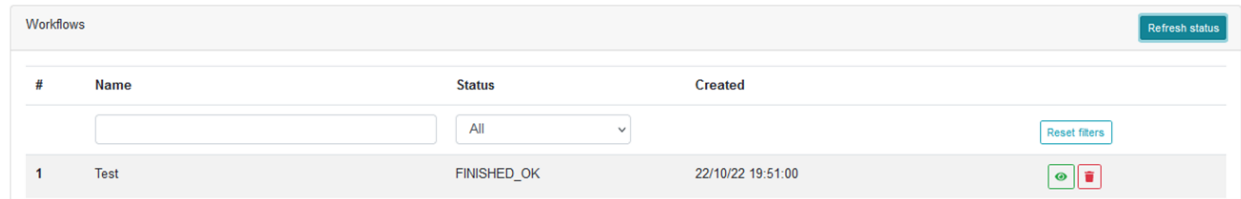


Figure 104. Workflow finished.

In order to see the obtained results, user needs to press the green eye below the Reset filters box. When the results window opens, user can see the input parameters (Figure 105).

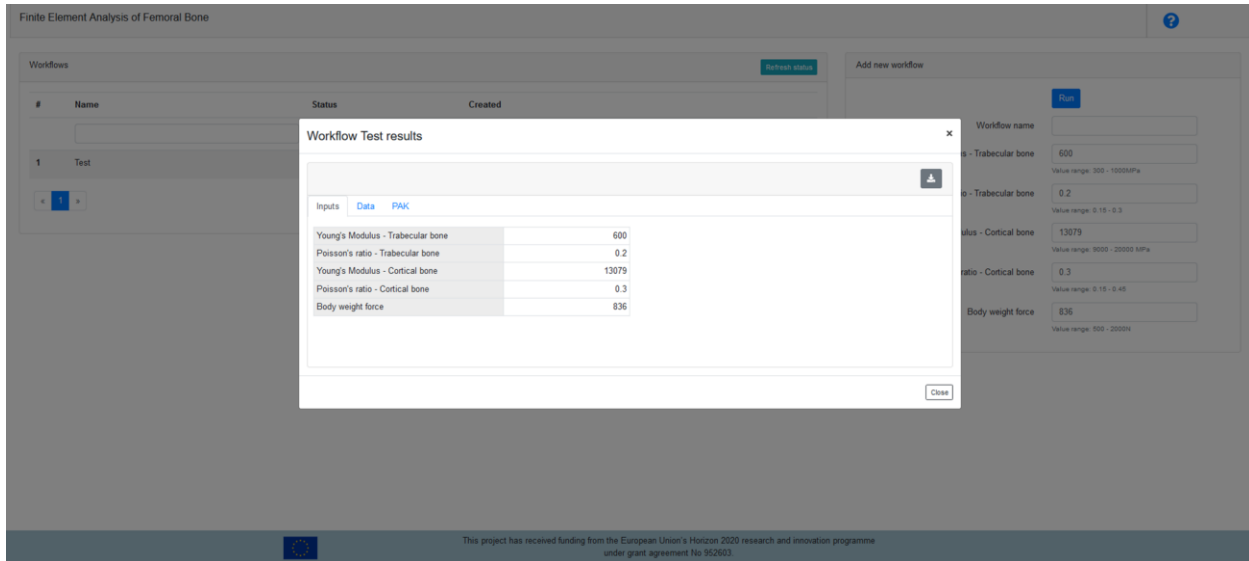


Figure 105. Results window – input parameters.

By choosing PAK tab (Figure 106) and View PakF001.vtk option, user can see Displacement and Stress distribution for the femoral bone.

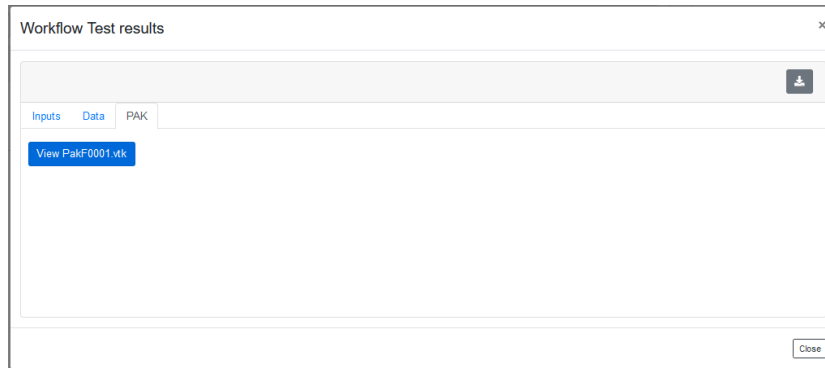


Figure 106. Results window – PAK tab.

By choosing View PakF001.vtk, a ParaView Glance will open (Figure 107).

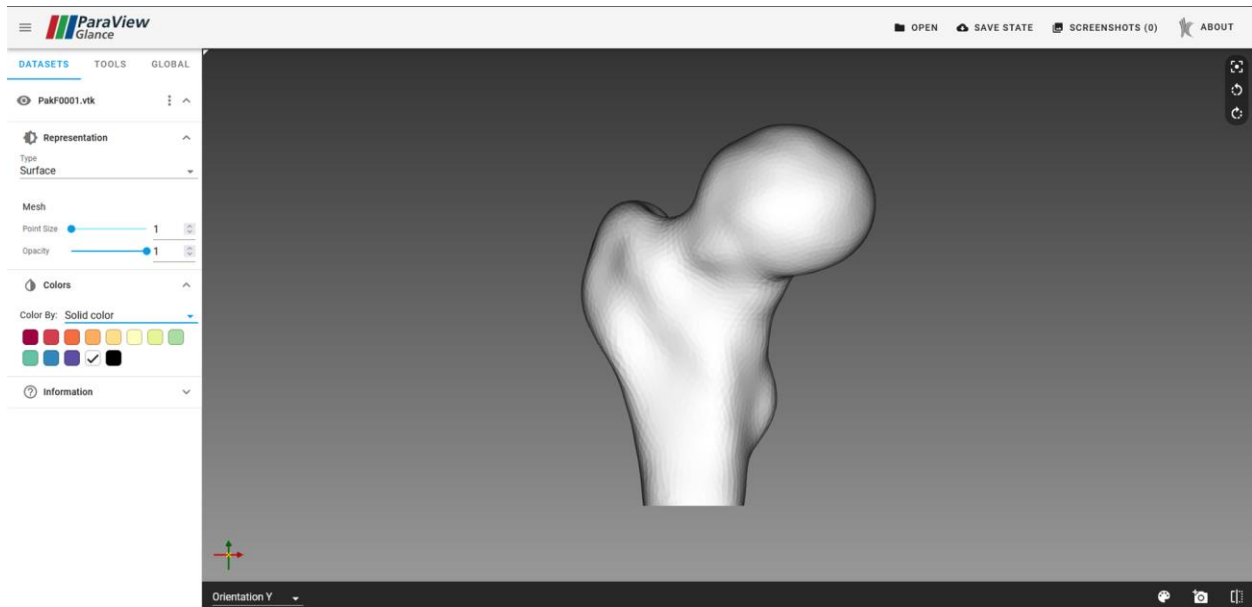


Figure 107. ParaView Glance.

In order to see the results, user needs to choose Solid color drop-down menu (Figure 108) and choose between displacement (Figure 109) and stress distribution (Figure 110).

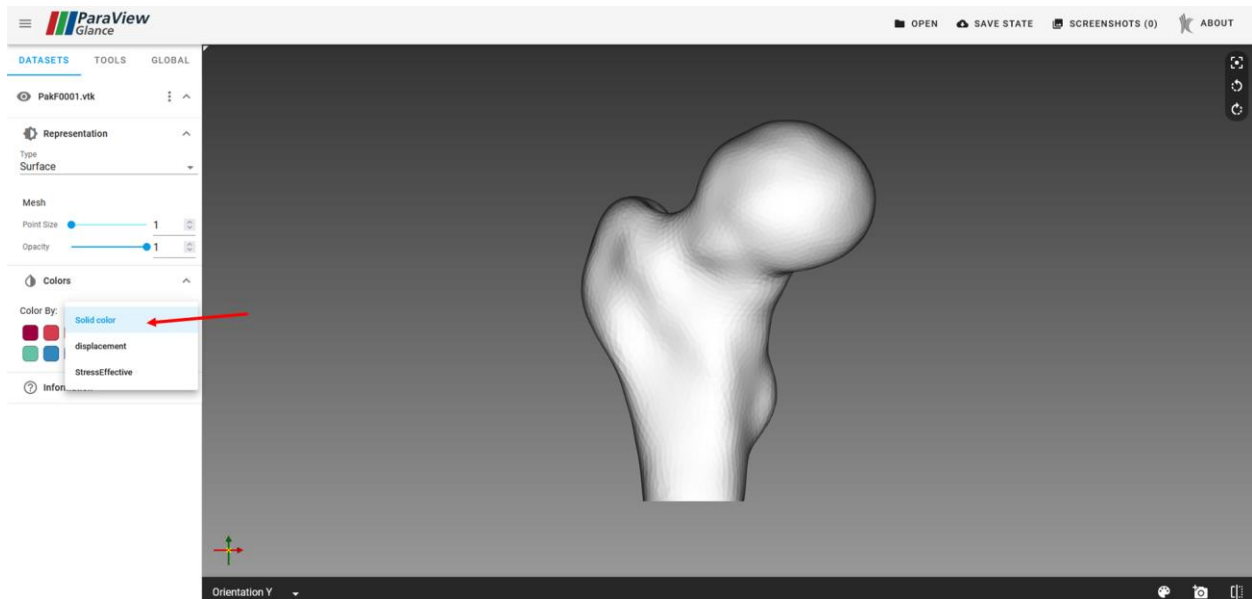


Figure 108. ParaView Glance – choosing results to visualize.

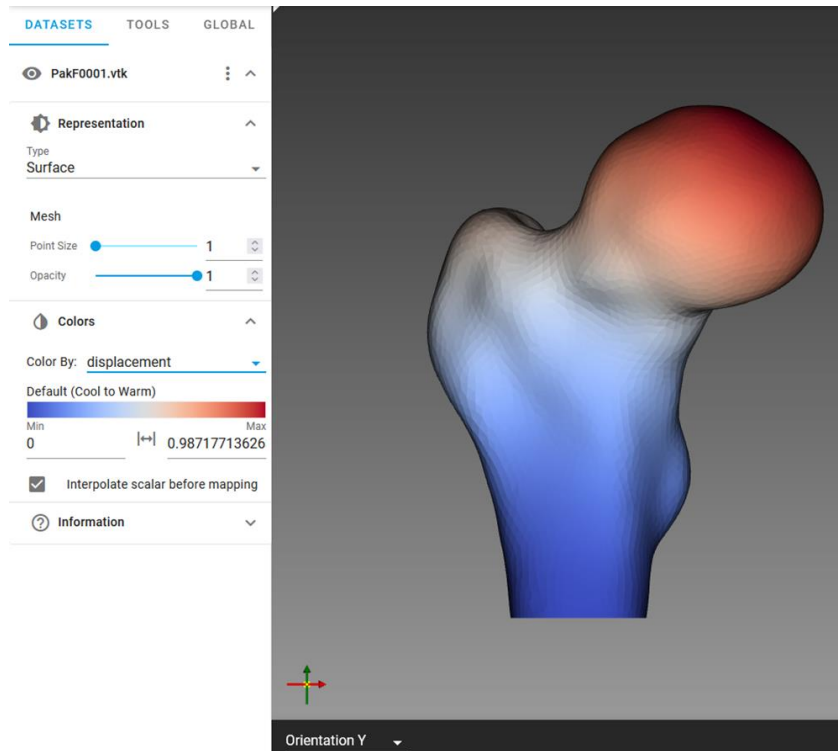


Figure 109. Displacement results.

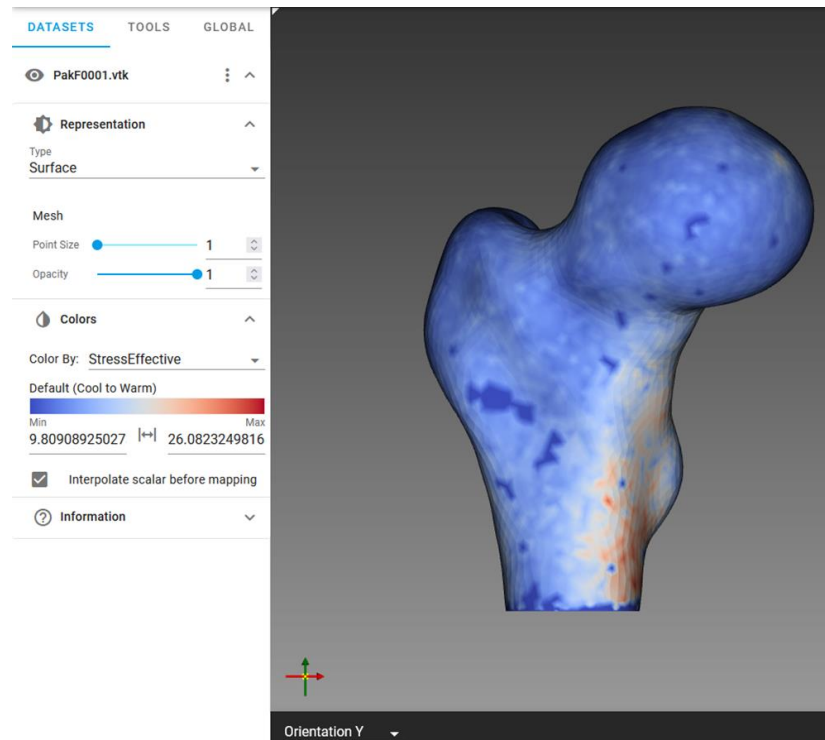


Figure 110. Stress results.

6.19 Model – Parametric Heart; Responsible partner - UKG

Model - Parametric Heart	Responsible partner - UKG
---------------------------------	----------------------------------

The access to the *Cardiovascular disease modeling* module on the SGABU platform is provided through the main dashboard as presented in the following Figure 111. A parametric heart model of the left ventricle is used to simulate the cardiac cycle with patient-specific dimensions, which are provided by the user. Based on user-provided parameters, the left ventricle model is generated and finite element simulation is run with prescribed boundary conditions. Boundary conditions consist of inlet and outlet velocities and/or pressures, which are prescribed to the valves of the model. Users are also allowed to change stiffness of left ventricle wall, and calcium concentration which controls the muscle contraction.

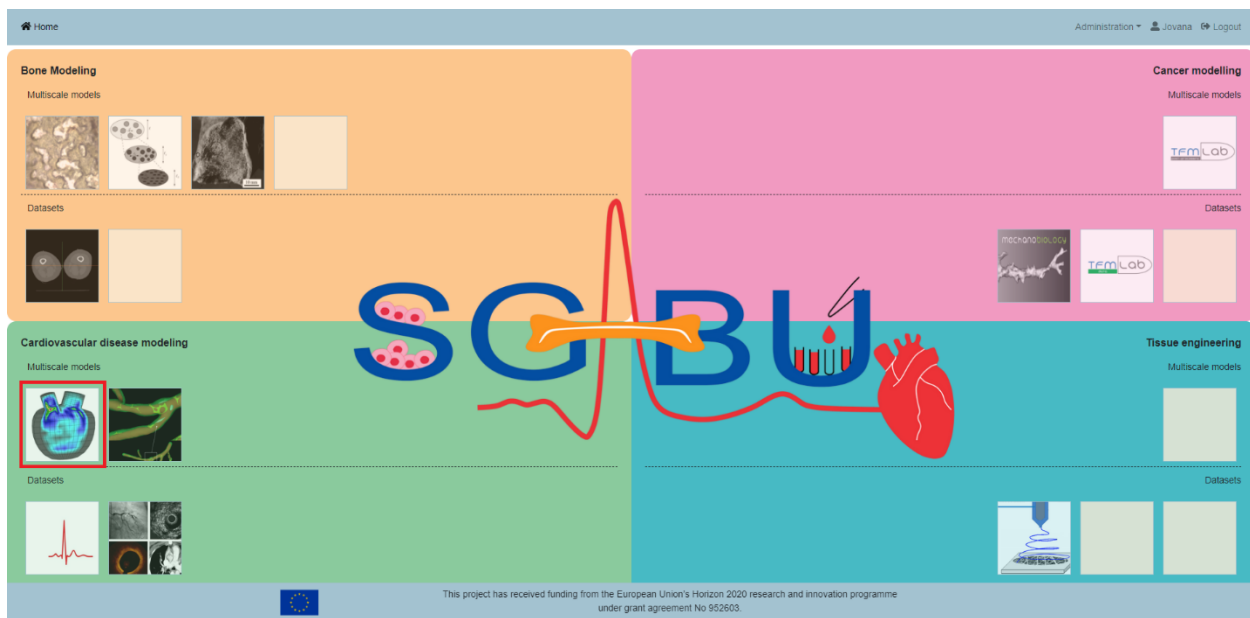


Figure 111. Main platform dashboard.

User Interface for ParametricHeart example is shown in Figure 112. The window is divided into 2 sections – *Workflows* and *Add new workflow*. The basic execution unit in SGABU is a workflow. In the upper section of the window, users are able to see names and status of the workflows. Possible statuses of the workflow are:

- Not yet executed
- Terminated
- Running
- Finished OK
- Finished Error

In the below section of the window, users can create new workflows for this submodule. Each of the forms needs to be filled out in order for simulation to run. Users are expected to fill out the following forms:

- Workflow name

- Left section:
 - Base division
 - Connection division
 - Aortic division
 - Wall division
 - Valves division
 - Mitral division
- Right section:
 - IVS-diastolic [cm]
 - LVID-diastolic [cm]
 - LVPW-diastolic [cm]
 - IVS-systolic [cm]
 - LVID-systolic [cm]
- Inlet Velocity time function
- Outlet velocity time function

The divisions control the number of finite elements within the model. Base division controls number of finite elements along the height of left ventricle base. Connection division controls the number of finite elements along the height between base and the valves. Valves division controls the number of finite elements along the width of valves. Aortic/mitral division controls the number of finite elements along the height of the aortic/mitral valve. Wall division controls the number of finite elements along the width of heart wall. Regarding the dimensions that need to be filled in, IVS-diastolic/systolic [cm] represents the interventricular septum (IVS) in diastole/systole, LVID-diastolic/systolic [cm] represents left ventricular internal diameter (LVID) in diastole/systole and LVPW-diastolic/systolic [cm] represents left ventricular posterior wall (LVPW) in diastole/systole.

All forms except for Workflow name are numerical and value ranges are provided for the users (Figure 112).

#	Name	Status	Created
1	Test_tijana	FINISHED_OK	24/10/21 13:56:07

Parameter	Value
Base division	6
Connection division	3
Aortic division	10
Wall division	1
Valves division	5
IVS-diastolic [cm]	1.298
LVID-diastolic [cm]	6.313
LVPW-diastolic [cm]	0.912
IVS-systolic [cm]	2.245
LVID-systolic [cm]	4.735

Figure 112. User Interface for ParametricHeart module.

In Figure 113 we showed the velocity functions. Inlet velocity function is prescribed to the mitral valve of the left ventricle, while outlet velocity function is prescribed to the aortic valve. Interactive graphs with inlet and outlet velocity time functions are also shown in Figure 113.

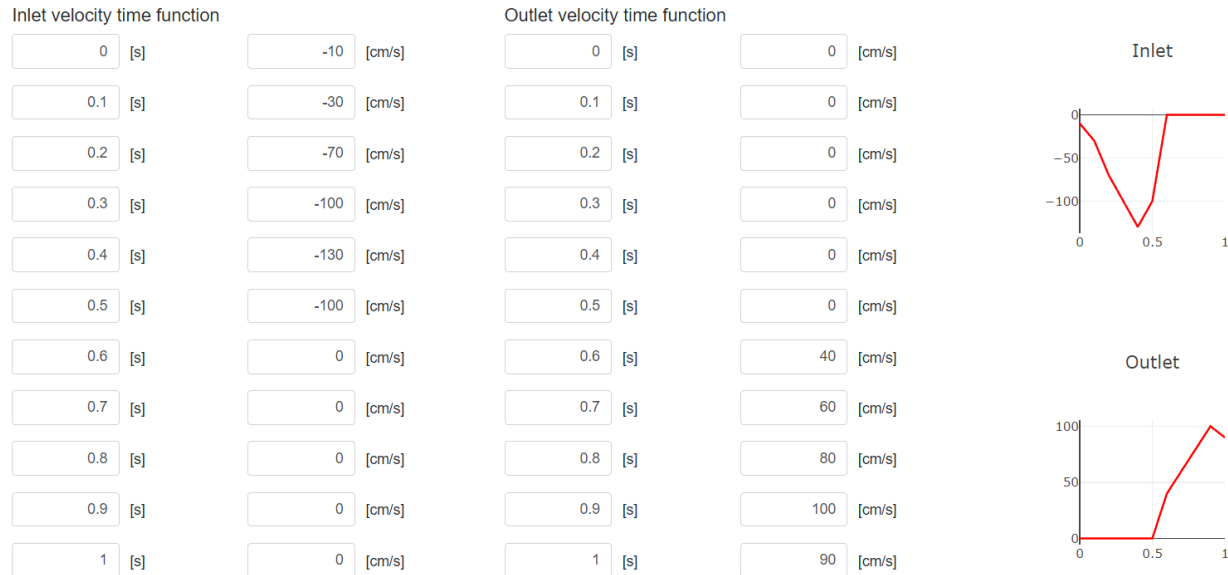


Figure 113. Prescribing inlet and outlet time function for ParametricHeart module.

The exception handling is integrated into the user interface (UI) of the SGABU platform (Empty forms, Non-numerical forms, Out of range values). Once everything is correctly filled, the workflow can be started. The user can monitor the current status of the workflow in the left section of the window (Figure 114).

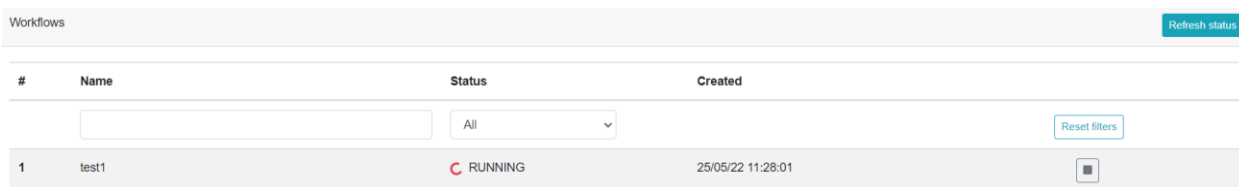


Figure 114. Running the workflow.

Results are displayed in the form of tables, data, video and Paraview. The result of the simulation consists of velocity, pressure and displacement fields during full cardiac cycle. Along the physical fields we also provided the pressure-volume diagrams and diagrams of myocardial work during cardiac cycle. In Figure 115 we showed input divisions, dimensions of the model and inlet velocity prescribed to the mitral valve.

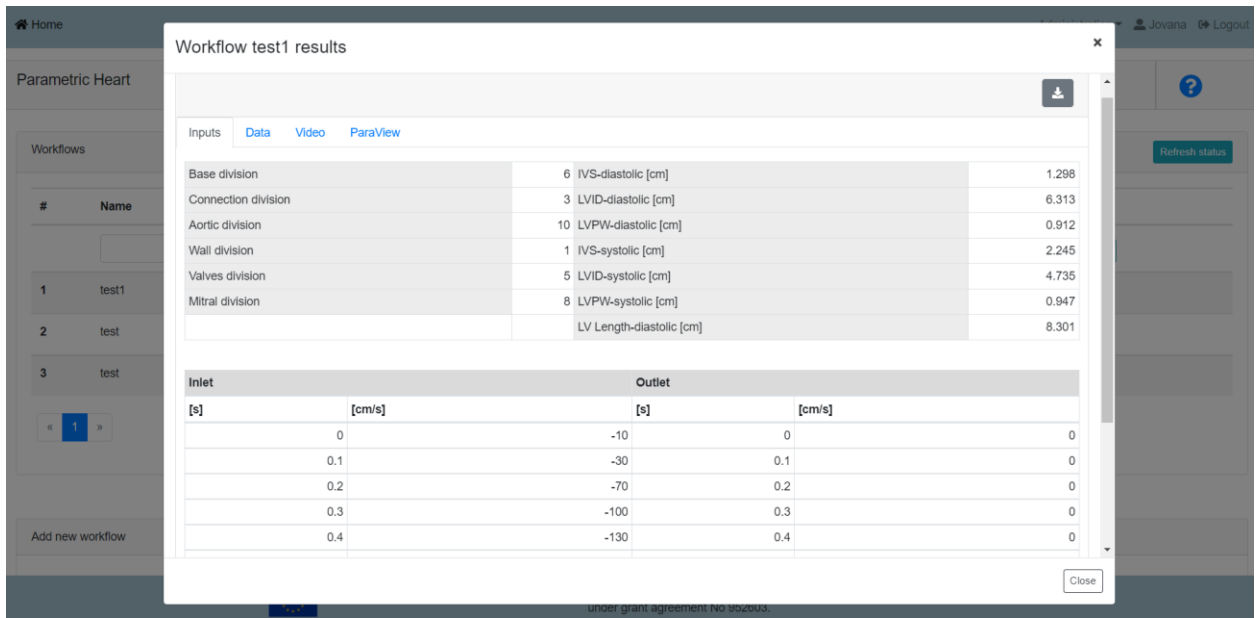


Figure 115. Inputs tab of the results section.

The results can also be downloaded in the form of csv files. In Figure 116 we showed Pressure-Volume (PV) diagram, ejection fraction and global work efficiency that we have got after executing our finite element simulation.

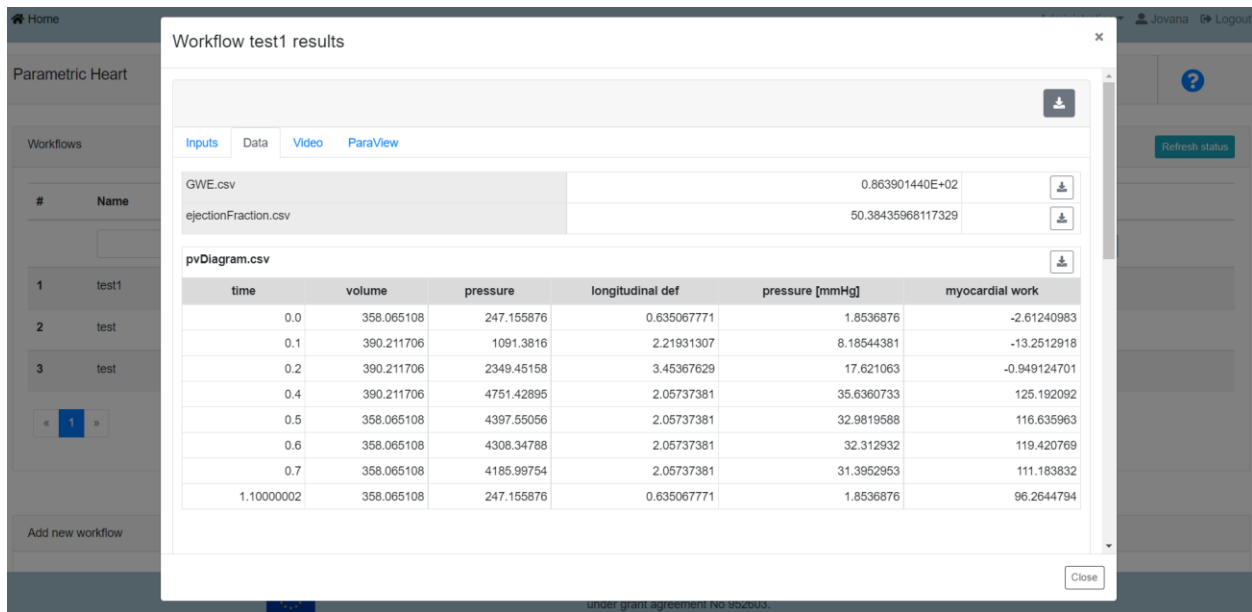


Figure 116. Data tab of the results section.

In Figure 117 we showed pressure field within left ventricle model. Pressure is the largest during systolic phase of the cycle.

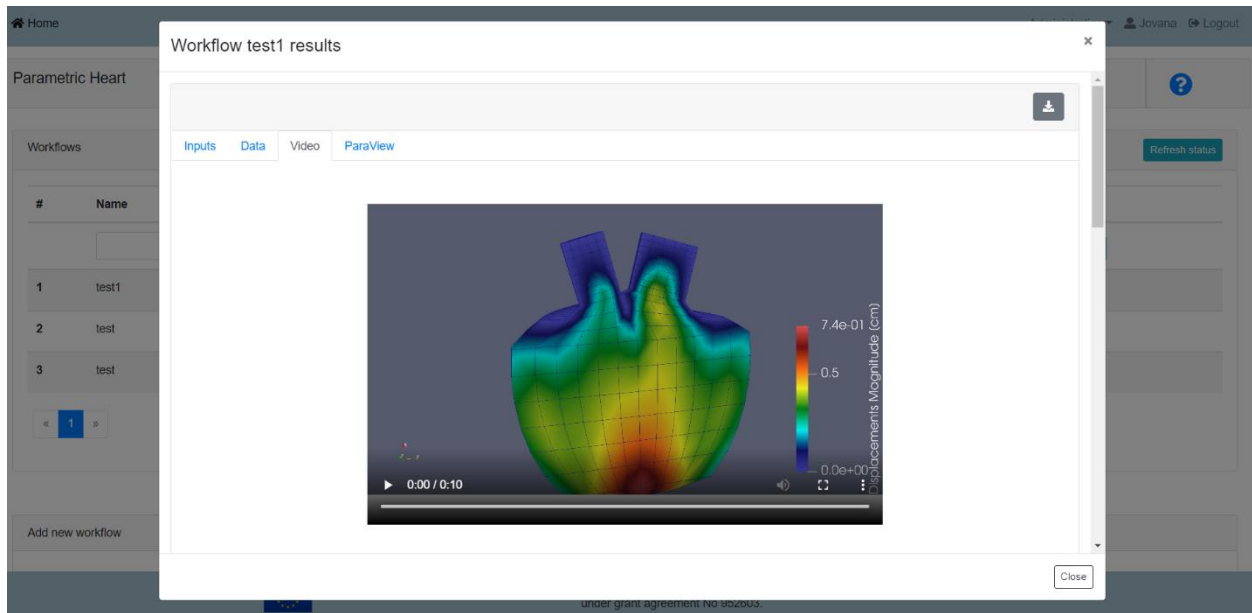


Figure 117. Video tab of the results section.

Clicking on the Paraveiw tab will open a new browser tab with results. In Figure 118 we showed geometry of the left ventricle.

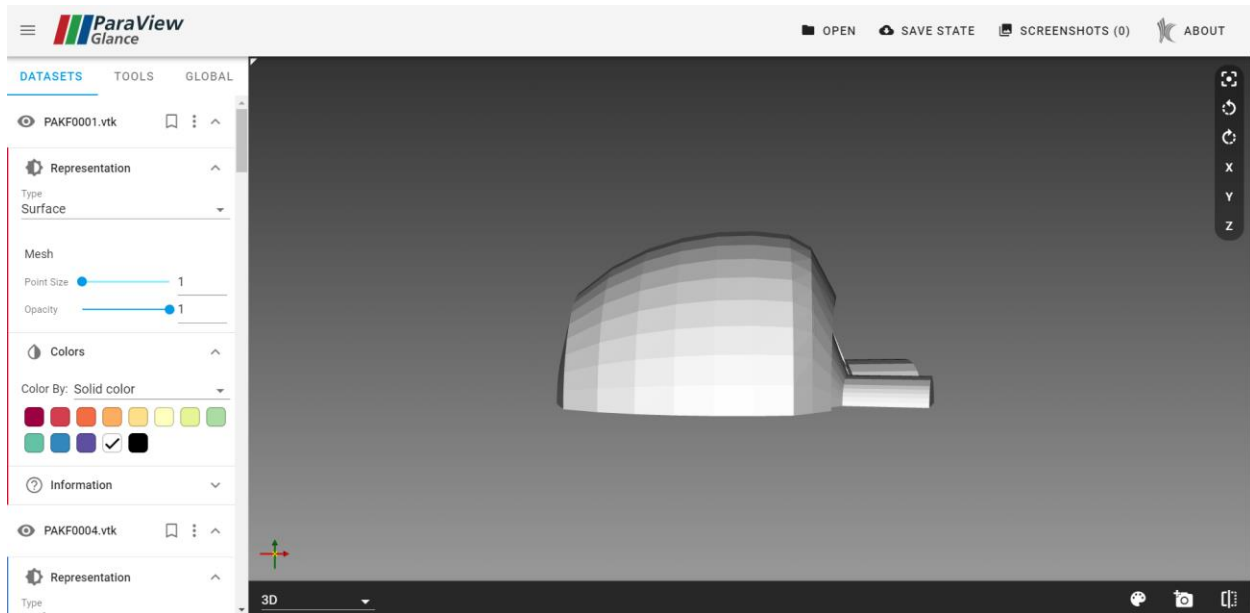


Figure 118. Paraveiw tab of the results section.

In Figure 119 we showed the velocity field³⁸. Inlet velocities rise during diastole and during systole inlet velocities are equal to zero. During systole muscles are activated and they push the blood out of left ventricle. At start of the systole the velocities are largest at the bottom of the heart. At the middle of the systole the velocities are the largest at the aortic valve.

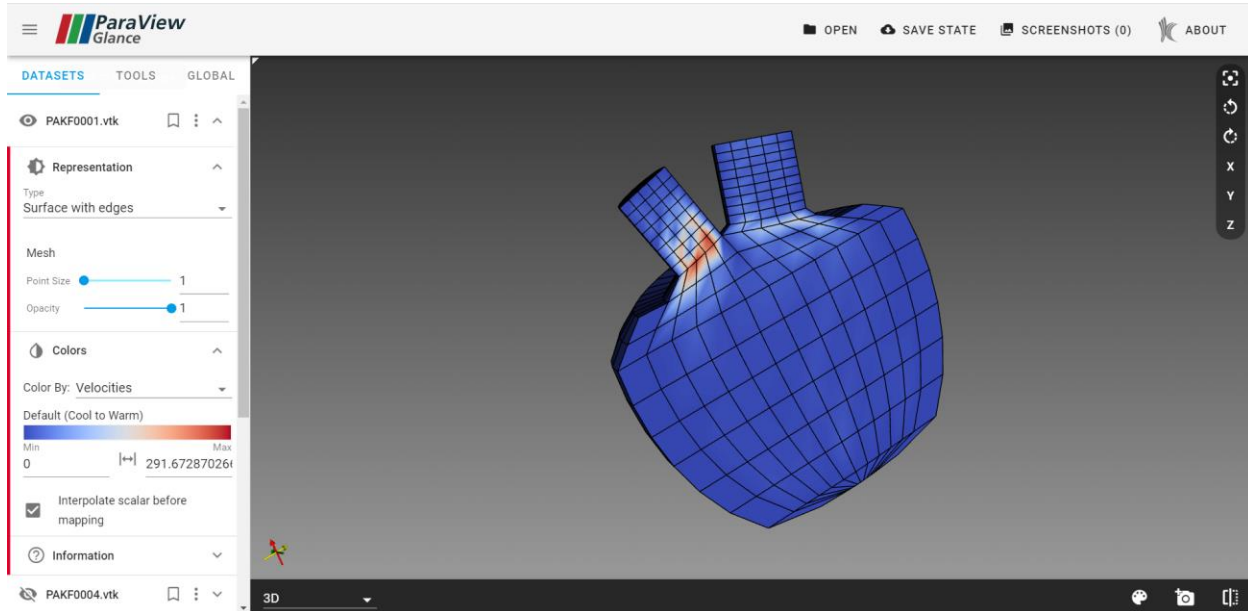


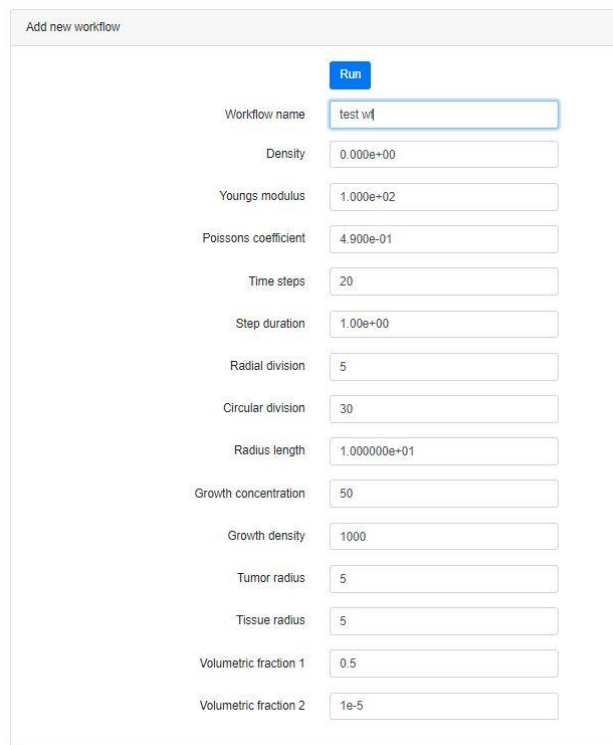
Figure 119. Paraview velocities of PAKF0001.vtk.

³⁸ M. Anić, S. Savić, A. Milovanović, M. Milošević, B. Milićević, V. Simić and N. Filipović, "Solution of fluid flow through the left heart ventricle," Applied Engineering Letters, vol. 5, pp. 120-125, 2020., <https://doi.org/10.18485/aeletters.2020.5.4.2>

6.20 Model – Smearred tumor growth model; Responsible partner - UKG - UKG

Model - Smearred tumor growth model	Responsible partner - UKG
-------------------------------------	---------------------------

Before executing the workflow provide input parameters for the finite element simulation³⁹ as shown in Figure 120. Default parameters are already preloaded on the platform so user can modify them or can just run the simulation with default parameters. “Workflow name” is necessary to run the simulation. Here user can put any word(s) which will help to identify user’s simulation.

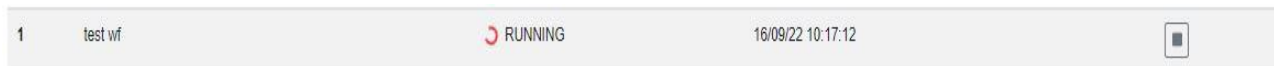


The screenshot shows a form titled "Add new workflow" with a "Run" button at the top. Below the button are several input fields with their respective values:

- Workflow name: test wf
- Density: 0.000e+00
- Youngs modulus: 1.000e+02
- Poissons coefficient: 4.900e-01
- Time steps: 20
- Step duration: 1.00e+00
- Radial division: 5
- Circular division: 30
- Radius length: 1.000000e+01
- Growth concentration: 50
- Growth density: 1000
- Tumor radius: 5
- Tissue radius: 5
- Volumetric fraction 1: 0.5
- Volumetric fraction 2: 1e-5

Figure 120. Input parameters.

Once user press the “Run” button new workflow will appear in the list with the status “running” as shown in Figure 121. This workflow takes a few minutes to execute. User might need to refresh the webpage to see if the workflow finished running. Once the simulations are finished the status will change from “running” to “finished_ok” (Figure 122). Press the green eye button to see the results of the simulation.



The screenshot shows a table with one row representing a workflow:



1	test wf	 RUNNING	16/09/22 10:17:12	
---	---------	---	-------------------	---

Figure 121. Workflow running.

³⁹ V. Simic, M. Milosevic, V. Milicevic, N. Filipovic, and M. Kojic, “A novel composite smearred finite element for mechanics (CSFEM): Some applications,” Technology and Health Care. IOS Press, pp. 1–15, Oct. 14, 2022. doi: 10.3233/thc-220414



Figure 122. Workflow finished.

In the result window, user can review the inputs as shown in Figure 123.

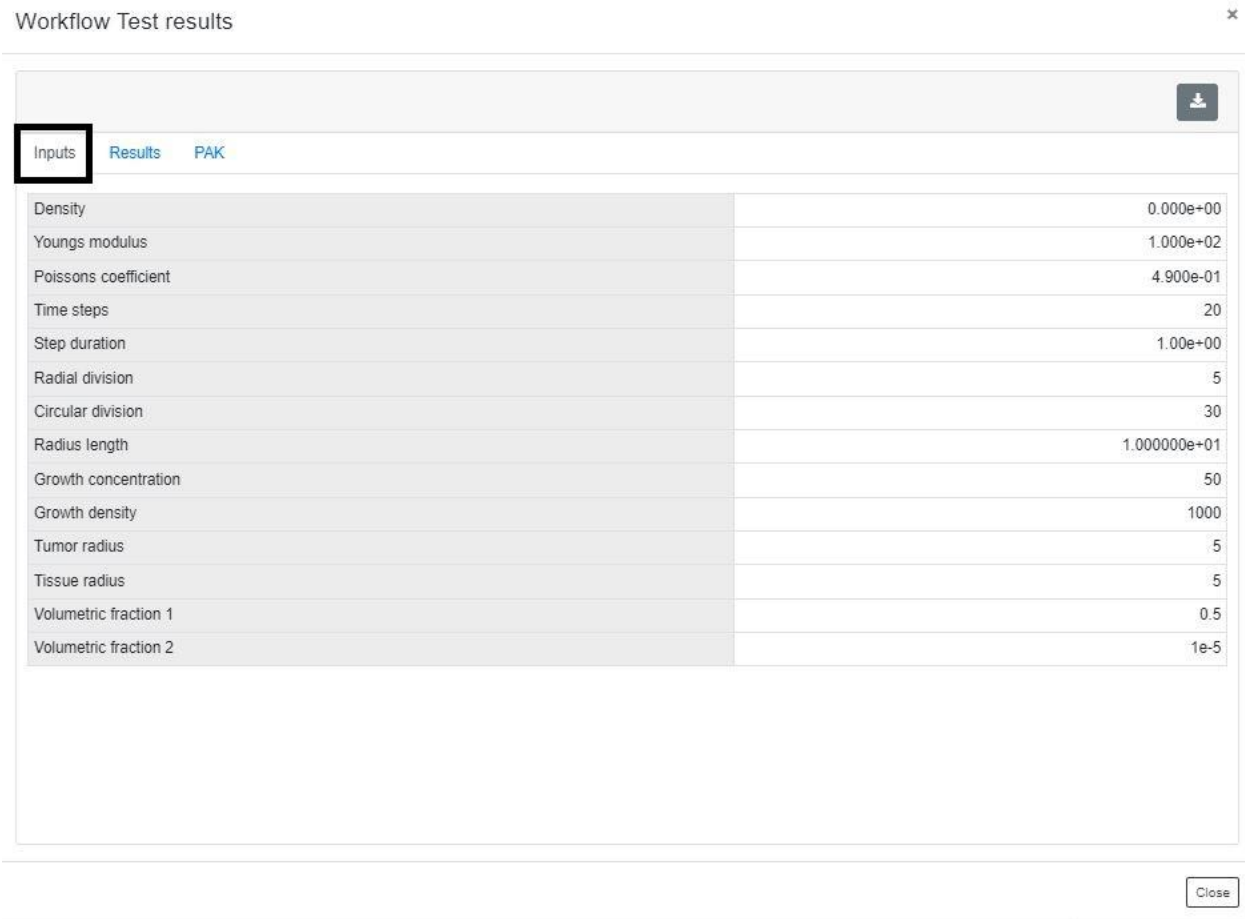
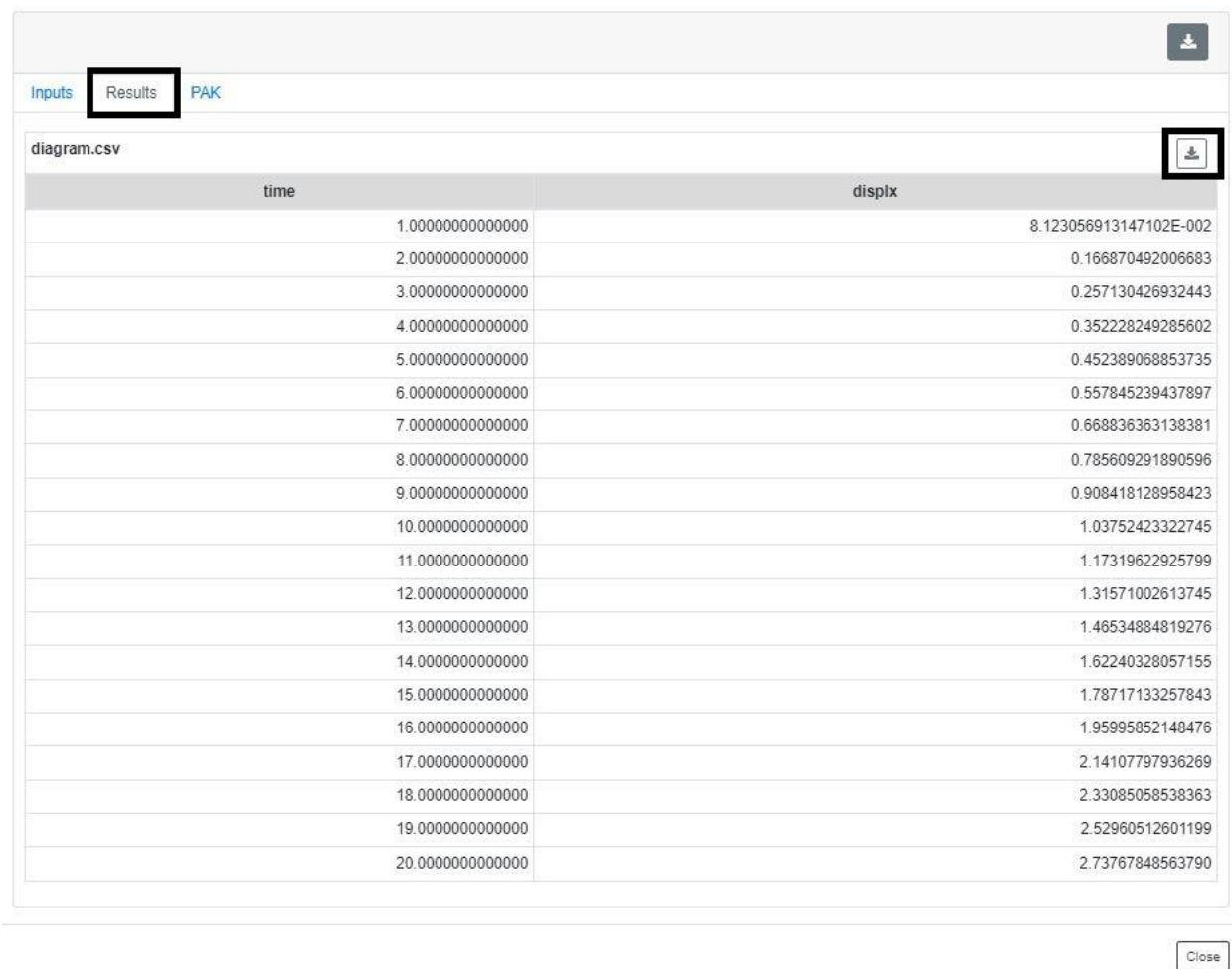


Figure 123. Review of the inputs once the workflow is finished.

By pressing the “Results” tab user can see diagram.csv data which can be downloaded to user’s computer by pressing the download button (arrow pointing down). These results represent the displacements of the rightmost tumor point in the x direction (Figure 124).

Workflow Test results



time	displx
1.0000000000000000	8.123056913147102E-002
2.0000000000000000	0.166870492006683
3.0000000000000000	0.257130426932443
4.0000000000000000	0.35228249285602
5.0000000000000000	0.452389068853735
6.0000000000000000	0.557845239437897
7.0000000000000000	0.668836363138381
8.0000000000000000	0.785609291890596
9.0000000000000000	0.908418128958423
10.0000000000000000	1.03752423322745
11.0000000000000000	1.17319622925799
12.0000000000000000	1.31571002613745
13.0000000000000000	1.46534884819276
14.0000000000000000	1.62240328057155
15.0000000000000000	1.78717133257843
16.0000000000000000	1.95995852148476
17.0000000000000000	2.14107797936269
18.0000000000000000	2.33085058538363
19.0000000000000000	2.52960512601199
20.0000000000000000	2.73767848563790

Figure 124. Diagram data (Displacements vs time).

By pressing the “PAK” tab user will see the list of all available vtk files (Figure 125). These files contain displacement fields. By pressing one of the files, a ParaView glance will open it. Here user should change the orientation to “Z” and choose the visualization of the “displacements” as shown in Figure 126.



Figure 125. List of vtk files.

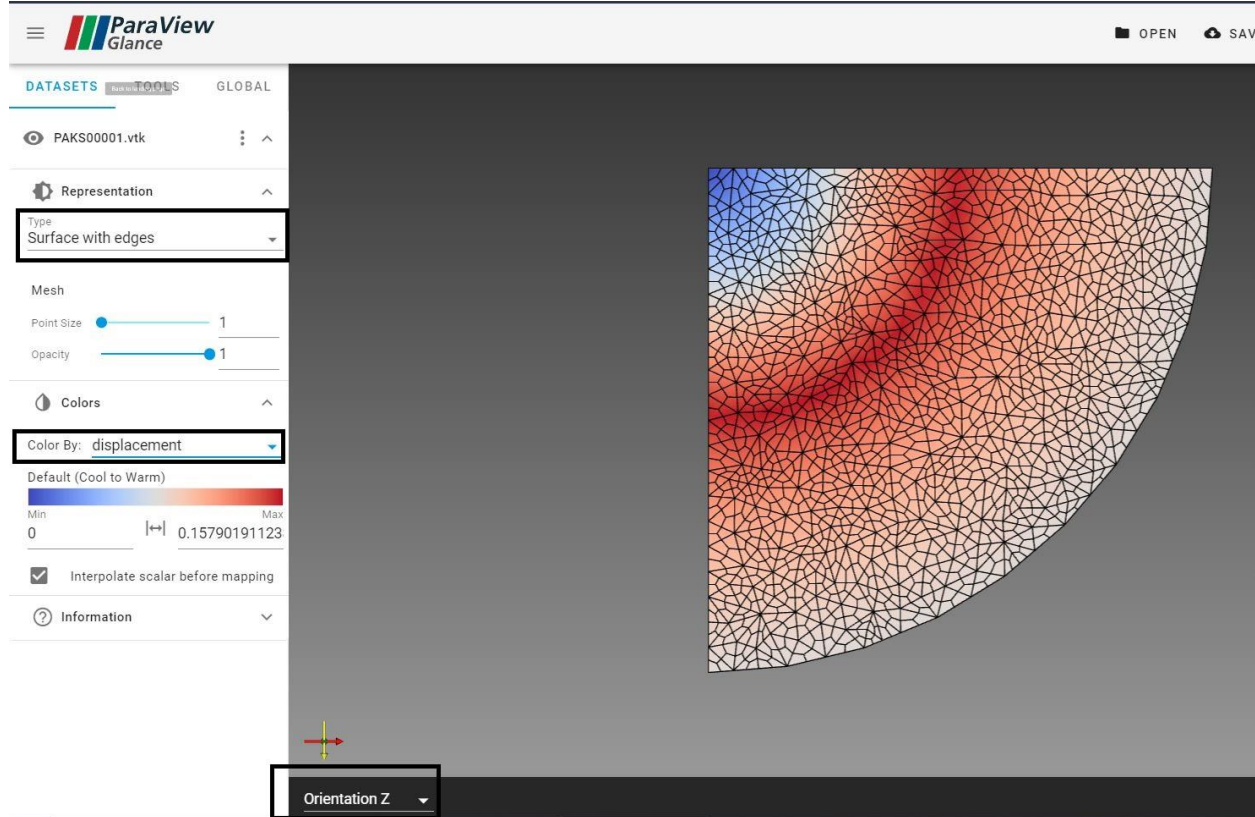


Figure 126. Visualization of the vtk file.

6.21 Model – Semicircular canal model; Responsible partner - UKG

Model - Semicircular canal model	Responsible partner - UKG
---	----------------------------------

The semicircular canal workflow can be accessed in the tissue engineering module through the main dashboard of the SGABU platform (Figure 127).

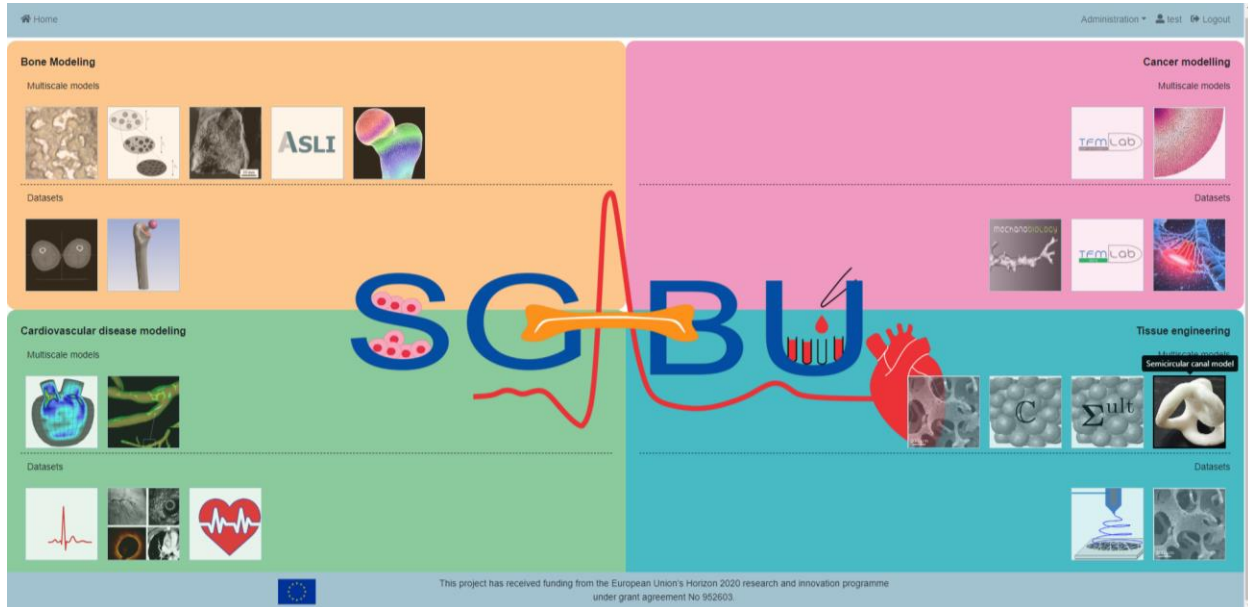


Figure 127. Locating the semicircular canal workflow in the SGABU platform.

Upon accessing the semicircular canal workflow, a user will observe two sections, namely the “Workflows” and “Add new workflow”, which are depicted in Figure 128. The workflows section includes a collection of simulation runs along with their current status and the date in which they were created. Namely possible status states include: “NOT_YET_EXECUTED”, “TERMINATED”, “RUNNING”, “FINISHED_OK” and “FINISHED_ERROR”.

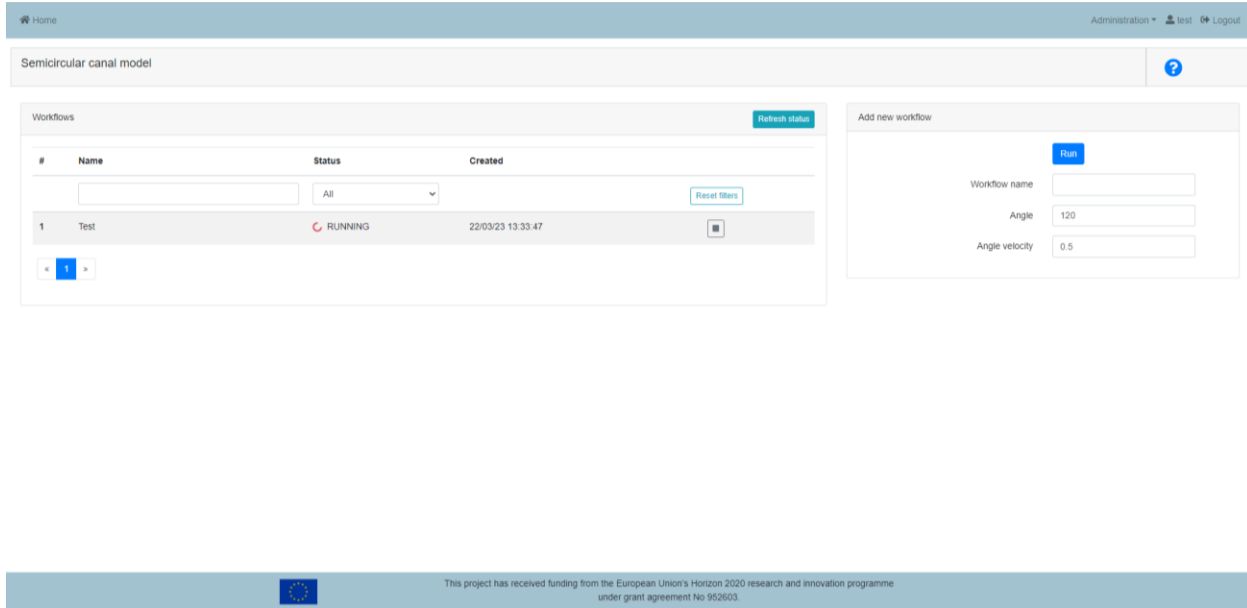


Figure 128. The dashboard of the semicircular canal workflow.

The vestibular apparatus together with cochlea make inner ear. Translational motion is regulated by the utricle and saccule placed within the vestibule. Utricle is a sort of fluid chamber, placed in vestibule and in front of the semicircular canals, containing the membrane as well. The utricle detects linear accelerations and head-tilts in the horizontal plane. The saccule detects linear accelerations and head tilts in the vertical plane. Rotational movements are detected by three semicircular canals for each ear, filled with fluid. This model focuses on the dynamic part of the vestibular apparatus. Detailed description of the model and used methodology is given in reference⁴⁰. This model enables the comparison of the numerical and analytical results of cupula displacement with the one obtained using FE analysis.

Once all the input parameters are inserted and the simulation is finished successfully, the FINISHED-OK status will appear. The FINISHED-ERROR status corresponds to a simulation run which could not run successfully due to an error. The RUNNING status corresponds to an analysis which is still running in the background. The TERMINATED status corresponds to an analysis which has been paused by the user, and lastly the NOT-YET-EXECUTED status corresponds to an analysis which has not been initiated by the user.

The add-new-workflow section enables the user to define angle and angle velocity. Upon successful simulation, the platform allows the user with the provision of several tabs – inputs, displacement, force, movie. First tab – inputs gives an overview of the chosen input parameters (Figure 129).

⁴⁰ Vulovic R., Nikolic M., Filipovic N. (2018), "Smart Platform for the Analysis of Cupula Deformation caused by Otoconia Presence within SCCs", *Computer Methods in Biomechanics and Biomedical Engineering*, Vol. 22, No. 2, pp. 130-138, Published online: 24 Dec 2018, ISSN 1476-8259, <https://doi.org/10.1080/10255842.2018.1539166>

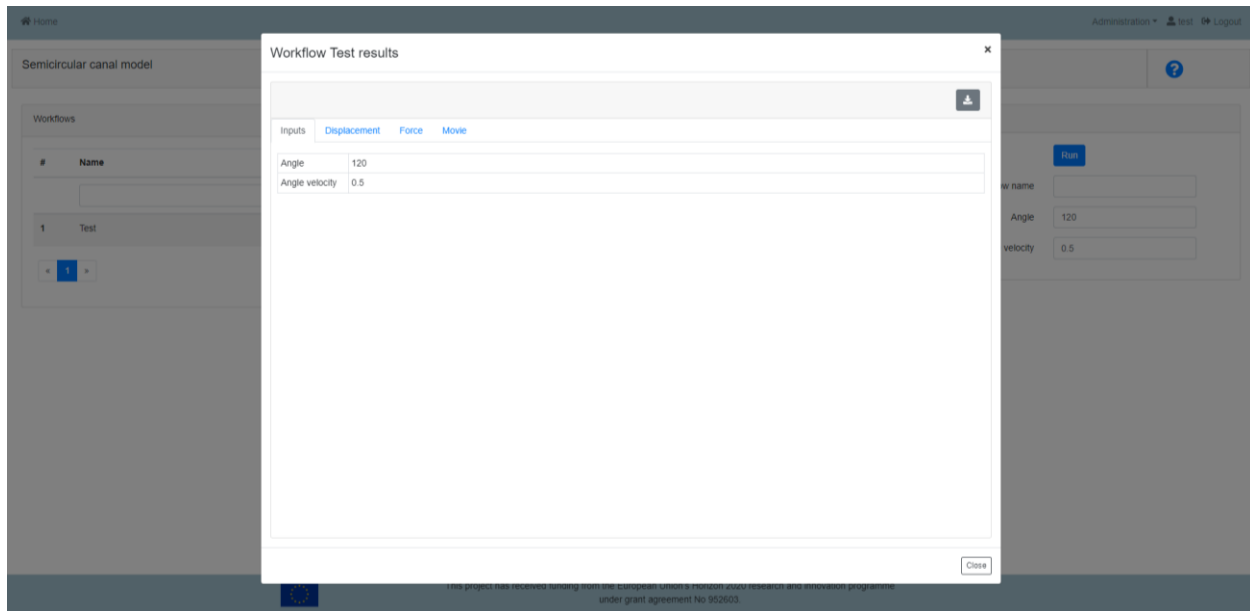


Figure 129. Input Tab in the Workflow results section.

Second tab relates to the displacement results (Figure 130), while third tab represents the forces obtained during the simulation.

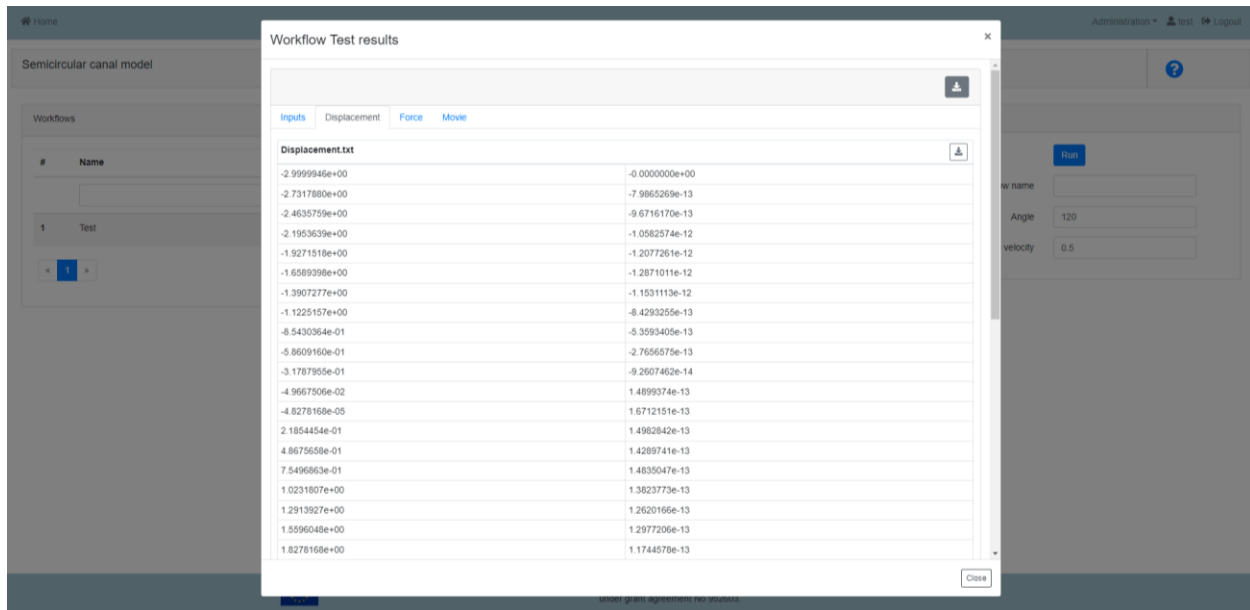


Figure 130. Displacement Tab in the Workflow results section.

The last tab represents the movie or animation of the particles inside semicircular canal (Figure 131).

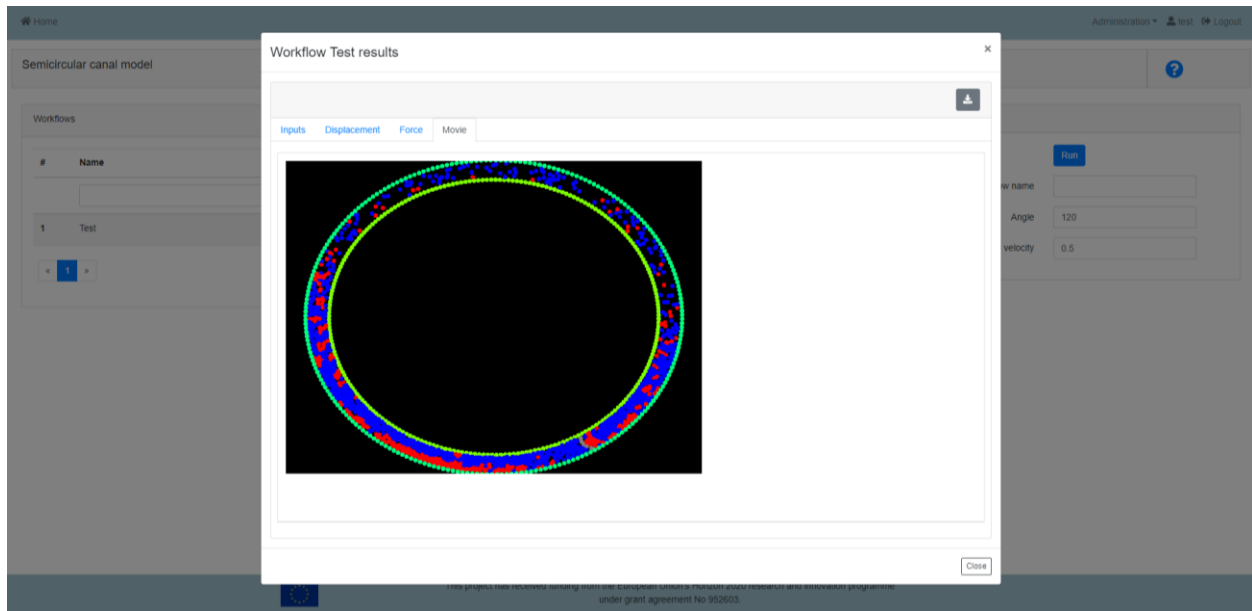


Figure 131. Movie Tab in the Workflow results section.